Title
Studies on the Evolution of Silencing in Budding Yeasts Using Comparative Genomics

Author
Ellahi, Aisha

Publication Date
2015

Peer reviewed|Thesis/dissertation

Studies on the Evolution of Silencing in Budding Yeasts Using Comparative Genomics

by

Aisha Ellahi

A dissertation submitted in partial satisfaction of the

requirements for the degree of

Doctor of Philosophy

in

Molecular and Cell Biology

in the

Graduate Division

of the

University of California, Berkeley

Committee in charge:

Professor Jasper Rine, Chair
Professor Michael Eisen
Professor Nicole King
Professor John Taylor

Fall 2015

Studies on the Evolution of Silencing in Budding Yeasts Using Comparative Genomics

by Aisha Ellahi

Abstract

Studies on the Evolution of Silencing in Budding Yeasts Using Comparative Genomics

by

Aisha Ellahi

Doctor of Philosophy in Molecular and Cell Biology

University of California, Berkeley

Professor Jasper Rine, Chair

Regional promoter-independent gene silencing is critical in the establishment of cellular identity in *Saccharomyces*. Domains of transcriptionally silent regions in the genome are associated with certain heritable modifications made to chromatin, such as histone hypoacetylation and methylation. In *Saccharomyces cerevisiae*, this type of gene repression occurs through the activity of the four Silent Information Regulator, or *SIR* genes (*SIR1-4*). From an evolutionary perspective, the *SIR* genes are unique: except for *SIR2*, all are specific to budding yeasts. Many other organisms, from *Schizosaccharomyces pombe* to human, utilize the RNA interference (RNAi) pathway, whereas most budding yeasts lack this pathway entirely. Interestingly, *SIR1*, *SIR3*, and *SIR4* are also rapidly evolving among *Saccharomyces* yeasts, providing a model by which to examine the essential principles governing successful silencing across various species and the relationship between rapid sequence evolution and evolution of function.

To examine the relationship between gene duplication, extreme sequence divergence, and functional evolution, I studied the *SIR1* gene in *S. cerevisiae* and its most ancestral paralog, *KOS3*, in the pre-whole-genome-duplication budding yeast, *Torulaspora delbrueckii*. *T. delbrueckii* also possesses genes for RNAi, *AGO1* and *DCR1*, allowing us the possibility of exploring how the evolutionary divergence of RNAi and *SIR* silencing occurred. In the process, I developed genetic tools for *T. delbrueckii.* To fully characterize *SIR1* function in *S. cerevisiae* and *SIR* gene function in *T. delbrueckii*, I utilized chromatin immunoprecipitation followed by deep-sequencing (ChIP-Seq) of tagged Sir proteins in both species. This strategy allowed for the discovery of potential novel functions, as well, revealing functions that may have been gained or lost throughout *SIR1*'s evolution. To identify loci that were directly repressed by Sir proteins, I also generated whole-transcriptome data by performing mRNA-Seq on wild-type and *sir* mutants in both species.

Collectively, these data revealed that though *SIR1* in both species is still involved in silencing, its role in that process has dramatically shifted. Previous data suggested that *SIR1* is primarily associated with the establishment or nucleation phase of silencing and not involved in telomeric silencing. The Sir1 ChIP data in *S. cerevisiae* corroborated this assessment. In *T. delbrueckii*, however, *KOS3* was essential for silencing, and was also found at telomeres. Thus, Sir1 in its early evolution had a more essential role in silencing; this role may have changed due to the duplication and diversification of the other Sir complex members. This diversification may

be contributing to the continual change in interactions between Sir1 and other Sir complex members across budding yeasts, leading to different mutant phenotypes in each species. Assays of silencer function in *T. delbrueckii* answered critical questions about when in the phylogeny important shifts in transcription factor binding sites took place. My work showed that the arrival of the Rap1, ORC, and Abf1 binding sites in the silencers of budding yeasts took place prior to the whole-genome duplication event. Analysis of silencer structure also revealed the diversity of chromatin architecture in budding yeasts: *S. cerevisiae* silent mating type loci have two silencers on either side of each locus, whereas in *T. delbrueckii*, there appears to be a single silencer on one side of each mating type locus. Transcriptome analysis of RNAi mutants revealed that this pathway in *T. delbrueckii* does not function in heterochromatic gene silencing, suggesting that this pathway has already been repurposed for some other biological process.

The examination of whole-transcriptome data in *S. cerevisiae* in conjunction with the enrichment patterns of the Sir proteins at telomeres allowed us to evaluate widely accepted models regarding the molecular architecture of heterochromatin and expression at *S. cerevisiae* telomeres. I established that repression of gene expression at native telomeres is not as widespread as previously thought, and that many genes in proximity to regions of Sir protein enrichment were, in fact, expressed just as equally in wild type as they were in *sir* mutant genetic backgrounds. However, twenty-one genes were convincingly repressed by Sir proteins, highlighting the complex and individual nature of native telomeres and subtelomeric genes. The sensitivity of RNA-Seq also uncovered a previously under-appreciated class of haploid-regulated genes: genes that were not fully repressed or de-repressed in the diploid a/α-cell type, but rather weakly repressed or de-repressed. Thus, my work has expanded the set of known a/α-regulated genes in *S. cerevisiae*. In conclusion, this dissertation has broadened our understanding of the functional constraints dictating silencing gene evolution across species that diverged prior to and after the whole-genome-duplication event. My data speaks to the actual chromatin architecture and expression state of native *S. cerevisiae* telomeres, leading to the refinement of existing models and an appreciation for how heterogeneous these regions of the genome can be.

Table of Contents

Chapter 1: An Introduction To The Use Of Comparative Genomics To Examine The Evolution Of Silencing In Budding Yeasts 1

1.1 Sir-Based Transcriptional Silencing *Saccharomyces cerevisiae* 2
1.2 Telomeres And Telomeric Silencing In *Saccharomyces cerevisiae* 5
1.3 The Role Of *SIR1* In Silencing 6
1.4 The Evolutionary History Of *SIR1* 7
1.5 RNAi And Sir-Based Silencing: Two Ways To Form Repressive Chromatin 8
1.6 *Torulaspora delbrueckii* As A Model To Study *SIR1* Evolution And The Emergence Of Sir-Based Silencing From RNAi 10

Chapter 2: The Chromatin And Transcriptional Landscape Of Native *Saccharomyces cerevisiae* Telomeres And Subtelomeric Domains 12

2.1 Abstract 13
2.2 Introduction 13
2.3 Materials And Methods 15
2.4 Results 20
2.4.1 Sir Proteins Associated At Discrete Positions At Natural Telomeres 20
2.4.2 Catalytic Activity Of Sir2 At Telomeres 30
2.4.3 Most *S. cerevisiae* Telomeres Have Expressed Genes 33
2.4.4 Telomeres Produced Significantly Fewer Transcripts Than Non-Telomeric Loci 37
2.4.5 Only ~6% Of Subtelomeric Genes Were Silenced By Sir Proteins 38
2.4.6 At Least Thirteen Y' Elements Were Expressed 44
2.4.7 Newly-Identified Haploid Or Diploid-Regulated Genes 45
2.5 Discussion 49
2.5.1 Transcription Occurs Near Telomeres, But At Lower Levels Than At Non-Telomeric Regions 50
2.5.2 Only A Small Fraction Of Subtelomeric Genes Were Repressed By Sir Proteins 51
2.5.3 The Functional Significance Of Sir Proteins At Telomeres 52
2.5.4 Discovery Of Novel Haploid-Specific Genes 52

Chapter 3: Evolution And Functional Trajectory Of Sir1 In Gene Silencing 53

3.1 Abstract 54
3.2 Introduction 54
3.3 Materials And Methods 56
3.4 Results 60

3.4.1 *S. cerevisiae* Sir1 Localized To The Autonomous Silencers Of *HML* And *HMR-E* 60
3.4.2 *S. cerevisiae* Sir1 Was Absent From Telomeres 63
3.4.3 The *Torulaspora delbrueckii* Genome Contains *KOS3*, An Ancestral *SIR1* Paralog 67
3.4.4 *KOS3* Was Indispensible For Silencing In *T. delbrueckii* 69
3.4.5 *T. delbrueckii* Kos3 Co-Localized With Sir2 And Sir4 At All Heterochromatic Locations 70
3.4.6 *T. delbrueckii SIR2* Had Roles Outside Of Its Functions With *KOS3* And *SIR4* 75
3.4.7 *T. delbrueckii* Kos3 Bound To The Silencers Of *HMLα* And *HMRa* 86
3.4.8 *T. delbrueckii* Silencers Contained Rap1 Binding Sites That Were Important For Silencing 89
3.4.9 *KOS3* Expression Was Autoregulated By De-Repression At *HMRa* 91
3.4.10 *KOS3* Was Necessary For The Recruitment Of *SIR2* And *SIR4* To Silenced Loci 92
3.4.11 Sir1 And *T. delbrueckii* Kos3, Sir2, And Sir4 Enriched At Centromeres 94
3.4.12 *T. delbrueckii AGO1* And *DCR1* Had No Function In Silencing 98
3.5 Discussion 103
3.5.1 Sir1 Associated With Silencers Except For The *HMR-I* Silencer 103
3.5.2 *KOS3* Was Essential For Silencing, Whereas *SIR1* Was Not 104
3.5.3 Kos3 Functioned At Telomeres, Whereas Sir1 Did Not 104
3.5.4 *T. delbrueckii SIR2* Had Roles In Addition To Silencing 104
3.5.5 Silencer Conservation And Diversity Among Budding Yeasts 105
3.5.6 The Presence Of Sir1 And Kos3 At Centromeres 105
3.5.7 The Role Of RNAi In *T. delbrueckii* 106

References 107

List Of Figures

1.1 Sir-Silencing In *S. cerevisiae* 3
1.2 The Structure Of Telomeres In *S. cerevisiae* 5
1.3 Phylogenetic Tree Of Yeast *SIR* And RNAi Genes 8
1.4 The RNAi Pathway Of *S. Pombe* 9

2.1 Positions Of Non-Uniquely Mapping Reads Across All Thirty-Two Telomeres From RNA-Seq Experiments 18
2.2 Sir2, Sir3 And Sir4 Enrichment At All Thirty-Two Yeast Telomeres 22
2.3 GFP-NLS ChIP-Seq Control At All Thirty-Two Yeast Telomeres 27
2.4 No Tag ChIP-Seq Control At All Thirty-Two Yeast Telomeres 28
2.5 Percentage Of Non-Uniquely Mapping Reads From ChIP-Seq Experiments At All Thirty-Two Telomeres 29
2.6 Sir Proteins Are Not Enriched At Y' Elements 30
2.7 H4K16 Exhibited Hypoacetylation In Regions Greater Than Sir2 Protein Association 31
2.8 Sir3 And Sir4 Association In Strains Lacking Sir2 Catalytic Activity 33
2.9 Transcription At All Thirty-Two Telomeres In Wild Type And *sir2*Δ 34
2.10 A Comparison Of Sir3 Protein Association And Expression In Wild Type And *sir3*Δ 35
2.11 Comparison Of Sir4 Protein Association And Expression In Wild Type And *sir4*Δ 36
2.12 FPKM Values For Subtelomeric Genes Were Significantly Lower Than FPKM Values For Non-Subtelomeric Genes 38
2.13 Genes That Were De-Repressed In *Sir* Mutants Tended To Be Located Near Peaks Of Sir Binding 43
2.14 Expression Confirmation Via qRT-PCR And Promoter Analysis Of Candidate Haploid-Specific Genes 47

3.1 ScSir1 Binding In *S. cerevisiae* 62
3.2 No Tag IP And Input Enrichment In *S. cerevisiae* 63
3.3 Lack Of Sir1 Enrichment At 31 Out Of 32 *S. cerevisiae* Telomeres 65
3.4 *SIR1* Paralogs And RNAi Genes In The *Saccharomycetaceae* Family 68
3.5 *T. delbrueckii kos3*Δ Mutants Exhibit A Complete Lack Of Silencing At *HMRa* 69
3.6 Enrichment Of Kos3, Sir2, And Sir4 In *T. delbrueckii* 71
3.7 Enrichment Of Kos3 At Eleven Telomeres In *T. delbrueckii* 72
3.8 Enrichment Of Sir2 At Telomeres In *T. delbrueckii* 73
3.9 Enrichment Of Sir4 At Telomeres In *T. delbrueckii* 74
3.10 Summary Of Genes That Significantly Increased In Expression In All Three *Sir* Mutants In *T. delbrueckii* 75
3.11 Kos3 Bound To The Silencer Of *HMLα* 86
3.12 Kos3 Bound To The Silencer Of *HMRa* 88

3.13 Mutations In Putative Abf1 Binding Sites And A Putative ARS Consensus Sequence Do Not Have An Effect On Silencing At The Chromosome V *HMR* In *T. delbrueckii* 90
3.14 The *T. delbrueckii* Chromosome V *HMR* C-Region Contains A Functional ARS 91
3.15 *KOS3* Expression Is Autoregulated By The Expression State Of The *HMR* On Chr V 92
3.16 *T. delbrueckii KOS3* Was Required To Recruit Sir2 And Sir4 To *HMRa* 93
3.17 Td Sir2 And Sir4 Display Reduced Enrichment At *HML* And *TEL01R* 94
3.18 Under-Enrichment Of IP And Input At *S. cerevisiae* Centromeres 95
3.19 Sir1 Enrichment At All 16 Centromeres In *S. cerevisiae* 96
3.20 Enrichment Of Kos3, Sir2, And Sir4 At *T. delbrueckii* Centromeres 98
3.21 RNAi Did Not Function In Silencing In *T. delbrueckii* 100

List Of Tables

2.1 Yeast Strains Used In Chapter 2 16
2.2 Percent Reads Mapped Of RNA-Seq Data 17
2.3 Oligos Used In qRT-PCR Expression Analysis 19
2.4 ChIP-Seq Peaks Called With MACS 23
2.5 Subtelomeric Genes Under Sir2/3/4 Repression 39
2.6 Complete List Of Genes Increasing In Expression In *sir2*Δ, *sir3*Δ, and *sir4*Δ 39
2.7 Reads Mapped To Y' Elements 44
2.8 Normalized Read Counts Of Uniquely-Mapped Reads At Y' Elements 45
2.9 Mating-Type Regulated Genes 48

3.1 Yeast Strains Used In Chapter 3 56
3.2 RNA-Seq Reads Per Data Set 58
3.3 ChIP-Seq Reads Per Data Set 59
3.4 Genes Increasing And Decreasing In Expression In *sir1*Δ 66
3.5 Genes Increasing In Expression In *T. delbrueckii sir* Mutants 76
3.6 Genes Increasing And Decreasing In Expression Relative To Wild Type In *T. delbrueckii kos3*Δ Mutant 77
3.7 Genes Increasing And Decreasing In Expression Relative To Wild Type In The *T. delbrueckii sir2*Δ Mutant 78
3.8 Genes Increasing And Decreasing In Expression Relative To Wild Type In The *T. delbrueckii sir4*Δ Mutant 85
3.9 Genes Increasing And Decreasing In Expression Relative To Wild Type In The *T. delbrueckii ago1*Δ Mutant 101
3.10 Genes Increasing And Decreasing In Expression Relative To Wild Type In The *T. delbrueckii dcr1*Δ Mutant 101
3.11 Genes Increasing And Decreasing In Expression Relative To Wild Type In The *T. delbrueckii ago1*Δ*dcr1*Δ Mutant 102

Acknowledgements

I would like to thank my advisor, Jasper Rine. He encouraged an incredible amount of scientific freedom and curiosity, providing a challenging and learning-filled environment. I appreciate that he was always willing to meet with me when I was stuck, and I'm grateful for his ability to review paper drafts and dissertations at lightening speed—it's a superpower!

I would also like to thank my committee members: Mike Eisen, John Taylor, and Nicole King. Special thanks goes to Nicole King who took the time to meet with me several times and gave me valuable advice. I thank everyone at the MCB Graduate Affairs Office for doing their best to support the graduate students.

The Rine lab has been an amazingly fun and stimulating place to do science. To all Rine lab members: thank you for providing such a positive and light-hearted yet scientifically rigorous atmosphere. There has never been a dull moment at the lunch table. I'd like to especially thank previous members Laura Lombardi, Oliver Zill, Debbie Thurtle, and Meru Sadhu, who were great science role models and whose advice I still, to this day, follow. To current members Anne Dodson, Ryan Janke, Katie Sieverman, David McCleary, Gavin Schlissel, Kripa Asrani, Nick Marini, and Jean Yan: I would be lucky to have colleagues half as awesome as you all wherever I end up next.

I am immensely grateful for the lifelong friends I've made in graduate school: Melissa Hendershott, Allison Craney, Caitlin Schartner, and all of my MCB 2010 classmates, especially Nick and Alisha Ellis, Anjali Zimmer, Priscilla Erickson, Anne Dodson, Courtney French, and Jenn Cisson. In addition to being awesome scientists, you are all wonderful and compassionate people—it is a privilege to have known you all at Berkeley. To Terry Meyers: your patience, empathy, and gentle reminders of what really matters in life kept my perspective in check. I'm extremely lucky to have found you at a time when I needed the support the most.

I would like to thank my parents, Zahoor and Fehmeeda, and my siblings, Asma, Zoobia, and Rehan. It was my father's love of learning and academics that inspired me to continue on the academic path after my undergraduate work. He was the first feminist in my life, and without his support and encouragement, it is no understatement to say that I would not be at Berkeley. I would like to also thank my siblings for always being there for me with care packages, a loving presence, and a sympathetic ear.

These acknowledgements wouldn't be complete without a special thank you to my cat, Darwin. Ever a source of unconditional love and solicitations for belly rubs, his insistence on sitting in my lap as I worked at my computer reminded me that I wasn't alone.

Lastly, words could never adequately express the amount of gratitude and love I have for my husband and best friend, Jared Matheson. His love, support, and encouragement gave me the strength to keep moving forward through many difficult periods. I would not have finished without his constant and unwavering belief in my abilities and intellect. Thank you, Jay.

Chapter 1

An Introduction to the Use of Comparative Genomics to Study the Evolution of Silencing in Budding Yeasts

1.1 Sir-based Transcriptional Silencing in *Saccharomyces cerevisiae*

Cellular identity is defined by the particular genes a cell expresses and represses stably through mitotic divisions. Thus, two cells with an identical genome can exhibit vastly different phenotypes depending upon the array of genes each cell is expresses. In eukaryotes, these programs of epigenetic gene regulation are associated with the enzymatic activity of methylases and acetylases that make biochemical modifications to histones and/or DNA, and demethylases and deacetylases that remove them. Certain chromatin marks are thus correlated with the transcriptional state of different regions of the genome. For example, euchromatin, or the chromatin at transcriptionally active loci, is characterized by acetylated histones H3 and H4 on nucleosomes (MILLAR and GRUNSTEIN 2006; GUILLEMETTE *et al.* 2011). Heterochromatin, or chromatin associated with transcriptionally repressed or silenced regions of the genome, is associated with histone hypoacetylation, hypomethylation, and in some eukaryotes, DNA methylation (MILLAR and GRUNSTEIN 2006; GOLDBERG *et al.* 2007; BANNISTER and KOUZARIDES 2011).

In *S. cerevisiae*, domains of heterochromatin are established and maintained by the activity of four Sir proteins: Sir1, Sir2, Sir3, and Sir4. The Sir proteins mediate silencing at the silent mating type loci *HML*α and *HMRa*, telomeres, and at the rDNA locus. Specifically, all four act at the silent mating type loci; Sir2, Sir3, and Sir4 act at the telomeres; and Sir2 in conjunction with the RENT complex acts at the rDNA, where it functions in suppressing recombination between the rDNA repeats (RUSCHE *et al.* 2003). Silencing at *HML*α and *HMRa* is a paradigm for the study of epigenetic gene silencing, and decades of careful genetic and biochemical work have identified the molecular principles governing the establishment and maintenance of silencing, and the role of the Sir proteins in this process (Figure 1.1). *HML*α is flanked by two DNA silencer elements, *E* and *I*, which contain combinations of binding sites for the Origin Recognition Complex (ORC), Rap1, and Abf1 (red boxes, Figure 1.1A). The collective protein-protein interactions between the Sir proteins and these silencer bound proteins recruit the Sir proteins to the locus and facilitate silencing (dotted gray lines, Figure 1.1B). Sir1 interacts with Orc1 (within ORC) and Sir4 (TRIOLO and STERNGLANZ 1996; BOSE *et al.* 2004; HSU *et al.* 2005). Sir4 interacts with Rap1 and Sir2, and Sir3 interacts with both Sir2 and Rap1.

The function of each Sir protein within the silencing complex is defined by its mutant phenotype on silencing, its specific protein-protein interactions, and, where applicable, its catalytic activity. Sir2 is an NAD^+-dependent deacetylase and therefore the catalytic component of the complex; it deacetylates lysines 9 and 14 on histone H3 and lysine 16 on histone H4 (H4K16) (IMAI *et al.* 2000). Deleting *SIR2* results in a complete loss of silencing, and in haploids, loss of the ability to mate. Hypoacetylated H4K16 is found across silent regions of the genome, where its association overlaps with Sir2/Sir3/Sir4 binding patterns (THURTLE and RINE 2014b; ELLAHI *et al.* 2015). Sir3 has an affinity for hypoacetylated nucleosomes and together with Sir4 comprises the structural component of the complex (ARMACHE *et al.* 2011). Neither Sir3 nor Sir4 have any catalytic activity, yet like *SIR2* are clearly required for silencing, as haploid *sir3*Δ and *sir4*Δ mutants are unable to mate and display a complete loss of silencing at *HML*α and *HMRa*. Sir1's role in silencing is complex and will be discussed in more detail below.

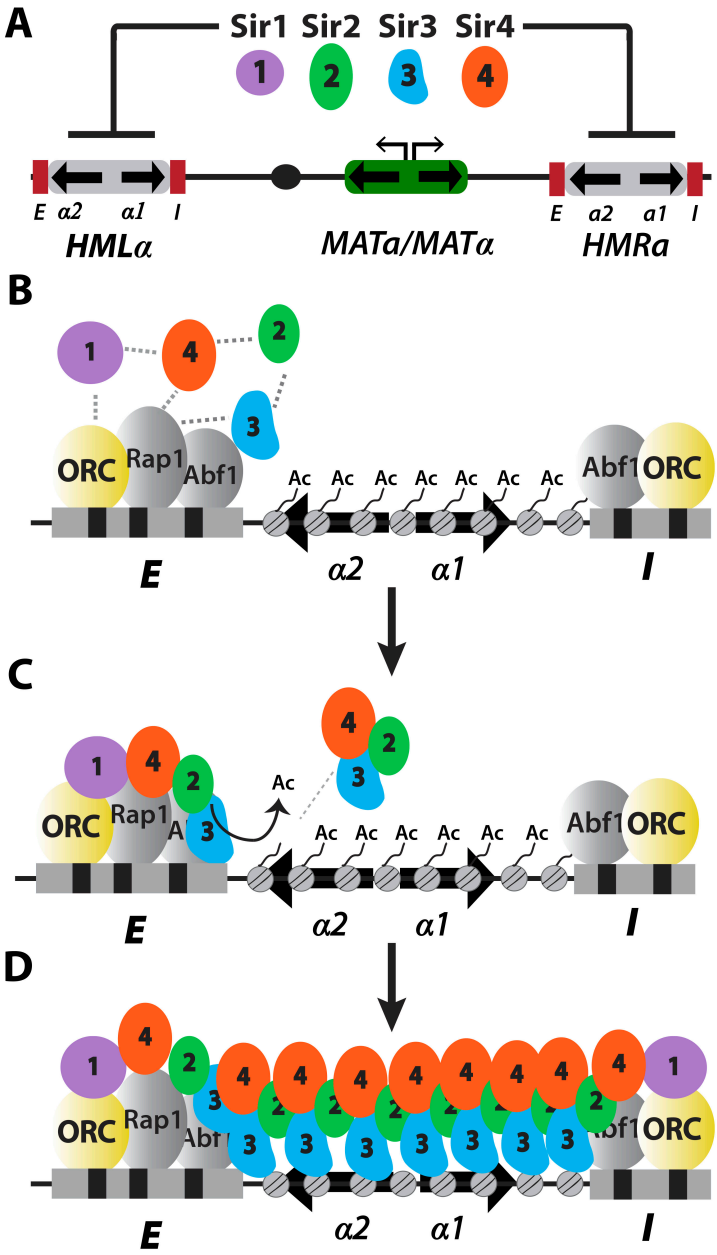

Figure 1.1 Sir-silencing in *S. cerevisiae*. The four Sir proteins (Sirs 1-4) mediate heterochromatin formation in *S. cerevisiae*. (A) Depiction of the structure of the *MAT* locus (green box) on chromosome III which is expressed, and the silent loci *HMLα* and *HMRa* present on the left and right sides of the chromosome III centromere, respectively. (B) Zoom in on *HMLα* depicting the molecular interactions that exist between the four Sir proteins and proteins binding at the *E* silencer during nucleation. Dashed gray lines represent known protein-protein interactions. (C) First step of spreading in the nucleation and spreading model of Sir-silencing: deacetylation of a nucleosome within the silent locus by Sir2, and subsequent recruitment of another Sir2/3/4 complex. (D) Depiction of spreading of the Sir2/3/4 complex after iterative cycles of deacetylation and Sir2/3/4 recruitment to hypoacetylated nucleosomes.

One prominent model for how silencing occurs divides the formation of heterochromatin into two stages: nucleation and spreading (RUSCHE *et al.* 2002). Nucleation occurs at the silencers, whereby ORC, Rap1, and Abf1 recruit the Sir proteins through the interactions detailed above. Sir1's role is primarily restricted to the silencer, as it interacts only with Orc1 and Sir4. Sir2, Sir3, and Sir4 are hypothesized to interact as a complex (MOAZED *et al.* 1997). Once the Sir2/3/4 complex arrives at the silencer, Sir2 could then deacetylate a neighboring nucleosome within the silent locus (gray circles in Figure 1.1B), creating a high-affinity binding site for Sir3. A second Sir2/3/4 complex might bind to this nucleosome (by way of Sir3's affinity for the deacetylated nucleosome). The Sir2 molecule in this second complex could then deacetylate the next nucleosome, thereby recruiting another complex of Sir2/Sir3/Sir4, and so on and so forth, leading to iterative cycles of deacetylation and subsequent Sir2/3/4 recruitment that eventually result in spreading of the Sir2/3/4 complex. Among the proposed mechanisms for how spreading of Sirs2-4 prevents transcription is the steric occlusion of RNA polymerase II (LOO and RINE 1994).

More recent data using the high-resolution genomic method of chromatin immunoprecipitation following by deep-sequencing (ChIP-seq) have refined this model (THURTLE and RINE 2014b). Though it is clear that Sir2, 3 and 4 associate with nucleosomes within the silent loci, their enrichment topography (at least in cross-linked chromatin) was not consistent with a simple spreading model, as the apparent enrichment levels were not constant throughout silent loci. This was true for both silent mating type loci as well as telomeres (ELLAHI *et al.* 2015). Differences in the nucleosome enrichment in cross-linked versus MNase digested chromatin across silent loci suggested the presence of a specialized chromatin structure mediated by Sir proteins.

Another important structural feature of the silent mating type loci is the presence of two silencers, one on either side of *HML*α and *HMRa* (red boxes, Figure 1.1A). In principle, if the sole purpose of the silencers were to provide a nucleation point for spreading to occur, one silencer at each locus could be sufficient. However, the presence of two suggests that either the degree of spreading afforded by one is insufficient, or that two silencers may contribute in some other way that is integral to repression (for example, by mediating formation of a higher-order structure). At *HML*α, deletion of either silencer by itself has no effect on silencing; thus, each is sufficient on its own to silence (MAHONEY and BROACH 1989). At *HMRa*, however, the two silencers are not functionally equivalent: deletion of the *E* silencer results in the de-repression of *HMRa*, but deletion of the *I* silencer has no effect on silencing when evaluated in the chromosome context (BRAND *et al.* 1985). Thus, it would appear that *HML*α has one more silencer than it needs, and that *HMRa* has only one fully functional silencer. Yet ORC, Rap1, and Abf1 binding sites in three of the four silencers (*HMR-E*, *HMR-I*, and *HML-I*) are evolutionarily conserved within the *sensu stricto* yeasts (TEYTELMAN *et al.* 2008). Furthermore, chromosome confirmation capture (3C) methods show that the silencers at *HMR* interact, suggesting that silencers allow the formation of a three-dimensional structure (VALENZUELA *et al.* 2008). Future studies may illuminate the selective advantage of the evolutionarily conserved two-silencer structure in *S. cerevisiae*.

1.2 Telomeres and Telomeric Silencing in *Saccharomyces cerevisiae*

The linear chromosomes of eukaryotic organisms are capped by specialized structures called telomeres. Telomeres protect chromosome ends from degradation, suppress recombination between repetitive telomeric sequence, prevent activation of the DNA damage response, and provide a mechanism that allows replication to occur without resulting in progressively shorter and shorter chromosomes (reviewed in (WELLINGER and ZAKIAN 2012)). In *Saccharomyces cerevisiae*, three sequence features define telomeres: (i) telomeric repeats, which are tracts of $(TG_{1\text{-}3})_n$ repeated units of 300±75bp in length; (ii) X-elements, which are further subdivided into the Core-X sequence and subtelomeric repeats; and (iii) Y' elements, which are ~5-6kb in length and contain ORFs for putative helicase genes. Core-X sequences contain ARS consensus sequences (ORC binding sites) and Abf1 binding sites. Native telomeres are one of two types, based on the sequence features they contain: X-only telomeres, which contain telomeric repeats and X-elements; or X-Y' telomeres, which contain all three sequence features (Figure 1.2). Thus, all telomeres contain X-elements and telomeric repeats, and about half of all *S. cerevisiae* telomeres contain one or more Y' elements.

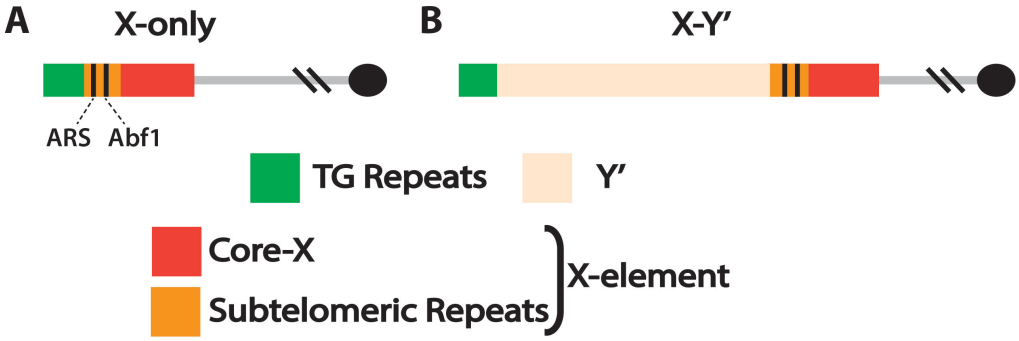

Figure 1.2 The Structure of Telomeres in *S. cerevisiae*. Two classes of telomeric sequence exist in *S. cerevisiae*: X-only telomeres (A), and X-Y' telomeres (B). Both types contain telomeric repeats (green boxes) and X-elements (orange boxes). X-elements consist of the Core-X sequence, which contains an ARS consensus sequence and an Abf1 binding site (black lines).

Telomeric chromatin in many organisms is heterochromatic, or transcriptionally repressive. As a result, genes adjacent to or within telomeric regions are often silenced. This effect, dubbed "telomere position effect," was first discovered in *Drosophila melanogaster* and has since been found to be a general feature of telomeric chromatin in many organisms (SCHULTZ 1947; HAZELRIGG *et al.* 1984). Telomere position effect was first described in *S. cerevisiae* by use of the *URA3* and *ADE2* reporter genes, which when placed adjacent to an artificially truncated telomere and was observed to be reversibly repressed. Additionally, the transcriptional state of *ADE2* was heritable, as evidenced by sectored colonies in which it was observed that red *ade2* mutants gave rise to *ade2* mutant daughter cells (GOTTSCHLING *et al.* 1990a). These assays in *S. cerevisiae* demonstrated several important principles of telomere position effects. First, the heritability of transcriptional state suggested that the effect on expression was epigenetic. Second, the finding that multiple reporter genes (*URA3*, *ADE2*, *HIS3*,

and *TRP1*) could be silenced when placed adjacent to this artificial telomere demonstrated that silencing was independent of promoter sequence, and therefore akin to the regional, promoter-independent repression characteristic of heterochromatin. Third, the strength of silencing varied directly as a function of the distance of the reporter gene from the telomeric end: the farther away the reporter gene was, the less it was silenced (and thereby, the more it was expressed). And finally, *SIR2*, *SIR3*, and *SIR4* (but not *SIR1*) were found to be required for telomeric silencing.

These early studies with reporter genes and artificial telomeres suggested that telomeric silencing was robust and widespread in *S. cerevisiae*. However, a subsequent study utilizing the same *URA3* reporter at native telomeres found that few of the telomeres assayed exhibited any silencing, and that furthermore, silencing abruptly decreased as a function of the reporter gene's distance from the telomere (rather than following a gradual decrease, as studies with artificial telomeres had shown) (PRYDE and LOUIS 1999). These data suggested that silencing was not widespread at native telomeres. Since then, other genome-wide microarray-based studies have corroborated this observation (WYRICK *et al.* 1999; TAKAHASHI *et al.* 2011). Furthermore, the *URA3* reporter gene assay, which measures silencing as a function of growth on media containing 5-fluoroorotic acid (5FOA), was shown to not always be a reliable indicator of *URA3*'s transcriptional status (ROSSMANN *et al.* 2011); cells can be sensitive to 5FOA without robust transcription of *URA3*.

1.3 The Role of *SIR1* in Silencing

SIR1 remains the most enigmatic members of the Sir complex. In *S. cerevisiae*, *sir1*Δ mutants show a partial loss of silencing (as compared to *sir2*Δ, *sir3*Δ, and *sir4*Δ mutants) as measured at the population level by *HMRa1* expression levels in *MAT*α strains. By bulk analysis, *sir1*Δ cells also show no apparent mating defect. At the single-cell level, however, a population of *sir1*Δ cells constitutes a mix of fully repressed and de-repressed cells. De-repressed haploid *MATa sir1*Δ cells lose sensitivity to α-factor, while repressed cells are as sensitive to it as wild-type cells (PILLUS and RINE 1989). The transcription state in *sir1*Δ cells is mitotically heritable for mutiple cell divisions. Furthermore, cells can switch from the repressed to de-repressed state and vice versa at a low frequency. Single-molecule RNA FISH data on *sir* mutants supports the observation that a population of *sir1*Δ strains consists of two groups of cells: cells that have the same number of transcripts on a per cell basis as *sir4*Δ cells, and another group that has the same rare number of transcripts as wild type (DODSON and RINE 2015).

The observation that some fraction of *sir1*Δ cells remain silenced in the absence of Sir1 led to the hypothesis that Sir1 primarily functions in the establishment of silencing (as opposed to Sirs 2,3 and 4, which function in both establishment and maintenance). This view, however, is incomplete, as it is clear that silencing can be re-established, even if inefficiently, in *sir1*Δ mutants. Sir1 likely contributes to establishment and stability of repression. Chromatin immunoprecipitation of Sir 2,3 and 4 in *sir1*Δ mutants showed that even in the absence of Sir1, that are able to associate with the silencers of *HML* (RUSCHE *et al.* 2002). The only identified domain in the Sir1 protein is the Orc1-interacting region (OIR); Sir1 actually has two such domains, an OIR and an OIR', and both appear to contain residues important for silencing function, although most previous work has focused on the OIR domain (BOSE *et al.* 2004; HOU *et al.* 2009). Because Sir1 interacts with Sir4 and Orc1, its primary function may be to stabilize interactions between Sir4, and thereby the Sir protein complex .

The only function attributed to Sir1 beyond silencing is its binding to at least six centromeres in *S. cerevisiae* (SHARP *et al.* 2003). This study found that strains that lack *SIR1* and *CAC1* show elevated rates of non-disjunction, suggesting that Sir1 may also function in ensuring proper chromosome segregation in mitosis.

1.4 The Evolutionary History of *SIR1*

In contrast to *SIR2*, which is widely conserved across organisms, *SIR1* is a budding yeast-specific gene with a dynamic evolutionary history in the *Saccharomyces* family of yeasts (Figure 1.3). While the *S. cerevisiae* genome contains one *SIR1* paralog, some species, like *S. bayanus v. uvarum* have up to four: *SIR1* and three additional *Kin Of SIR1* (*KOS*) paralogs, *KOS1-3*. These *SIR1* paralogs are highly divergent at the protein sequence level, both within and between species (GALLAGHER *et al.* 2009).

Furthermore, it appears that *SIR1*, *KOS1*, and *KOS2* are the products of an internal duplication as well, as the earliest *SIR1* paralog, *KOS3*, is about half the length of the other two and contains one instead of two Orc1 Interacting Regions (OIRs). The lack of conserved synteny around the *KOS* paralogs and the high sequence divergence has made it difficult to trace the sequence of duplications, and whether any paralogs are related by the whole-genome duplication. Phylogenetic analysis of the OIR and OIR' domains within Sir1 suggests that the OIR domain duplicated once in its evolutionary history; thus, the most parsimonious explanation is that the *KOS3* paralog arose first, prior to the whole-genome duplication event, then subsequently underwent an internal duplication as well as several whole-gene duplications, either before or after the whole-genome duplication. Many of these paralogs have been lost in *S. mikatae*, *S. paradoxus*, and *S. cerevisiae* (Figure 1.3).

It is interesting to note, from a functional perspective, that some species have four *SIR1* paralogs that function in silencing, while others have zero (namely, *K. lactis* and *C. glabrata*). These species seem to have innovated multiple solutions to the problem of achieving silencing, with some requiring many Sir1 proteins, and others requiring none. *SIR1*'s dynamic evolutionary history raises questions about how much a gene's function can change through duplication and rapid sequence divergence, as well as the essential principles guiding the selection of *SIR1* paralogs.

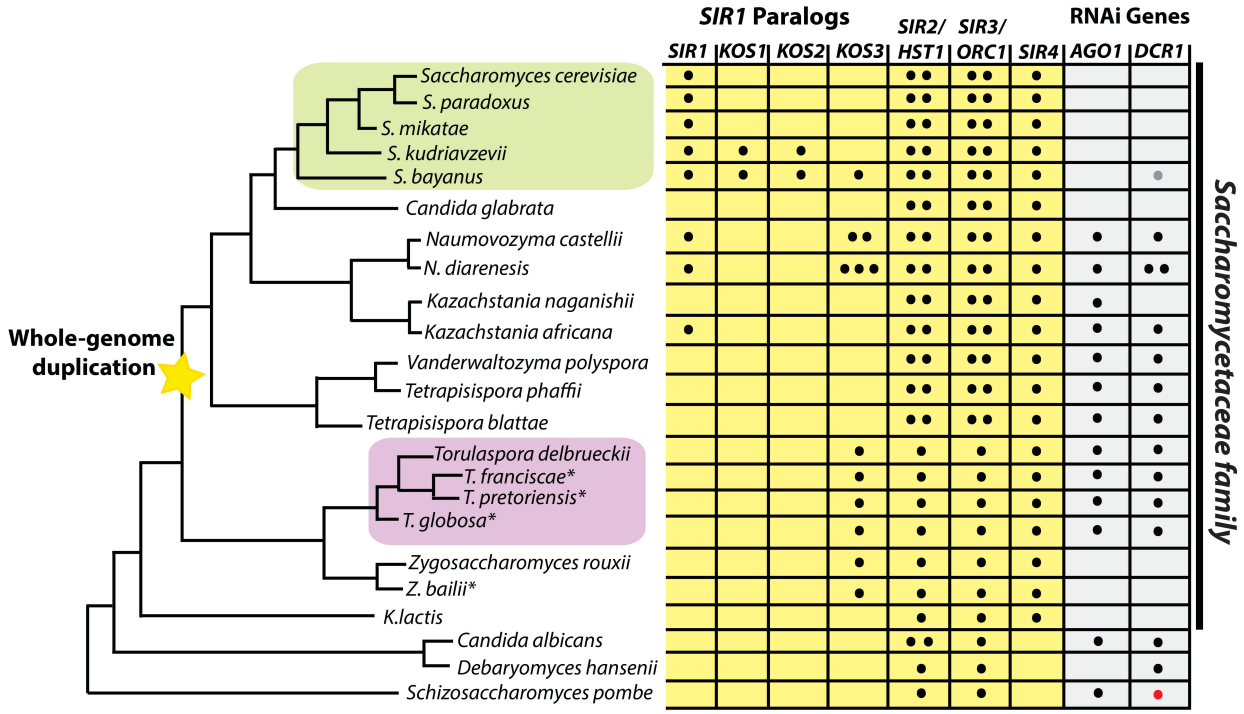

Figure 1.3. Phylogenetic Tree of Yeast *SIR* and RNAi Genes. Shown is a phylogenetic species tree of budding yeasts and the silencing gene paralogs present in their genomes, with *Schizosaccharomyces pombe* (fission yeast) shown as an outgroup. The *sensu stricto* yeasts are highlighted in green. *Torulaspora* yeasts are highlighted in pink. Black dots denote numbers of gene copies (i.e., three dots in the *KOS3* column for *N. diarenesis* denotes that this species has three highly similar copies of a *KOS3* gene). The gray dot in the *DCR1* column in *S. bayanus* denotes the presence of a *DCR1* pseudogene. The red dot in the same column in the *S. pombe* row highlights that though the gene names are identical, *DCR1* in *S. pombe* and *DCR1* in budding yeasts are not orthologous. Up to four *SIR1* paralogs have been identified: *SIR1*, and three *Kin Of SIR1* (*KOS*) paralogs, *KOS1-3*. *Naumovozyma castellii* has a fourth paralog, *KOS4*, not shown for simplicity. *KOS3* is the earliest pre-whole genome duplication *SIR1* paralog identified. The *SIR2*/*HST1* and *SIR3/OCR1* gene pairs are whole-genome duplicates; therefore, pre-whole genome duplicates only have one ancestral ortholog of these genes. *T. delbrueckii* contains an ancestral *SIR1* paralog, *KOS3*, as well as budding yeast orthologs of *AGO1* and *DCR1*.

1.5 RNAi and Sir-based Silencing: Two Ways To Form Repressive Chromatin

In eukaryotes, two major mechanisms for forming heterochromatin have been described: Sir-based silencing, and RNAi. RNAi is by far the most common pathway, present in a diverse array of organisms, ranging from the fission yeast *Schizosaccharomyces pombe* to metazoans (flies, humans, and worms). RNAi is absent from *S. cerevisiae,* however, as well as many budding yeasts in the *Saccharomyces* group (Figure 1.3). Meanwhile, the Sir proteins (with the

important exception of Sir2), are unique to budding yeasts. While Sir2 is widely conserved from bacteria to humans (GREISS and GARTNER 2009), Sir1, Sir3, and Sir4 are not found outside of the *Saccharomyces* group of budding yeasts (HICKMAN *et al.* 2011).

A major unanswered question in the evolution of silencing is how this unique Sir-based silencing machinery evolved independently of the more ubiquitous RNAi machinery. *SIR2* is the only gene common to both mechanisms across *S. pombe* and *S. cerevisiae*, and in both species, *SIR2* functions in heterochromatin formation (i.e., *sir2*Δ mutants in *S. pombe* exhibit silencing defects like *S. cerevisiae sir2*Δ mutants) (SHANKARANARAYANA *et al.* 2003). Three proteins constitute the core of the RNAi machinery: an RNA-dependent RNA polymerase, which converts transcribed single-stranded RNA to double-stranded RNA; Dicer, which cleaves the double-stranded RNA into small interfering RNAs (siRNAs); and Argonaute, which binds to siRNAs and recruits chromatin modifiers to target loci that are complementary to siRNAs (Figure 1.4, reviewed in (GREWAL 2010). Examination of the evolutionary history of these three genes reveals that the filamentous fungi of the Pezizomycotina subphylum (*Neurospora crassa*, *Aspergillus nidulans*, and *Magnaporthe grisea*) are the group of fungi closest to the budding yeast group that retain all three genes of the RNAi machinery. Thus, most budding yeast species lack Argonaute, and all lack any gene orthologous to the *S. pombe* Dicer as well as any gene reminiscent of an RNA-dependent RNA-polymerase (DRINNENBERG *et al.* 2009a).

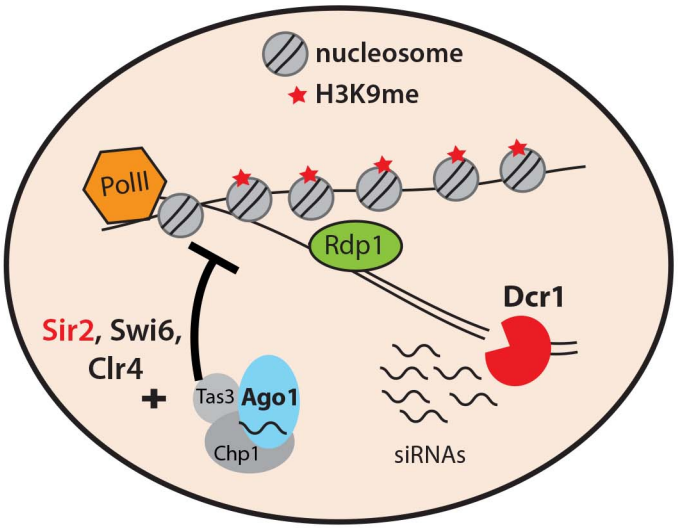

Figure 1.4. The RNAi pathway in *S. pombe*. Shown is a cartoon of the three major protein components of the RNAi pathway in *S. pombe* and their role in the formation of heterochromatin. Rdp1 converts Pol II-generated transcripts into dsRNAs, which are then cleaved by Dcr1, generating small interfering RNAs (siRNAs). Ago1 is part of a three-member complex composed of Ago1, Chp1, and Tas3, which binds the siRNAs and recruits chromatin modifying enzymes such as Sir2 to the locus targeted for repression. An important histone modification correlated with silencing that is present in *S. pombe* but absent in budding yeasts is the methylation Lysine 9 on histone H3 (H3K9 methylation).

There remain a handful of budding yeast species that do contain an Argonaute (or *AGO1*) ortholog, and a few of these species in turn possess a non-canonical *DCR1* ortholog that has been

identified as a duplicate of *RNT1*. Importantly, this budding-yeast specific *DCR1* gene is not orthologous to the *S. pombe* and *N. crassa DCR1* orthologs; despite their identical names, they are not evolutionarily related. The most thorough characterization of this budding yeast-version of RNAi has been in *Naumovozyma castellii* (*N. castellii*), where it was shown to repress the expression of Ty elements (DRINNENBERG *et al.* 2009a). Ago1 bound to siRNAs that were complementary to Ty sequences, and Dcr1 generated the siRNAs from longer Ty transcripts that formed hairpins through base-pairing at long-terminal repeat regions. Thus, the double-stranded portion of the hairpins stimulated Dcr1 activity, obviating the need for an RNA-dependent RNA polymerase to generate double-stranded RNAs.

Why would such an important biological pathway be completely lost in an entire group of species? Again, data from *N. castellii* and other related species suggests an answer: the cost of possessing RNAi is susceptibility to yeast killer double stranded RNA (dsRNA) viruses (DRINNENBERG *et al.* 2011). The dsRNA genomes of killer viruses encode a protein toxin that kills neighboring cells as well as a protein conferring immunity to the cell producing the toxin (SCHMITT and BREINIG 2006). Thus, the virus is able to quickly turn over a population of uninfected cells to infected cells because all non-infected cells are killed, while infected cells survive and pass toxin immunity onto their daughters. Restoring *N. castellii AGO1* and *DCR1* genes in *S. cerevisiae* leads to the degradation of the double-stranded RNA virus genome, thereby leaving cells unable to make the protein that confers toxin immunity, and therefore susceptible to the virus. The extreme fitness cost of having RNAi may have imposed a strong selective pressure to lose the pathway entirely. In support of this hypothesis, most species known to possess a killer dsRNA virus lack RNAi (DRINNENBERG *et al.* 2011). Interestingly, no toxin-producing killer viruses have been identified in *S. pombe* (HEINTEL *et al.* 2001). Whether this is because some other resistance mechanism exists or that the fitness of *S. pombe* strains lacking RNAi is poor because of other essential functions the pathway performs in natural environments is unknown. As for budding yeasts, the loss of RNAi may have facilitated the innovation of an entirely novel silencing mechanism, such as Sir-based silencing, with silencing functions analogous to RNAi.

1.6 *Torulaspora delbrueckii* as a model to study *SIR1* Evolution and the Emergence of Sir-based Silencing From RNAi

The growing number of sequenced yeast species, their experimental tractability, and the representation of many millions of years of evolutionary time offers unprecedented advantages in using yeast species to study how evolution unfolds at the molecular level (DUJON 2010; HITTINGER 2013). The development of additional experimentally tractable species adds to the toolkit of yeast evolutionary genetics and expands the repertoire of evolutionary questions one can ask and rigorously test in an experimental setting. The *Torulaspora* group of yeasts represents one such (until now) untapped resource. The genomes of four species in this clade were recently sequenced: *T. delbrueckii*, *T. pretoriensis*, *T. globosa*, and *T. franciscae* (Devin Scannell, unpublished). The most commonly used genome assembly is of *T. delbrueckii* (GORDON *et al.* 2011). *T. delbrueckii* and all of the *Torulaspora* yeasts, like *K. lactis*, are pre-whole genome duplication budding yeasts. *T. delbrueckii* is found in many commercial processes where *S. cerevisiae* is used: wine fermentation, beer, baking, and even dairy (WELTHAGEN and VILJOEN 1998; HERNANDEZ-LOPEZ *et al.* 2003; ALBERTIN *et al.* 2014). More recently, mixtures of *T. delbrueckii* and *S. cerevisiae* are being explored in wine production for their potential to

enhance desired flavors (PACHECO *et al.* 2012). Wild isolates of *T. delbrueckii* have been found in a variety of locations, including grapes and other fruit, soil, insects, and plants (ALBERTIN *et al.* 2014). Thus, like *S. cerevisiae*, *T. delbrueckii's* habitat range is quite extensive.

T. delbrueckii's position on the phylogenetic tree offered the opportunity to answer two important Sir-silencing evolution questions introduced in this chapter: the functional evolution of *SIR1*, and the evolution of the Sir-silencing mechanism (Figure 1.3). The genomes of all four aforementioned *Torulaspora* species contain the earliest identified pre-whole genome duplication *SIR1* paralog, *KOS3*, as well as orthologs for budding yeast RNAi, *AGO1* and *DCR1*. To explore if any of these *Torulaspora* species could be used to answer these questions, all were evaluated in the lab for their genetic and experimental tractability. Four metrics were used in evaluation: growth in standard *S. cerevisiae* media, transformational ability and the ease of targeted gene deletion, the occurrence of mating in the lab, and compatibility with existing *S. cerevisiae* genetic tools (*CEN/ARS* and 2 μm plasmids). *T. delbrueckii* was the most compatible species and easiest to transform with existing *S. cerevisiae* protocols, and therefore, experimental work was continued using this species. The only unresolved metric that remains in this species is mating. Despite the characterization of both haploid *MATa* and *MATα* wild isolates, we have not observed mating of this species in the lab.

Chapter 2

The Chromatin and Transcriptional Landscape of Native *Saccharomyces cerevisiae* Telomeres and Subtelomeric Domains

(Portions of this chapter are adapted from: *Ellahi A*, Thurtle D*, Rine J (2015) The Chromatin and Transcriptional Landscape of Native Saccharomyces cerevisiae Telomeres and Subtelomeric Domains. Genetics 200:1–17.*)

2.1 Abstract

S. cerevisiae telomeres have been a paradigm for studying telomere position effects on gene expression. Telomere position effect was first described in yeast by its effect on the expression of reporter genes inserted adjacent to truncated telomeres. The reporter genes showed variable silencing that was dependent on the Sir2/Sir3/Sir4 complex. Later studies examining subtelomeric reporter genes inserted at natural telomeres hinted that telomere position effects were less pervasive than previously thought. Additionally, more recent data using the sensitive technology of ChIP-Seq revealed a discrete and non-continuous pattern of co-enrichment for all three Sir proteins at a few telomeres, calling the generality of these conclusions into question. Here, we combined the ChIP-Seq of the Sir proteins with RNA-Seq of mRNAs in wild type and in *sir2*, *sir3* and *sir4* deletion mutants to characterize the chromatin and transcriptional landscape of all native *S. cerevisiae* telomeres at the highest achievable resolution. Most *S. cerevisiae* chromosomes had subtelomeric genes that were expressed, with only ~6% of subtelomeric genes silenced in a *SIR*-dependent manner. In addition, we uncovered twenty-nine genes with previously unknown cell-type-specific patterns of expression. These detailed data provided a comprehensive assessment of the chromatin and transcriptional landscape of the subtelomeric domains of a eukaryotic genome.

2.2 Introduction

Telomeres are specialized structures at the end of eukaryotic chromosomes critical for various biological functions. Telomeres bypass the problem of replicating the ends of linear DNA, protect chromosome ends from exonucleases and nonhomologous end-joining, prevent the linear DNA ends from activating a DNA-damage checkpoint, and exhibit suppressed recombination (reviewed in (WELLINGER and ZAKIAN 2012)). In *Saccharomyces cerevisiae*, telomeres are composed of three sequence features: telomeric repeats, which consist of 300 ± 75 bp of $(TG_{1\text{-}3})n$ repeated units produced by telomerase; X elements; and Y' elements, which contain an open reading frame for a putative helicase gene. The X elements are subdivided into a core X (consisting of an ARS consensus sequence and Abf1 binding site) and subtelomeric repeats that have variable repeated units containing a binding site for Tbf1 (LOUIS 1995). All telomeres contain telomeric repeats plus an X element, and about half of *S. cerevisiae's* 32 telomeres also contain a Y' element (X-Y' telomeres). "X-only" telomeres contain an X element but not a Y' element. Unlike the Y' elements, the telomeric repeats and X elements are bound by proteins critical for the maintenance of telomeres. Rap1 binds the $TG_{1\text{-}3}$ telomeric repeats and recruits the Sir2/Sir3/Sir4 protein complex, the trio of heterochromatin structural proteins critical for the repression of the silent mating loci, *HMLα* and *HMRa*. Sir proteins are also recruited to the core X sequence through interactions with Abf1 and the Origin Recognition Complex (ORC), which binds the ARS consensus sequence within the core X. Thus, telomeres have a heterogeneous sequence composition, recruit proteins that can form heterochromatin-like structures**,** and are critical to maintaining the genomic integrity of the cell.

As first described in *Drosophila* (SCHULTZ 1947; HAZELRIGG *et al.* 1984), the heterochromatic structure of telomeric chromatin results in the transcriptional silencing of adjacent genes, an effect known as "telomere position effect." Since then, telomere position effects have been observed in other organisms, where it can be an important means of regulating

gene expression. For example, the malarial parasite *Plasmodium falciparum* genome contains subtelomeric *var* genes encoding cell-surface antigens that utilize Sir2-dependent telomeric heterochromatin for their repression (GUIZETTI and SCHERF 2013). *Var* genes are selectively expressed, one at a time, and switch expression states allowing *Plasmodium* to stay ahead of the host's immune response. This selective expression of one antigen over all the other antigen genes is maintained by the epigenetic silencing of all *var* copies except the expressed one (TONKIN *et al.* 2009; GUIZETTI and SCHERF 2013). Similarly, in *Candida glabrata*, the *EPA* adhesion genes essential for colonization of the host urinary tract are located in subtelomeric regions, and their expression is regulated by a Sir-protein-based silencing mechanism that is responsive to the differences in niacin concentration in the blood stream versus the urinary track (PEÑAS *et al.* 2003; DOMERGUE *et al.* 2005). In *S. cerevisiae,* genes encoding cell-wall components and genes required for the metabolism of certain nutrients tend to be located in subtelomeric regions and are expressed specifically under certain stressful conditions (AI *et al.* 2002).

Telomere position effect was first described in *S. cerevisiae* by the attenuated expression of reporter genes placed adjacent to a synthetic telomere on either the left arm of chromosome VII or the right arm of chromosome V (GOTTSCHLING *et al.* 1990b; RENAULD *et al.* 1993; FOUREL *et al.* 1999). Reminiscent of general epigenetic silencing, the effect was concluded to be independent of gene identity and promoter sequence. Furthermore, much like silencing at the mating type cassettes *HMLα* and *HMRa,* the silenced state of telomere-adjacent *URA3* and *ADE2* was heritable and dependent on the *S*ilent *I*nformation *R*egulator proteins Sir2, Sir3, and Sir4. Unlike *HMLα* and *HMRa*, deletion of *SIR1* had no effect on telomeric silencing (APARICIO *et al.* 1991). These and other early studies led to the view that Sir proteins were in a continuous gradient, highest at the telomere and extending inward for a few kilobase pairs, depending in particular on the level of Sir3 protein (RENAULD *et al.* 1993; HECHT *et al.* 1996; STRAHL-BOLSINGER *et al.* 1997).

More recent findings have questioned the earlier view of telomere position effect in *S. cerevisiae*. For example, when inserted adjacent to the native telomeres *TEL10R, TEL04L,* and *TEL03R*, the same *URA3* reporter detects little transcriptional repression (PRYDE and LOUIS 1999). For the few natural telomeres at which *URA3* appears repressed (*TEL13R, TEL11L*, and *TEL02R*), silencing is discontinuous across the length of the telomere and largely restricted to positions close to the X element. Similarly, Sir proteins also associate discretely at select natural telomeres with the highest levels of enrichment proximal to the X element (ZILL *et al.* 2010; RADMAN-LIVAJA *et al.* 2011; THURTLE and RINE 2014b). The natural telomeres that repress the *URA3* transgene exhibit a characteristic array of phased nucleosomes specific to those telomeres (LONEY *et al.* 2009). Additionally, some Y' elements are transcribed, a fact that is inconsistent with Sir protein-mediated repression of all Y' elements (FOUREL *et al.* 1999; PRYDE and LOUIS 1999). In addition to these discrepancies, metabolic reporters are not biologically neutral, and some complexity regarding these reporters has emerged (ROSSMANN *et al.* 2011; TAKAHASHI *et al.* 2011). For example, *DOT1, SWI4,* and *ARD1*, all of which abrogate H3K79 methylation, had been implicated in telomeric silencing as assayed by the *URA3* reporter at artificial telomeres. However, transcription of native genes at telomeres as measured by microarray analysis revealed little change in expression level in a *dot1* mutant and other mutants proposed to disrupt H3K79 methylation (TAKAHASHI *et al.* 2011). Subsequent interrogation of the *URA3* reporter found that *dot1* and other mutants are actually differentially sensitized to the drug 5-FOA used to monitor *URA3* expression (ROSSMANN *et al.* 2011). Therefore, the phenotypes of these mutants as measured by 5-FOA-sensitivity do not reliably reflect the transcriptional status of *URA3* at

telomeres.

In summary, establishing the prevalence of telomere position effect, and identifying the set of genes and proteins that mediate it has been complicated by three issues: (1) non-systematic studies of different telomeres in *S. cerevisiae;* (2) the influence of metabolism on telomeric reporters; and (3) limitations on the resolution of ChIP and microarray analysis. To resolve these confounding issues, we undertook a high-resolution analysis of chromatin architecture and expression state at all natural *S. cerevisiae* telomeres, free of reporter genes, by utilizing ChIP-Seq analysis of Sir proteins combined with RNA-seq analysis of wild type and *sir2Δ*, *sir3Δ*, and *sir4Δ* mutants. ChIP-Seq of acetylated H4K16, a histone mark anti-correlated with silencing, was also analyzed to further evaluate specific histone modifications with respect to expression data from RNA-Seq. This study provided a definitive analysis of the chromatin landscape and degree of silencing at telomeres in *S. cerevisiae*, and highlighted the functional variation among telomeres, befitting the accelerated sequence changes seen in these cauldrons of genetic innovation.

2.3 Materials and Methods

Yeast Strains. Yeast strains and plasmid-containing strains are listed in Table 2.1. All yeast strains were generated in the W303 background. Deletion alleles were constructed through one-step integration of knockout cassettes (LONGTINE *et al.* 1998).

RNA Isolation. Cells were grown at 30°C in rich medium (YPD) to A_{600} of 0.8. RNA was extracted from fifteen A_{600} units of cells using the hot acid-phenol and chloroform method (COLLART and OLIVIERO 2001). Briefly, cells were incubated in TES buffer (10mM Tris HCl pH 7.5, 10mM EDTA, 0.5% SDS) and citrate-saturated phenol (pH 4.3) for 1 h at 65°C, and vortexed every 10 minutes. RNA was isolated from lysed cells with two rounds of phenol-chloroform extraction, pelleted, then resuspended in RNase-free water and treated with DNase I (Roche) to digest genomic DNA. A final round of phenol-chloroform extraction was performed prior to library preparation and/or cDNA synthesis.

RNA Library Preparation and Sequencing. Paired-end sequencing was performed to accurately assign reads. 100bp paired-end RNA-Seq libraries were prepared using the Illumina TruSeq Stranded mRNA sequencing kit with 4ug of total RNA as starting material, as described in the TruSeq Stranded mRNA sequencing kit protocol. Libraries were quantified using a Bioanalyzer (Agilent) and sequenced on an Illumina HiSeq 2000 machine. Reads have been deposited under accession number SRP055208. Telomeric regions that contributed multi-mapping (or non-uniquely mapping reads) are shown in Figure 2.1.

TABLE 2.1 Yeast Strains Used in Chapter 2

Name	Genotype	Source
JRY9316	*matΔ::HygMX can1-100 his3-11 leu2-3,112 lys2- trp1-1 ura3-52*	TEYTELMAN *et al.* 2013
JRY9720	*matΔ::HygMX can1-100 his3-11 leu2-3,112 lys2- trp1-1 ura3-52 sir2Δ::KanMX*	This study
JRY9721	*matΔ::HygMX can1-100 his3-11 leu2-3,112 lys2- trp1-1 ura3-52 sir2Δ::KanMX*	This study
JRY9722	*matΔ::HygMX can1-100 his3-11 leu2-3,112 lys2- trp1-1 ura3-52 sir2Δ::KanMX*	This study
JRY9723	*matΔ::HygMX can1-100 his3-11 leu2-3,112 lys2- trp1-1 ura3-52 sir3Δ::KanMX*	This study
JRY9724	*matΔ::HygMX can1-100 his3-11 leu2-3,112 lys2- trp1-1 ura3-52 sir3Δ::KanMX*	This study
JRY9725	*matΔ::HygMX can1-100 his3-11 leu2-3,112 lys2- trp1-1 ura3-52 sir3Δ::KanMX*	This study
JRY9726	*matΔ::HygMX can1-100 his3-11 leu2-3,112 lys2- trp1-1 ura3-52 sir4Δ::KanMX*	This study
JRY9727	*matΔ::HygMX can1-100 his3-11 leu2-3,112 lys2- trp1-1 ura3-52 sir4Δ::KanMX*	This study
JRY9728	*matΔ::HygMX can1-100 his3-11 leu2-3,112 lys2- trp1-1 ura3-52 sir4Δ::KanMX*	This study
JRY9741	*matΔ::HygMX can1-100 his3-11 leu2-3,112 lys2- trp1-1 ura3-52 sir2Δ::KanMX hmlΔ::SpHIS5MX*	This study

TABLE 2.2 Percent Reads Mapped of RNA-Seq Data

Strain	Alias	Replicate	Total Reads	Reads Mapped	% Reads Mapped	% Mapped Non-uniquely
JRY9316	Wild type	A	15,747,860	14,480,231	92	6.94
JRY9316	Wild type	B	20,204,590	18,636,063	92	6.76
JRY9316	Wild type	C	19,988,764	18,323,263	91.7	8.98
JRY9720	*sir2Δ*	A	13,176,140	12,290,225	93	7.58
JRY9721	*sir2Δ*	B	13,865,402	12,737,081	92	6.10
JRY9722	*sir2Δ*	C	12,505,868	11,519,936	92.1	6.71
JRY9723	*sir3Δ*	A	19,925,570	18,454,658	92.6	6.8
JRY9724	*sir3Δ*	B	20,806,146	19,352,189	93	6.45
JRY9725	*sir3Δ*	C	19,655,418	18,102,386	92.1	6.43
JRY9726	*sir4Δ*	A	14,217,780	12,973,038	91	5.51
JRY9727	*sir4Δ*	B	15,272,748	14,043,542	92	6.20
JRY9728	*sir4Δ*	C	13,785,048	12,561,860	91	5.85

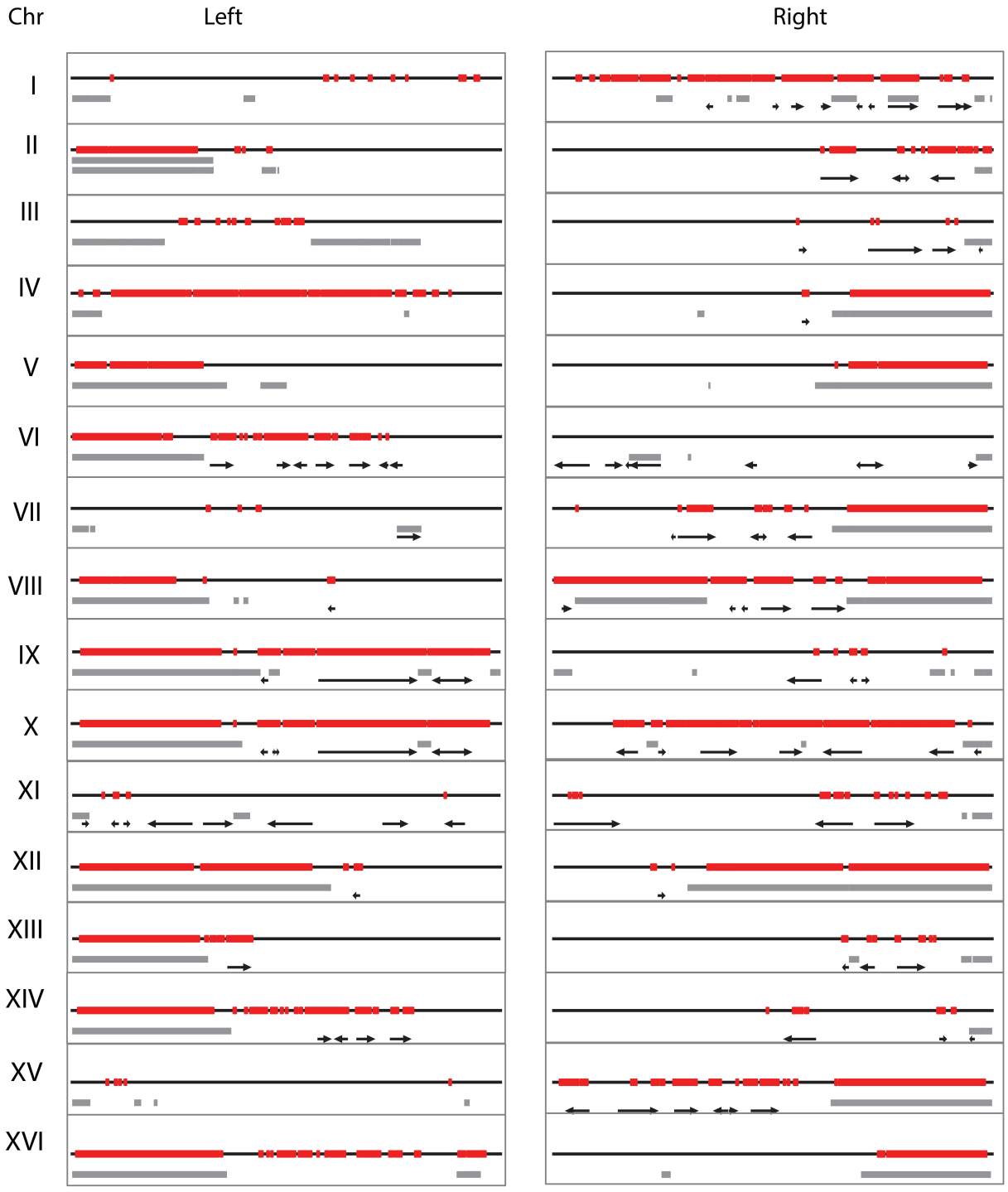

Figure 2.1. Positions of non-uniquely mapping reads across all thirty-two telomeres from RNA-Seq experiments. Shown in red are regions of all thirty-two telomeres that contribute non-non-uniquely mapping reads in RNA-Seq experiments. Positions of annotated Y' elements, Ty δ elements, telomeric repeats, and X elements are shown in gray boxes. Black arrows depict ORFs.

Quantitative Reverse Transcriptase-PCR (qRT-PCR) analysis. cDNA was prepared from 2ug total RNA using the Superscript III Reverse transcriptase kit (Invitrogen). qRT-PCR was performed using the SYBR Green real-time PCR master mix (Thermofisher) and was quantified using the Stratagene MX3000 quantitative PCR system. Standard curves were generated from wild type and from a *sir2Δ* strain, and all expression values were normalized to *ACT1*. Values shown are the average of three biological replicates. Error bars reflect standard error. Two-tailed Student's t-test was performed to evaluate significance of observed differences in expression. Oligos used are listed in Table 2.3.

TABLE 2.3 Oligos Used in qRT-PCR Expression Analysis

Gene	Forward	Reverse
ACT1	ggcatcataccttctacaacg	ctaccggaagagtacaaggacaaaac
STE14	gaagaccaagaaggagtccg	gtagctgagtgccaattgcc
TOS1	gccaagtgacaccagcggttct	ttggccgtcatggatgtgtgag
AXL2	acggaatcactcccacaacaatgtc	ggtcttctgtctggttccatgc
MHF2	tcattgatgaggcggtgctg	cttgatgcgataactctaagggac
STE2	gataggttttatccaggcacgctg	ttgaactcgtaggtgtgggcaactg
HO	gaaatcatgtcgaggctgctg	ccatagcatctagcacatactc
YGL193C	cctttcctatagctccagcg	ccggtcacataaattgacgg
YJL133C-A	tctcaaggatagccgctagc	agggaccatatgtcttggc

Data Analysis

ChIP-Seq Read Mapping. ChIP-Seq reads analyzed were from previous Sir protein ChIP studies (TEYTELMAN *et al.* 2013; THURTLE and RINE 2014b), accession numbers SRP030670 and SRP034921, respectively. Reads were mapped using BWA (LI and DURBIN 2009) to a modified sacCer 2 genome in which the *MAT* locus was replaced with the Hyg-MX cassette. Duplicate reads were removed using Picard (http://picard.sourceforge.net). Due to the repeated sequences shared among telomeres, some reads could not be mapped to specific telomeres. Making the simplifying assumption that all copies of a repeat sequence contributed to the production of sequence reads of that repeat, reads that mapped to repeated sequences were randomly assigned to copies of that repeat, allowing for an estimation of Sir-protein association even at the repetitive elements of the telomeres. However to indicate which reads were accurately mapped and which were inferred, we graphed the percentage of reads within each telomere that did not map uniquely (Figure 2.5). This analysis clearly showed that Y' elements at all telomeres are difficult to distinguish from each other except at positions of polymorphisms unique to individual Y' elements. Additionally, almost the entire 20 kbp region of *TEL01R*, *TEL04L*, *TEL09L*, *TEL10L*, *TEL10R*, *TEL14L*, *TEL15R* and *TEL16L* are not unique. The laboratory strain (derived from W303), which the ChIP-Seq experiments were performed on, had deletions in subtelomeric regions as compared to the S288C reference genome (*TEL07L*, *TEL14R*, and small gaps on *TEL01R* and *TEL13R*). These missing regions in the sequenced strain were indicated in the figures. Reads were mapped to the S288C genome to allow direct reference to the annotated features on *Saccharomyces* Genome Database (SGD). For each sample, per-base-read counts were determined using SAMtools (LI *et al.* 2009). Enrichment was determined as the number of IP reads divided by the number of input reads for that base-pair position.

MACS Peak Calling. MACS peak calling was performed on the default settings except that no model was used to optimize for the broader peaks typical of chromatin-interacting proteins. For each Sir protein chromatin sample, MACS was run on two biological replicates of ChIP-seq data from chromatin sheared by sonication and on a third sample for each Sir protein in which the chromatin sample was prepared by enzymatic digestion with MNase (THURTLE and RINE 2014b). For each chromatin sample analyzed with MACS, the IP sample was the "treatment" and the input sample was the "control." We defined peaks as reproducible if they were called in at least two of the three datasets, as noted in Table S1.

RNA-Seq. Reads were mapped using Tophat2 and per-gene transcript quantification was performed using Cufflinks and reported as "Fragments Per Kilobase per Million Reads," or FPKM (TRAPNELL *et al.* 2009, 2012). Genome-wide RNA read pileups per base pair were calculated using SAMtools (LI *et al.* 2009). The *DESeq* pipeline was used to perform differential gene expression analysis as outlined in the following steps: (1) First, raw read counts per gene were determined using htseq-count, which discards multi-mapped paired-end read fragments (ANDERS and HUBER 2010); therefore, only uniquely mapped reads were included in tests for differential expression of genes; (2) Read counts were normalized and subjected to differential expression analysis using the DESeq package in *R* (ANDERS and HUBER 2013). Genes that showed statistically-significant differences in expression of 2-fold or greater relative to wild type with a p-value of < 0.05 and a false-discovery rate of $< 10\%$ were included in the final list of candidate genes under *SIR2/3/4* repression or as possible haploid-specific genes.

Comparison of Transcription at Telomeres vs. Non-telomeric Loci. Genes were classified as either falling within ("telomeric") or not falling within ("non-telomeric") 20 kbp of a chromosome end, resulting in two distributions of FPKM values. A Wilcoxon rank-sums test was performed to compare the "telomeric" versus "non-telomeric" distributions.
MEME Analysis. The MAST program within the MEME package was used to scan the coding sequence, plus and minus 1000 base pairs, for a1/α2 and α2/Mcm1 binding sites in candidate haploid-specific genes (BAILEY *et al.* 2009). Results were filtered for E-values < 10.

Scanning Motif Binding Sites on The Yeast Transcription Factor Specificity Compendium. The Binding Site Genome Browser (http://nbrowse.ccbr.utoronto.ca/mgb2/gbrowse/yetfasco/) was used to search for a1/α2 and α2/Mcm1 binding sites within 1 kbp of each candidate gene. All a1/α2 and α2 binding sites with a score > 80% of the motif's maximum position-weighted matrix-score threshold were noted.

2.4 Results

2.4.1 Sir Proteins Associated at Discrete Positions at Natural Telomeres

To investigate Sir protein association at the 32 natural telomeres of *S. cerevisiae*, we analyzed ChIP-Seq datasets in the 20 kbp subtelomeric region of Myc-tagged Sir2, Sir3, Sir4 from our previous Sir ChIP-Seq studies (THURTLE and RINE 2014b) (Figure 2.2). Additionally, we analyzed ChIP-Seq datasets for green fluorescent protein endowed with a nuclear localization

signal (GFP-NLS) and a no-tag sample immunoprecipitated with the Myc antibody as controls for artifacts of ChIP-Seq analyses and non-specific enrichment, respectively (TEYTELMAN *et al.* 2013) (Figure 2.3, Figure 2.4). The telomeric regions are difficult to analyze due to their repetitive nature and incomplete sequencing at some of the telomere ends. Thus we made simplifying assumptions about ambiguously mapped reads as outlined in the Materials and Methods and supplement (Figure 2.5). The peaks at *TEL05L* and *TEL14L* chromosomes, for example, for which no telomeric repeats are annotated, presumably arose from ChIP-Seq reads that extended from telomeric repeats into sufficiently unique flanking sequences to allow mapping. Where the telomerase-generated repeats are present, the Rap1-protein binding sites embedded in those repeats were presumably responsible for the Sir-protein enrichment at those positions (e.g. *TEL08R* and *TEL08L*). Most strikingly, at the 32 natural telomeres the enrichment patterns of the three Sir-protein complex members were highly similar, illustrating both the remarkable degree of reproducibility of the enrichment patterns as well as the discontinuous nature of the Sir protein enrichments at each and every telomere (Figure 2.2). There was no evidence of a gradient of Sir proteins, as envisioned by early models of telomere position effect (HECHT *et al.* 1996). The discontinuous distribution of Sir proteins has previously been reported for specific telomeres (ZILL *et al.* 2010; THURTLE and RINE 2014b). Overall this analysis clearly established the generality of the discrete nature of Sir protein association at all 32 telomeres.

To provide a statistical evaluation of the Sir2, Sir3 and Sir4 peaks detected by eye, we called peaks of significant enrichment with MACS using the default p-value cutoff of .00001 (ZHANG *et al.* 2008). To control for non-specific enrichment we also called peaks of enrichment with MACS on a ChIP-Seq dataset from a heterologous protein control, GFP-NLS. For the GFP-NLS, only one small region on the *TEL02L* (base-pair positions 8824-10250) showed overlapping enrichment with Sir protein peaks. Thus, the Sir protein peak was adjusted to account for this non-specific enrichment. Otherwise, non-specific enrichment from highly expressed transcripts did not confound the ChIP enrichment at telomeres, in contrast to other places in the genome (TEYTELMAN *et al.* 2013). As determined by the MACS peak calling, all but five of the thirty-two yeast telomere X elements exhibited significant enrichment of Sir proteins (Table 2.4). For those five telomeres in which MACS did not identify a peak (*TEL1R, TEL2R, TEL10R, TEL13R, TEL14R*), there appeared to be ample enrichment by eye (Figure 2.2). All five of these telomeres were X-only telomeres in which the enrichment abutted the end of the chromosome, possibly resulting in MACS not calling the peak due to its abrupt end and the presence of repetitive sequence. Hence, Sir-protein enrichment appeared to be a property of all, or nearly all, X-elements. For 15 out of the 19 X-Y' telomeres, MACS positioned the peak of Sir protein enrichment as extending all the way from the chromosome end to the internal X element, spanning the entire Y' element (Table 2.4). To determine if there was actually detectable Sir-protein enrichment within the Y' element, or whether these large peaks called were due to the proximity of two distinct peaks, we calculated the average enrichment (IP/Input) for all the X elements and all the Y' elements for Sir2, Sir3 and Sir4 (Figure 2.6). For the three Sir proteins, the average X element enrichment was 4-fold for Sir2 and 8-fold for Sir3 and Sir4. In contrast, the Y' elements all showed IP/Input values less than 1 for all three Sir proteins, indicating that the IP values for this region were all below background. Thus, as reported previously for specific telomeres (ZHU and GUSTAFSSON 2009; ZILL *et al.* 2010; TAKAHASHI *et al.* 2011; THURTLE and RINE 2014b), the Y' elements did not exhibit any Sir-protein enrichment. In summary, Sir proteins showed the highest level of association at the core X element with average enrichment values between 4.5 to 8.2 for the three Sir proteins, where ORC and Abf1 bind, whether at an X-

element-only telomere or an X-Y' telomere (Figure 1 and Figure S4).

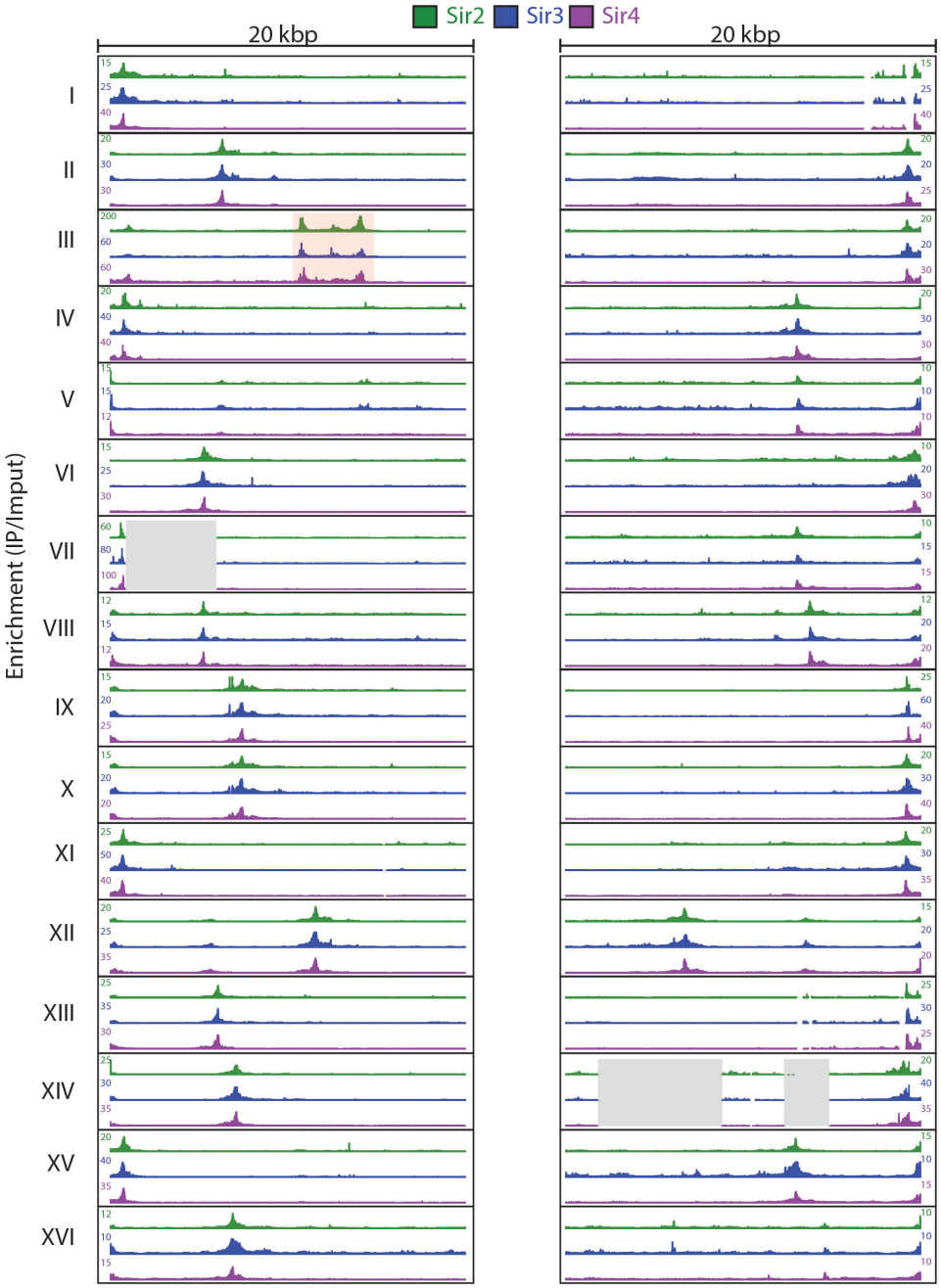

Figure 2.2. Sir2, Sir3 and Sir4 enrichment at all thirty-two yeast telomeres. ChIP-Seq of Myc-tagged Sir2, Sir3 and Sir4 was analyzed at all yeast telomeres. The left side shows the first 20 kbp of each chromosome and the right side shows the last 20 kbp of each chromosome. IP/Input enrichment values for Sir2 (green), Sir3 (blue) and Sir4 (green) are shown for each telomere. On chromosome III, *HML* is boxed in red, and regions absent in the sequenced W303 strain relative to the S288C sacCer2 genome are represented by a grey shaded box.

TABLE 2.4 ChIP-Seq Peaks Called with MACS

MACS was used to call peaks of significant enrichment for the Sir protein ChIP-Seq datasets. The "Sir" column indicates the Sir protein dataset (either Sir2, Sir3 or Sir4) that the peak was identified in. The start and end coordinates indicate the chromosomal coordinate of the peak as identified by MACS. A "yes" in columns 5-7 indicate that the peak was detected in that dataset for the particular Sir protein and a "No" indicates that the peak was not called in that dataset. The "Genome Features" column indicates the genome features within the starting and ending coordinates of the peak as annotated in SGD.

Sir	Telomere	start	end	Sonication Replicate 1	Sonication Replicate 2	MNase	Genome Features
Sir2	*TEL01-L*	1	3165	Yes	Yes	Yes	TR, X element, *PAU8*
Sir3	*TEL01-L*	1	3204	Yes	Yes	Yes	TR, X element, *PAU8*
Sir4	*TEL01-L*	1	3211	Yes	Yes	Yes	TR, X element, *PAU8*
Sir2	*TEL01-L*	1	1905	No	Yes	Yes	Y'
Sir3	*TEL02-L*	1	8824	No	Yes	Yes	X-Y', *PAU9*
Sir4	*TEL02-L*	1	8824	Yes	Yes	Yes	X-Y', *PAU9*
Sir2	*TEL02-L*	4924	8824	Yes	Yes	Yes	X element, *PAU9*
Sir2	*TEL03-L*	1	18568	Yes	Yes	Yes	TR, X element, *YCL076W, YCL075W, YCL074W, GEX1, VBA3, YCL068C, YCL065W, HML, CHA1*
Sir3	*TEL03-L*	1	18622	Yes	Yes	Yes	TR, X element, *YCL076W, YCL075W, YCL074W, GEX1, VBA3, YCL068C, YCL065W, HML, CHA1*
Sir4	*TEL03-L*	1	15202	Yes	Yes	Yes	TR, X element, *YCL076W, YCL075W, YCL074W, GEX1, VBA3, YCL068C, YCL065W, HML*
Sir4	*TEL03-L*	15460	18178	Yes	Yes	Yes	*HML*
Sir4	*TEL03-R*	312518	315021	Yes	Yes	Yes	TR, X element
Sir2	*TEL03-R*	313064	315102	Yes	Yes	Yes	TR, X element
Sir2	*TEL04-L*	1	1725	Yes	Yes	Yes	TR, X element
Sir3	*TEL04-L*	1	1800	Yes	Yes	Yes	TR, X element
Sir4	*TEL04-L*	1	1731	Yes	Yes	Yes	TR, X element
Sir4	*TEL04-R*	1521508	1525877	No	Yes	Yes	X element,

							PAU10
Sir3	*TEL04-R*	1522260	1526289	Yes	Yes	Yes	X element, *PAU10*
Sir2	*TEL04-R*	1522281	1526268	Yes	Yes	Yes	X element, *PAU10*
Sir3	*TEL04-R*	1526513	1529507	No	Yes	Yes	Y'
Sir2	*TEL09-L*	1	5882	Yes	Yes	Yes	Y'
Sir3	*TEL09-L*	1	5999	Yes	Yes	Yes	Y'
Sir4	*TEL09-L*	1	7027	Yes	Yes	Yes	Y'
Sir2	*TEL09-L*	6054	9980	Yes	Yes	Yes	X element, *PAU14*
Sir3	*TEL09-L*	6057	10087	Yes	Yes	Yes	X element, *PAU14*
Sir4	*TEL09-L*	7049	9980	Yes	Yes	Yes	X element, *PAU14*
Sir4	*TEL09-L*	16947	18692	No	Yes	Yes	IMA3
Sir4	*TEL09-R*	437481	439152	No	Yes	Yes	X element
Sir2	*TEL09-R*	437501	439339	No	Yes	Yes	X element
Sir2	*TEL05-L*	1	7618	Yes	Yes	Yes	X-Y'
Sir3	*TEL05-L*	1	7804	Yes	Yes	Yes	X-Y'
Sir4	*TEL05-L*	1	7826	Yes	No	Yes	X-Y'
Sir4	*TEL05-R*	567524	571291	No	Yes	Yes	X element
Sir2	*TEL05-R*	568755	571249	No	Yes	Yes	X element
Sir3	*TEL05-R*	568818	571793	No	Yes	Yes	X element
Sir4	*TEL06-L*	1	7113	Yes	Yes	Yes	X-Y', *YFL063W, COS4, YFL058W*
Sir3	*TEL06-L*	1	7067	No	Yes	Yes	X-Y', *YFL063W, COS4, YFL058W*
Sir2	*TEL06-L*	374	8410	No	Yes	Yes	X-Y', *YFL063W, COS4, YFL058W*
Sir4	*TEL06-R*	263978	265355	Yes	Yes	No	*IRC7*
Sir3	*TEL06-R*	263993	265339	Yes	Yes	Yes	*IRC7*
Sir2	*TEL06-R*	264026	265321	Yes	No	Yes	*IRC7*
Sir3	*TEL07-L*	1	875	Yes	Yes	No	TR, X-element
Sir4	*TEL07-R*	1081144	1083523	No	Yes	Yes	*COS6*
Sir2	*TEL07-R*	1082655	1085210	Yes	Yes	Yes	X element
Sir3	*TEL07-R*	1083258	1085832	No	Yes	Yes	X element
Sir3	*TEL07-R*	1085851	1087178	No	Yes	Yes	Y'
Sir2	*TEL08-L*	1	2478	Yes	Yes	Yes	X element
Sir3	*TEL08-L*	1	2476	Yes	Yes	Yes	X element
Sir4	*TEL08-L*	1	6631	Yes	Yes	Yes	X-Y'
Sir3	*TEL08-L*	4505	6572	No	Yes	Yes	X element
Sir2	*TEL08-L*	4521	6542	Yes	Yes	Yes	X element
Sir4	*TEL08-R*	552041	558152	Yes	Yes	No	X element, Y', *IMD2*
Sir3	*TEL08-R*	552750	562261	No	Yes	Yes	X element, Y',

							IMD2
Sir2	*TEL08-R*	552885	557851	Yes	Yes	Yes	X element, Y', *IMD2*
Sir2	*TEL10-L*	1	5942	Yes	Yes	Yes	Y'
Sir3	*TEL10-L*	1	7045	Yes	Yes	Yes	Y'
Sir4	*TEL10-L*	1	10006	Yes	Yes	Yes	X-Y'
Sir4, Y'*L10-L*	*TEL10-L*	6061	9999	Yes	Yes	Yes	X element
Sir3	*TEL10-L*	7070	10068	Yes	Yes	Yes	X element
Sir2	*TEL11-L*	1	3067	Yes	Yes	Yes	TR, X element, *PAU16*
Sir3	*TEL11-L*	1	3107	Yes	Yes	Yes	TR, X element, *PAU16*
Sir4	*TEL11-L*	1	3117	Yes	Yes	Yes	TR, X element, *PAU16*
Sir4	*TEL11-R*	658211	660866	Yes	Yes	Yes	*VBA5*
Sir3	*TEL11-R*	658212	660806	Yes	Yes	Yes	*VBA5*
Sir2	*TEL11-R*	658227	660267	Yes	Yes	Yes	*VBA5*
Sir3	*TEL11-R*	660881	663222	Yes	Yes	No	*GEX2*
Sir2	*TEL11-R*	661907	664824	X	No	Yes	*GEX2*
Sir3	*TEL12-L*	1	4543	No	Yes	Yes	Y'
Sir2	*TEL12-L*	1	4537	Yes	Yes	Yes	Y'
Sir4	*TEL12-L*	1	14200	Yes	Yes	Yes	X-Y'
Sir3	*TEL12-L*	4752	10100	Yes	Yes	Yes	X-Y'
Sir2	*TEL12-L*	4786	10091	Yes	Yes	Yes	X-Y'
Sir3	*TEL12-L*	10354	14187	No	Yes	Yes	X-Y'
Sir2	*TEL12-L*	10392	14195	Yes	Yes	Yes	X-Y'
Sir3	*TEL12-R*	1061965	1066024	No	Yes	Yes	X element, *PAU4*
Sir4	*TEL12-R*	1061988	1072866	Yes	Yes	No	X element, *PAU4*
Sir2	*TEL12-R*	1062036	1066015	Yes	Yes	Yes	X element, *PAU4*
Sir3	*TEL12-R*	1066129	1072549	No	Yes	Yes	Y'
Sir2	*TEL12-R*	1066155	1072450	Yes	Yes	Yes	Y'
Sir3	*TEL12-R*	1072672	1077188	No	Yes	Yes	Y'
Sir2	*TEL13-L*	1	4459	Yes	Yes	Yes	Y'
Sir3	*TEL13-L*	1	4429	Yes	Yes	Yes	Y'
Sir4	*TEL13-L*	1	7494	Yes	Yes	Yes	X-Y'
Sir3	*TEL13-L*	4617	7435	Yes	Yes	Yes	X element
Sir2	*TEL13-L*	4658	7401	Yes	Yes	Yes	X element
Sir2	*TEL14-L*	1	5012	Yes	Yes	Yes	Y'
Sir3	*TEL14-L*	1	5265	No	Yes	Yes	Y'
Sir4	*TEL14-L*	1	8603	Yes	Yes	Yes	X-Y'
Sir2	*TEL14-L*	5748	8491	Yes	Yes	Yes	X element
Sir3	*TEL14-L*	5748	8575	Yes	Yes	Yes	X element

Sir2	*TEL15-L*	1	2868	Yes	Yes	Yes	X element, *AAD15*
Sir4	*TEL15-L*	1	2883	Yes	Yes	Yes	X element, *AAD15*
Sir3	*TEL15-L*	1	2924	Yes	Yes	Yes	X element, *AAD15*
Sir4	*TEL15-L*	10818	12699	Yes	Yes	No	*PAU20*
Sir3	*TEL15-L*	10840	12798	Yes	Yes	No	*PAU20*
Sir3	*TEL15-R*	1082035	1085505	No	Yes	Yes	X element, *PAU21*
Sir2	*TEL15-R*	1082045	1085443	Yes	Yes	Yes	X element, *PAU21*
Sir3	*TEL15-R*	1085649	1090020	No	Yes	Yes	Y'
Sir2	*TEL16-L*	1	4519	Yes	Yes	Yes	Y'
Sir3	*TEL16-L*	1	5215	No	Yes	Yes	Y'
Sir4	*TEL16-L*	1	8760	Yes	Yes	Yes	Y'
Sir2	*TEL16-L*	5594	9094	Yes	Yes	Yes	X element
Sir3	*TEL16-L*	5648	9097	No	Yes	Yes	X element
Sir3	*TEL16-R*	941574	945387	No	Yes	Yes	X element
Sir2	*TEL16-R*	942173	944929	No	Yes	Yes	X element
Sir2	*TEL16-R*	945624	947502	No	Yes	Yes	Y'

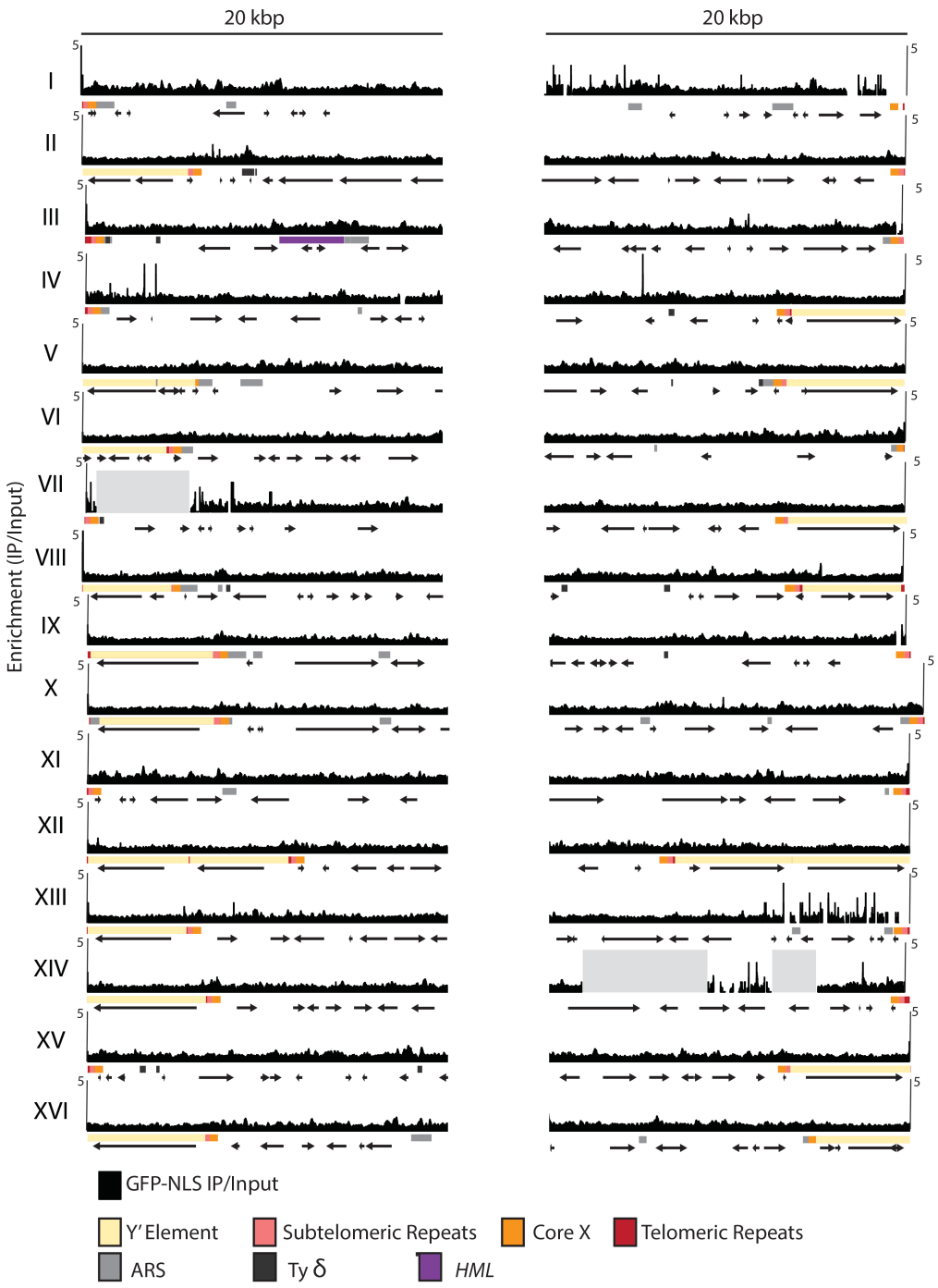

Figure 2.3. GFP-NLS ChIP-Seq control at all thirty-two yeast telomeres. The IP/Input enrichment values of the GFP-NLS ChIP-Seq dataset from (TEYTELMAN *et al.* 2013) was mapped at all thirty-two *S. cerevisiae* telomeres. 20 kbp for each telomere is shown. Salient features as annotated in SGD are indicated below the X-axis for each telomere. The light gray rectangles indicate regions deleted in the sequenced W303 derived lab strain relative to the SGD sacCer2 reference genome.

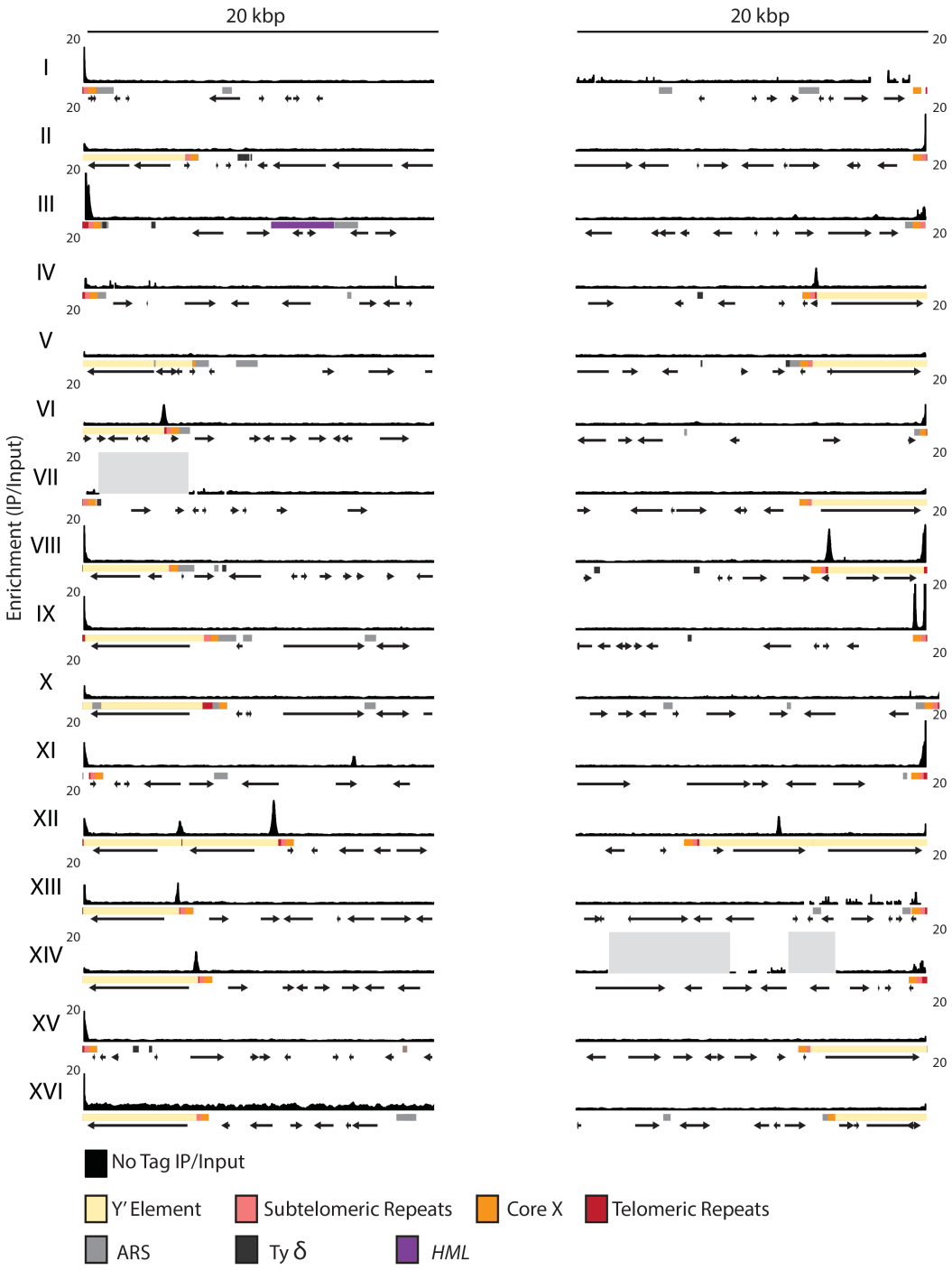

Figure 2.4. No tag ChIP-Seq control at all thirty-two yeast telomeres. The IP/Input enrichment values of the no tag ChIP-Seq dataset from (THURTLE and RINE 2014a) was mapped at all thirty-two *S. cerevisiae* telomeres. 20 kbp for each telomere is shown. Salient features as annotated in SGD are indicated below the X-axis for each telomere as in Figure 2.3. The light gray rectangles indicate regions deleted in the sequenced W303 derived lab strain relative to the SGD sacCer2 reference genome.

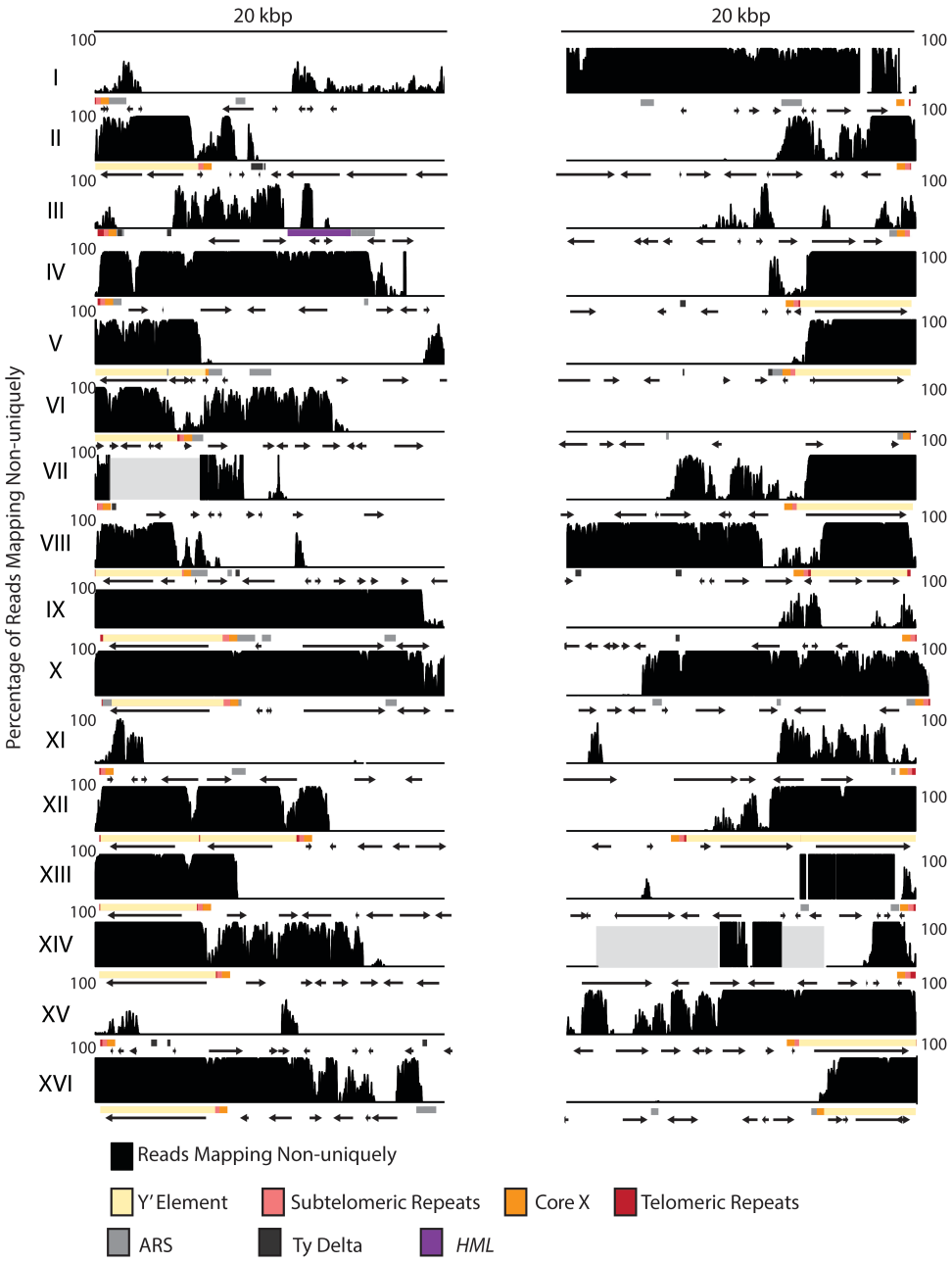

Figure 2.5. Percentage of non-uniquely mapping reads from ChIP-Seq experiments at all thirty-two telomeres. Reads that mapped non-uniquely in the Sir4 input dataset from (THURTLE and RINE 2014) were determined by those reads with a MAPQ flag of 0. The number of reads that mapped non-uniquely at that base-pair position was determined and divided by the total number of reads that mapped at that position. This percentage of non-uniquely mapped reads was plotted for each telomere. 20 kbp for each telomere is shown. Salient features as annotated in SGD are indicated below the X-axis for each telomere as in Figure 2.3. The light gray rectangles indicate regions deleted in the sequenced W303 derived lab strain relative to the SGD sacCer2 reference genome.

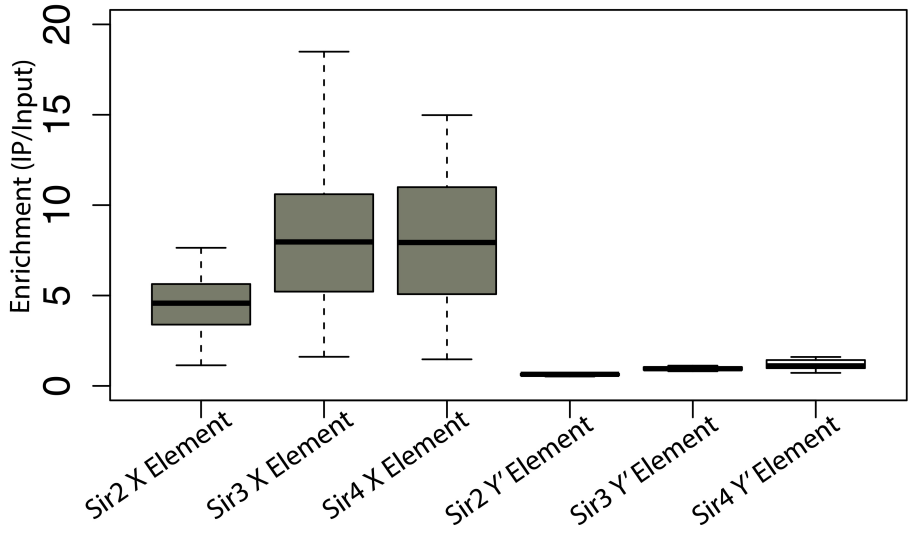

Figure 2.6. Sir proteins are not enriched at Y' elements. Average enrichment for all annotated X elements and Y' elements was calculated for all three Sir proteins. Enrichment was determined by the average IP/Input for that sample for the X elements and Y' elements for each chromosome as defined in SGD.

2.4.2 Catalytic Activity of Sir2 at Telomeres

To determine if positions of H4K16 hypoacetylation overlapped with Sir2 distribution at telomeres, we analyzed ChIP-Seq of H4K16-acetyl, and compared Sir2 ChIP-Seq profiles at all 32 telomeres to the H4K16-acetyl ChIP-Seq profiles (Figure 2.7). H4K16 was hypoacetylated in regions slightly larger than the X element, with the lowest levels of H4K16-acetyl at the core X sequence. Additionally, X-Y' telomeres showed a variable amount of H4K16-hypoacetylation within the Y' region. We also observed regions of H4K16-hypoacetylation without detectable Sir2 association, which presumably reflected the action of a different histone deacetylase such as Rpd3 or Hst1. Both have been shown to associate with subtelomeric chromatin (KURDISTANI *et al.* 2002; EHRENTRAUT *et al.* 2010; LI *et al.* 2013). Alternatively, the hypoacetylation of H4K16 in these regions could be due to transient Sir2 association not captured by ChIP-Seq. Previous studies have shown that Sir2, but not Sir3 or Sir4, controls some origins of replication (PAPPAS *et al.* 2004; CRAMPTON *et al.* 2008; YOSHIDA *et al.* 2014). However MACS did not detect any significant enrichment for Sir2 at subtelomeric ARSs outside of the core X element.

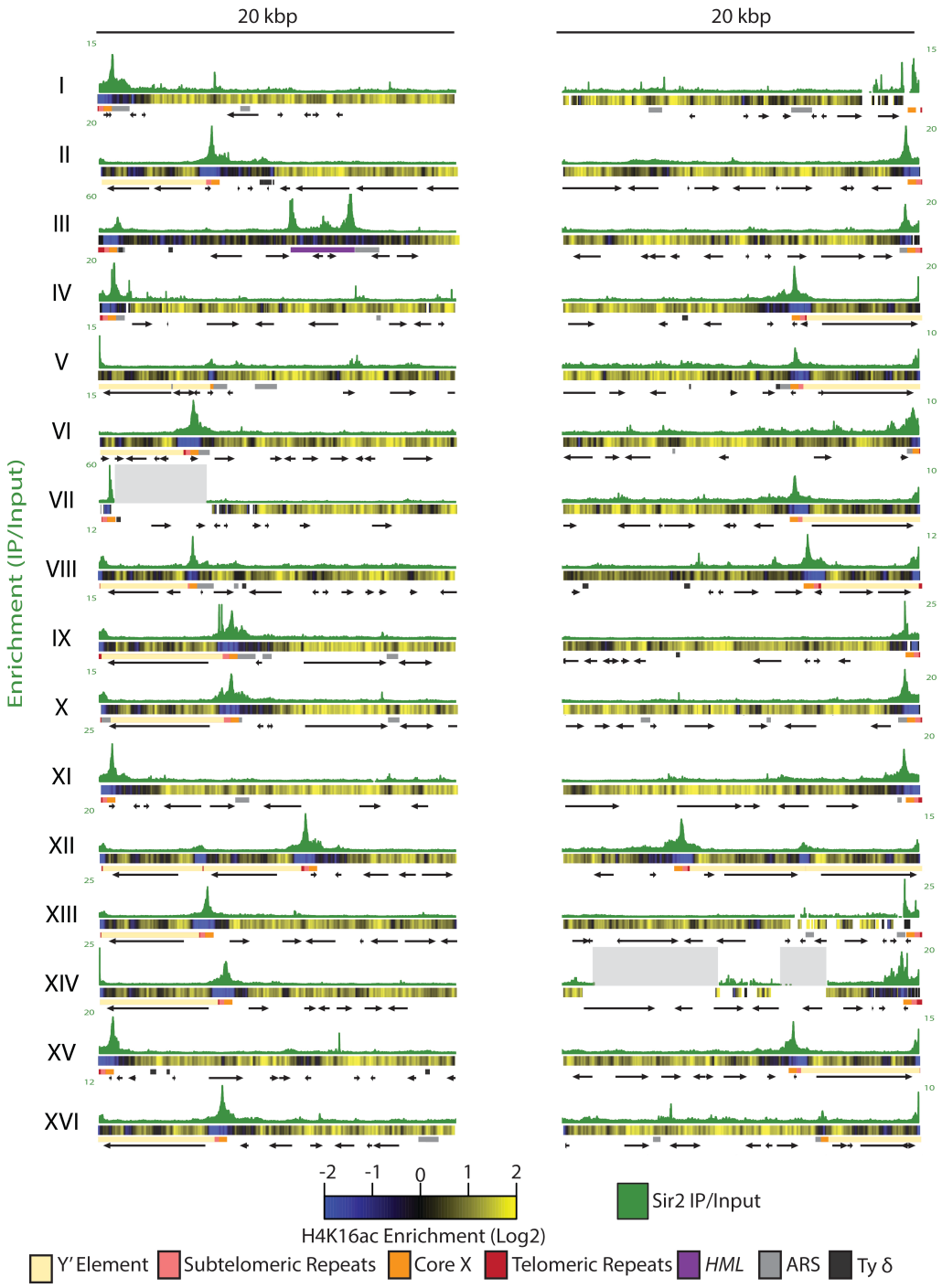

Figure 2.7. H4K16 exhibited hypoacetylation in regions greater than Sir2 protein association. Sir2 enrichment is shown for each telomere as the IP/input for that base-pair position. Below the Sir2 enrichment track for each telomere is a heat map representing the Log2 of H4K16 IP/input. Blue represents regions of hypoacetylation where the IP value is below the input value and yellow represents IP/input values greater than 1, which indicates acetylated regions. Salient features for each telomere are shown: telomeric repeats are red boxes, subtelomeric repeats as pink boxes, the core X as orange boxes and *HML* as a dark purple

rectangle. Origins of replication and Ty δ elements are marked in light grey and dark grey, respectively. Open reading frames are represented by black arrows. All features were mapped as annotated in SGD.

The deacetylation of H4K16-acetyl by Sir2 is thought to be key for the spreading of Sir proteins (HECHT *et al.* 1996; RUSCHE *et al.* 2002; HOPPE *et al.* 2002). In the standard model for spreading (reviewed in (RUSCHE *et al.* 2002)), Sir proteins are recruited to nucleation sites through protein interactions between ORC, Abf1 and Rap1, which are bound to DNA, Sir3, and a Sir2-Sir4 dimer. According to the model, Sir2 deacetylates nearby nucleosomes, which creates high-affinity binding sites for Sir3 and Sir4, resulting in the spreading of additional copies of the Sir protein complex. Thus, this model predicts that Sir protein enrichment should be continuously distributed along the length of a telomere. However, the distribution of Sir proteins at the telomeres was discrete (Figure 2.2 and Figure 2.7) and therefore not in support of the spreading model. To determine the role of Sir2's catalytic activity in Sir-protein association at the telomeres, Sir3 and Sir4 enrichment was examined at the telomeres in a strain lacking Sir2 catalytic activity (THURTLE and RINE 2014b). As shown for a representative X-only telomere (*TEL15L*) there seemed to be some indications of spreading for Sir3 as the association of Sir3 in the wild-type background extended about 800 bp beyond where Sir3 associated in a strain lacking Sir2 catalytic activity (Figure 2.8). This extended distribution was less prominent for Sir4 at the X-only telomere and both Sir3 and Sir4 at the internal X element of the X-Y' telomere *TEL09L* (Figure 2.8). These results indicate that if Sir complex spreading occurred at telomeres, it did so only to a slight extent. The prominent feature of all telomeres was the overall reduced Sir3 and Sir4 association at the core X in a strain lacking Sir2 catalytic activity, indicating that Sir2's catalytic activity was necessary for the association and/or stability of the Sir-protein complex with ORC and Abf1. Both Sir3 and Sir4 showed enrichment in the telomeric repeats in a strain lacking Sir2 catalytic activity. However, as reported previously (ZILL *et al.* 2010; TEYTELMAN *et al.* 2013), the telomeric repeats showed enrichment in the no-tag ChIP-Seq control sample as well, indicating that the telomeric repeats, whether at the chromosome ends of X-only telomeres or at internal locations at X-Y' telomeres, interact non-specifically with the anti-Myc antibody (Figure 2.4). This interaction seemed to be specific for the Myc antibody, as the GFP-NLS immunoprecipitated with an anti-GFP antibody did not show enrichment at the telomeric repeats (Figure 2.3). It was surprising that the no-tag ChIP-Seq control sample and the Sir3 and Sir4 samples in strains lacking Sir2 catalytic activity indicated greater enrichment at the telomeric repeats than the level of Sir-protein enrichment at the telomeric repeats in wild type. However this apparent greater enrichment may be a consequence of increasing the signal-to-noise ratio: there are less sites with lower amounts of Sir3 and Sir4 enrichment in a strain lacking Sir2 catalytic activity and very little association in the no tag sample; thus, there is more Myc antibody available to associate non-specifically with the telomeric repeats. Overall, Sir2's catalytic activity at telomeres was important for association of the Sir protein complex at the core X nucleation sites and less implicated in the spreading of the Sir complex into subtelomeric regions.

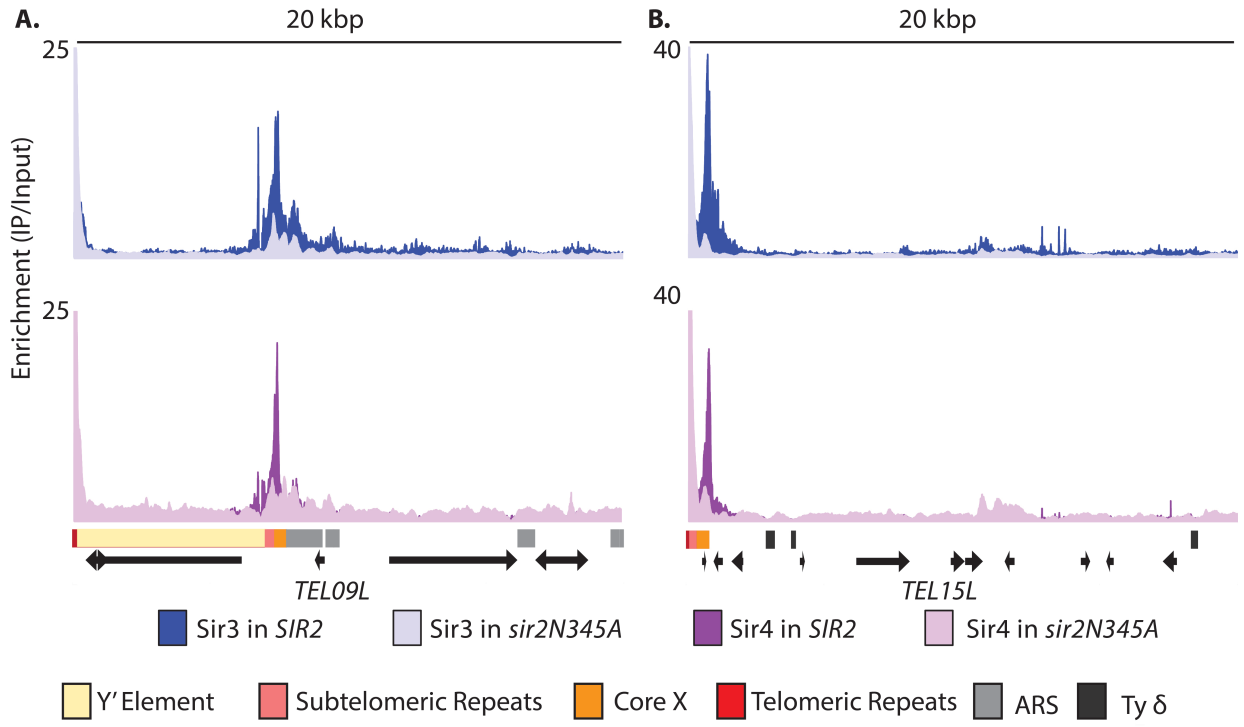

Figure 2.8. Sir3 and Sir4 association in strains lacking Sir2 catalytic activity. ChIP-Seq reads of Myc-tagged Sir3 and Sir4 in a strain expressing a catalytically inactive point mutant *SIR2* allele, *SIR2N345A*, were analyzed at the telomeres. A representative X-Y' telomere is shown in (A), and a representative X-only telomere is shown in (B). The upper panel shows Sir3 association in wild-type *SIR2* (dark blue) and mutant *sir2N345A* background (light blue). The lower panel shows Sir4 association in the wild-type *SIR2* (dark purple) and mutant *sir2N345A* background (light purple). Salient features for each telomere are as in Figure 2.7.

2.4.3 Most *S. cerevisiae* Telomeres Have Expressed Genes

To determine the expression state of all genes at all thirty-two *S. cerevisiae* telomeres, we performed mRNA-Seq on RNA samples from wild-type, *sir2Δ, sir3Δ,* and *sir4Δ* strains. The *MAT* locus, which specifies mating type, was deleted in these strains to allow nearly-complete unambiguous read mapping between the two silent mating-type cassettes, *HMLα* and *HMRa.* Analysis of mRNAs in wild type and in *sir2Δ* across all subtelomeric regions revealed several important generalizations (Figure 2.9; the highly similar results for *sir3Δ* and *sir4Δ* are shown in Figures 2.10 and 2.11). All chromosomes had numerous genes within 20 kbp of the end that were expressed. Transcription occurred within 5 kbp of most ends. Thus there was no evidence supporting widespread Sir-based repression of most genes near telomeres. For the majority of transcripts detected in subtelomeric regions, there was no detectable increase in transcript number in *sir2*Δ relative to wild type. For some loci, transcription increased modestly in *sir2*Δ (ORFs shown in red; genes listed in Table 1).

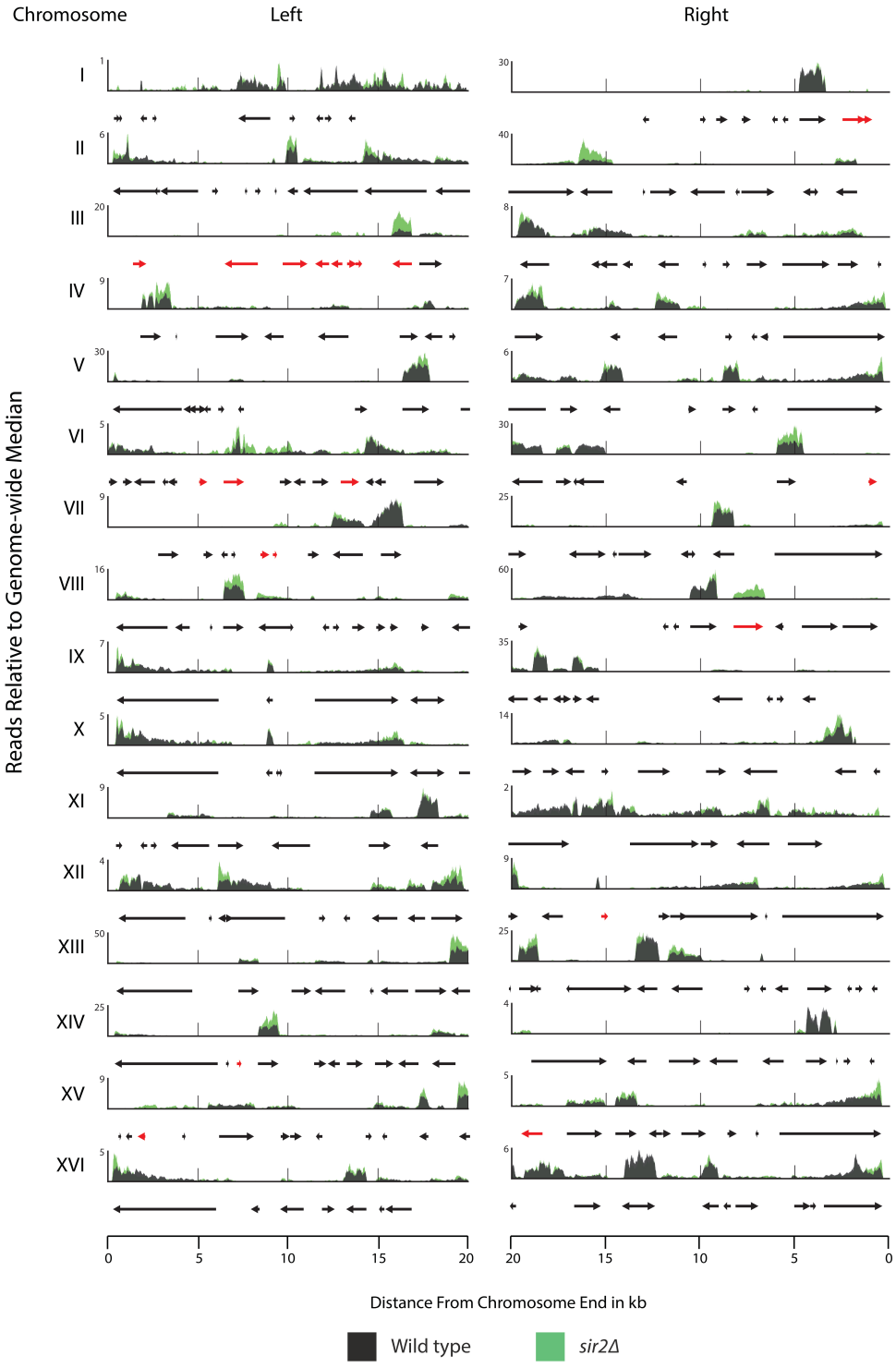

Figure 2.9. Transcription at all thirty-two telomeres in wild type and *sir2Δ*. RNA-seq was performed on wild-type and *sir2Δ* strains. Shown are read pileups from wild type (black) and *sir2Δ* (green). Read pileups are normalized to the median genome-wide coverage and are the average of three biological replicates. Genes that showed a two-fold or greater increase in expression in all three *sir* mutants (*sir2Δ*, *sir3Δ*, and *sir4Δ*) are colored as red arrows. Genes that showed no significant change in expression between wild type and all three *sir* mutants are in black.

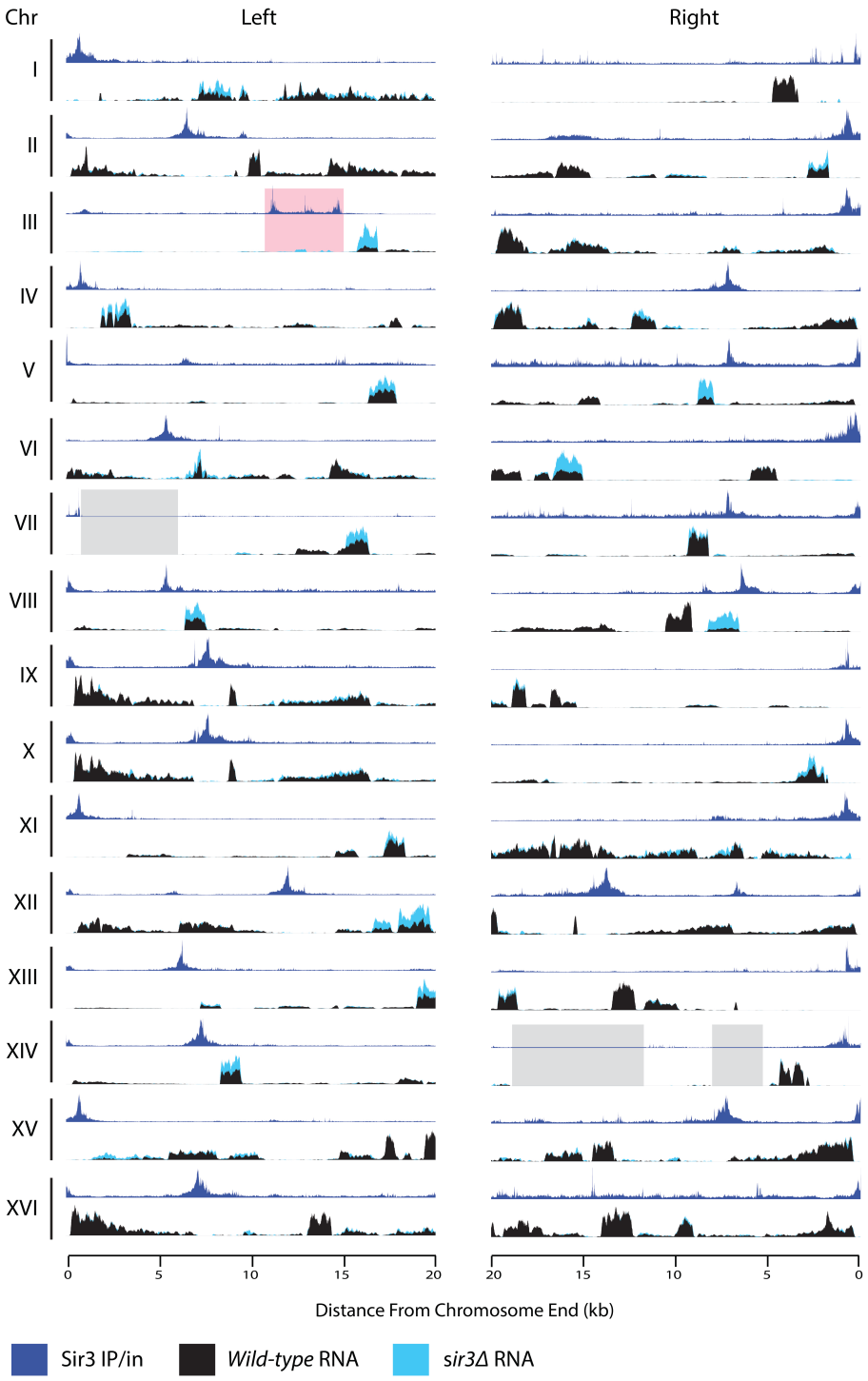

Figure 2.10. A comparison of Sir3 protein association and expression in wild type *sir3Δ*. For each telomere arm, top axis shows Sir3 IP/input (dark blue) and lower axis displays transcription as RNA read pileups in wild type (black) and *sir3Δ* (light blue).

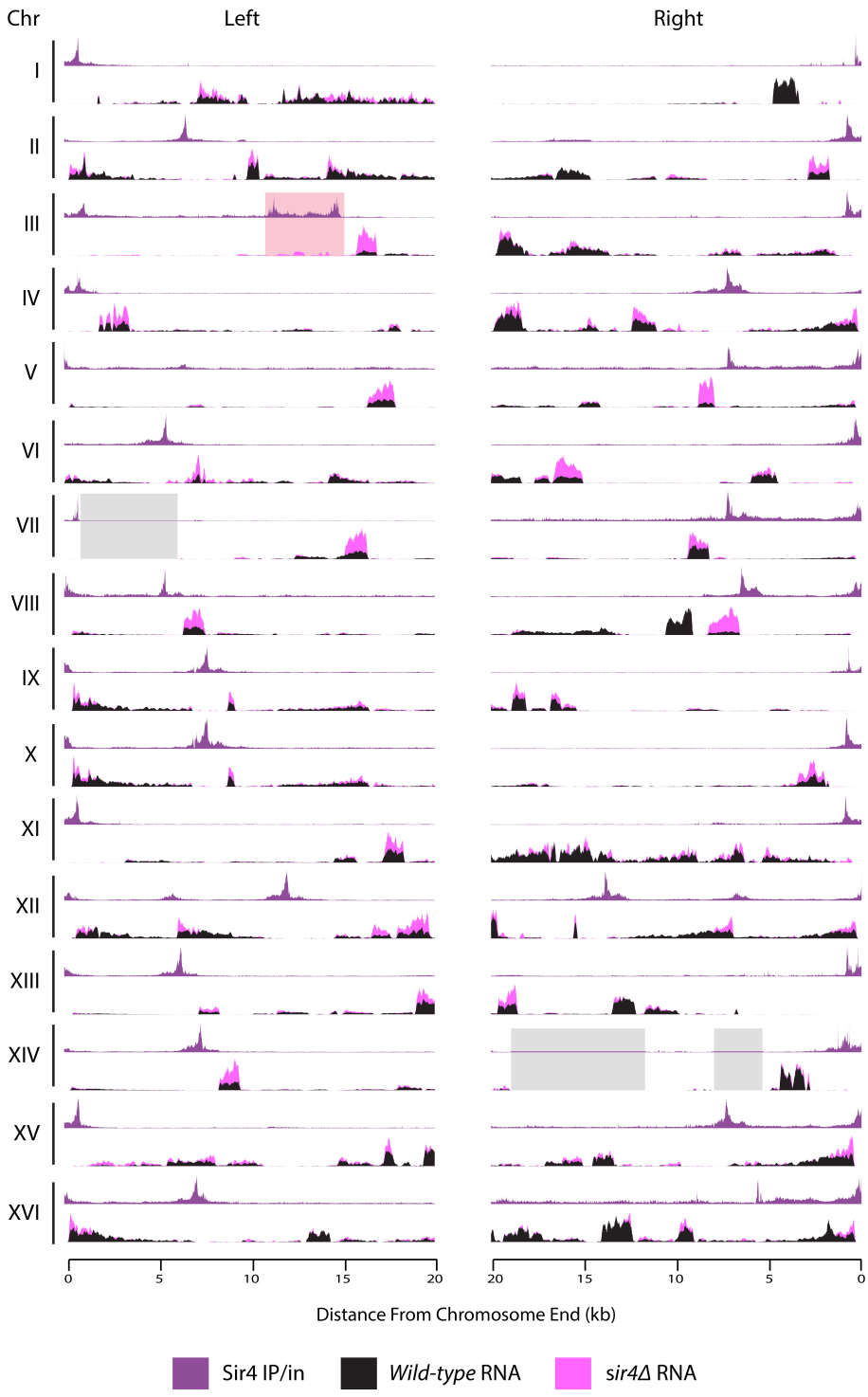

Figure 2.11. Comparison of Sir4 protein association and expression in wild type and *sir4Δ*. For each telomere arm, top axis shows Sir4 IP/input (dark purple) and lower axis shows transcription as RNA read pileups in wild type (black) and *sir4Δ* (pink).

An important and expected exception were *HMLα1* and *HMLα2*; these genes showed a substantial increase in expression in *sir2*Δ (see *TEL03L* 15 kbp from end). Interestingly, repression at *TEL03L* extended approximately 12 kilobases beyond *HMLα* to the end of chromosome III, as all annotated ORFs in this region increased in expression in *sir2*Δ (Table 2.5). Sir2 was found to be enriched across this entire domain as well, along with hypoacetylated H4K16. Thus, the expression status in wild type correlated with these two marks of heterochromatin. This was the only telomere for which there was evidence of a Sir-protein-mediated domain of repression.

2.4.4 Telomeres Produced Significantly Fewer Transcripts Than Non-Telomeric Loci

Once observing transcription at subtelomeric domains, we wanted to determine how transcription at telomeres and subtelomeric domains compared to transcription at non-telomeric loci. Though transcripts were detected from many of the genes at subtelomeric regions, these genes had lower expression levels (FPKM) as compared to non-telomeric genes. We compared the distribution of FPKM values of subtelomeric protein coding genes to non-subtelomeric protein coding genes and found a statistically significant lower level of FPKM values among subtelomeric genes (Figure 2.12). These data corroborate previous subtelomeric transcript quantification in *S. cerevisiae* (WYRICK *et al.* 1999; TEYTELMAN *et al.* 2008). This decreased transcription at telomeres could be attributed, in part, to decreased ORF density at telomeres (LOUIS 1995).

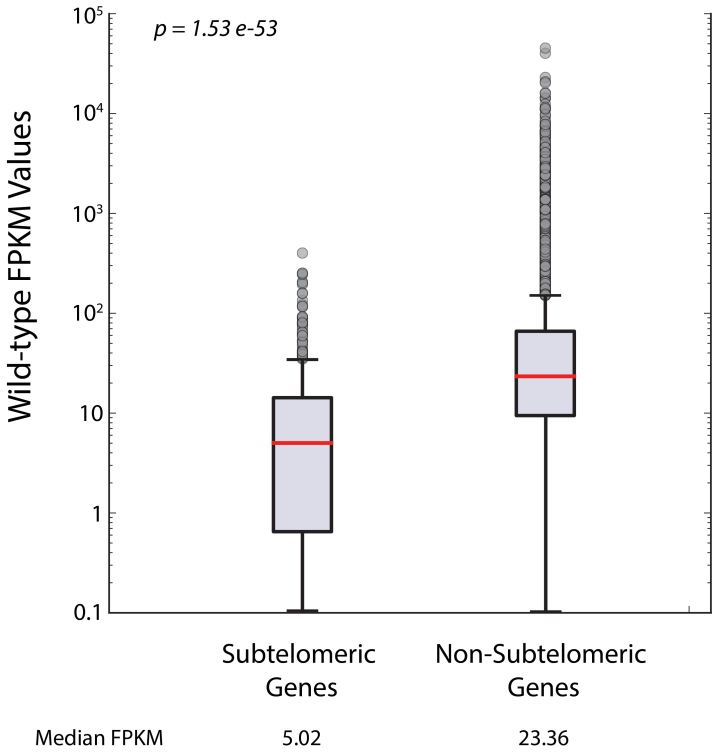

Figure 2.12. FPKM values for subtelomeric genes were significantly lower than FPKM values for non-subtelomeric genes. The distribution in FPKM values of subtelomeric genes was compared to the distribution of FPKM values of non-subtelomeric genes in the wild type genetic background using the Wilcoxon rank sums test. The median FPKM value for subtelomeric genes was 5.02, whereas the median FPKM value for non-subtelomeric genes was 23.4 (p-value = 1.53^{-53}).

2.4.5 Only ~6% Of Subtelomeric Genes Were Silenced by Sir Proteins

To determine the extent to which Sir proteins affect the expression of subtelomeric genes, we performed a differential gene expression analysis using the DESeq package in R (ANDERS and HUBER 2013). Genes showing a statistically-significant difference in expression from wild type (as indicated by a p-value < 0.05), a greater than 2-fold change in expression, and a false discovery rate of less than 10% (to control for the multiple-testing problem) were included in the final list of differentially expressed genes. Using these criteria, forty-two genes appeared to be upregulated in all three *sir* mutants (for a complete list of all statistically significant observed expression changes, see Table S7). In principle, these forty-two genes were expected to fall into either of two categories: (1) genes directly subject to Sir-based repression (for example, genes at *HMLα*, *HMRa*, and subtelomeric regions), and (2) genes normally expressed more highly in a/α diploids as a result of simultaneous *HML* and *HMR* de-repression in *sir* mutants. Of these forty-two genes, twenty-one (50%) were in subtelomeric regions (Table 2.5 and red arrows in Figure 2.9). Of these, thirteen were completely repressed or averaged less that one FPKM among

replicate experiments in wild-type cells. However, even in *sir* mutant conditions, many of these genes had low expression levels, averaging at ~3.8 FPKM (Table 2.5). The remaining genes were expressed from 2 to 6-fold higher in *sir* mutants than in wild type, with some highly expressed even in wild type (e.g. *CHA1* and *HXK1*). A previous study found *BNA1* to increase in *sir2Δ* strains (BERNSTEIN *et al.* 2000); our data did not reproduce this finding.

TABLE 2.5 Subtelomeric Genes Under Sir2/3/4 Repression

Shown below are the expression values in FPKM for the twenty-one subtelomeric genes that increased in expression in *sir2Δ*, *sir3Δ* and *sir4Δ*. *COS6* specifically increased *sir4Δ* and was also associated with a Sir4 ChIP peak. Genes are ordered by chromosome number and map position. FPKM values represent the average of three biological replicates. Distances to nearest Sir peaks were calculated by taking the difference of the midpoint of the gene and the genomic coordinate of the highest nearby Sir protein IP/input enrichment value.

Gene	Systematic Name	Wild type	*sir2Δ*	*sir3Δ*	*sir4Δ*	Distance To Nearest Sir Peak (bp)
IMD1	*YAR073W*	0.1	1.1	1.1	1.1	1575
YAR075W	*YAR075W*	1.6	26	21.9	25	846
YCL076W	*YCL076W*	0	3.3	2.8	3.5	0
YCL075W	*YCL075W*	0	1.9	2.6	2.8	0
YCL074W	*YCL074W*	0	4.5	6.5	4.9	0
GEX1	*YCL073C*	0.1	0.4	0.5	0.5	0
VBA3	*YCL069W*	0.4	3.5	3.9	4.5	0
YCL068C	*YCL068C*	0.1	4.8	0.5	7.4	0
YCL065W	*YCL065W*	0	14.9	9.1	9.2	0
CHA1	*YCL064C*	51.2	148	229.4	242.2	0
YFL063W	*YFL063W*	0	1.7	1.2	0.4	175
COS4	*YFL062W*	5	12.5	15.3	18.1	1527
THI5	*YFL058W*	1.3	4.4	3.8	3.1	7972
YFR057W	*YFR057W*	0.2	12	9.7	10.8	529
YPS5	*YGL259W*	0.2	2.9	3.3	2.7	2836
YGL258W-A	*YGL258W-A*	3.4	13.1	27.8	29.7	3396
IMD2	*YHR216W*	61.5	234.2	331.9	352.5	989
PAU4	*YLR461W*	0.5	1.1	1.6	1.9	1239
YNL337W	*YNL337W*	0	2.2	0.4	0.6	77
AAD15	*YOL165C*	2.1	7.2	10.1	10.4	0
FDH1	*YOR388C*	1.4	2.7	2.5	2.7	11622

TABLE 2.6 Complete List of Genes Increasing in Expression in *sir2Δ, sir3Δ*, and *sir4Δ*

Shown below are expression levels in FPKM for the 107 genes that significantly increased in expression across all three *sir* mutants (*sir2Δ, sir3Δ*, and *sir4Δ*). Genes are listed in alphabetical

order by gene name. Expression changes were filtered based on a p-value < 0.05 and a false-discovery rate of < 0.10. Forty-two genes (bold-faced type) showed expression changes of 2-fold or greater in *sir* mutants relative to wild type as analyzed by DESeq in terms of read counts (NOT FPKM). Transcript quantification in terms of FPKM was done with Cufflinks.

Gene	Systematic Name	Wild type	*sir2Δ*	*sir3Δ*	*sir4Δ*
AAD15	***YOL165C***	**2.1**	**7.2**	**10.1**	**10.4**
ADH7	*YCR105W*	11	15.1	15.3	15.3
ADI1	*YMR009W*	146.4	182.5	264.1	287.1
AHP1	***YLR109W***	**218.2**	**480.6**	**438.6**	**526.6**
ARO9	*YHR137W*	62.4	75.7	116.2	91.7
BNA2	*YJR078W*	7.7	11.2	14.1	12.5
BNA4	*YBL098W*	27.3	37.9	42.7	45.7
BNA5	*YLR231C*	26.8	44.2	71	69.8
CAR1	*YPL111W*	47.6	84.3	73.4	83.5
CHA1	***YCL064C***	**51.2**	**148**	**229.4**	**242.2**
CMC4	*YMR194C-B*	12.5	14.8	20.7	23.5
COA2	*YPL189C-A*	64.4	152.4	128	140.4
COS1	*YNL336W*	134	191.3	252.7	302.1
COS4	***YFL062W***	**5**	**12.5**	**15.3**	**18.1**
COS7	*YDL248W*	36	51.3	67.6	71.9
COS8	*YHL048W*	115.6	161.5	233.2	266.9
COX5A	*YNL052W*	198.4	240.4	394.7	248.9
COX6	*YHR051W*	175.9	235.6	255.3	243.4
COX7	*YMR256C*	204.3	322.7	408.4	286.6
CRC1	*YOR100C*	1.4	3.3	3.2	3.1
CYB5	*YNL111C*	146.4	254.6	572	316.5
CYC1	***YJR048W***	**130.8**	**444.2**	**513.5**	**267.8**
CYC7	***YEL039C***	**11.2**	**26.8**	**99.7**	**62.9**
CYT1	*YOR065W*	55.5	82.3	172.5	105.1
DLD1	*YDL174C*	31	40	49.8	47
EDC1	*YGL222C*	17.4	21.9	23.2	23.6
ERG13	*YML126C*	302.4	372.5	544	388
ERG6	*YML008C*	161.4	188.7	219.9	206.6
ERG8	*YMR220W*	49.2	60.6	71.6	61.8
FDH1	***YOR388C***	**1.4**	**2.7**	**2.5**	**2.7**
FMP43	***YGR243W***	**1.3**	**10.4**	**8.5**	**8.3**
GEX1	***YCL073C***	**0.1**	**0.4**	**0.5**	**0.5**
GTO3	***YMR251W***	**3.7**	**7.6**	**8.5**	**10.6**
HAP4	*YKL109W*	53.7	96.6	124.1	92.8
HMLALPHA1	***YCL066W***	**0**	**20.7**	**16.6**	**14.1**

HMLALPHA2	***YCL067C***	**0**	**38.7**	**32.3**	**48.9**
HMRA1	***YCR097W***	**0**	**40.6**	**33.4**	**39.5**
HMRA2	***YCR096C***	**0.1**	**31.9**	**23.9**	**39.5**
HMX1	***YLR205C***	**6.7**	**29.3**	**44**	**24.5**
HOR2	*YER062C*	52.9	98.8	137.2	133.8
HPF1	*YOL155C*	61.2	82.2	114.6	118.9
HSP12	*YFL014W*	51.7	126	113.8	80.1
HSP31	*YDR533C*	38.9	50.6	59.5	51.9
ICY1	*YMR195W*	97.8	209.9	154.8	175.8
IDH2	*YOR136W*	131.4	170.1	228.2	205.1
IDI1	*YPL117C*	97.6	140.3	143.1	128.8
IMD1	***YAR073W***	**0.1**	**1.1**	**1.1**	**1.1**
IMD2	***YHR216W***	**61.5**	**234.2**	**331.9**	**352.5**
JID1	***YPR061C***	**3.2**	**9.1**	**8.3**	**8.5**
MCR1	*YKL150W*	126.7	171.6	266	258.6
MET10	*YFR030W*	18.4	24.5	37.1	29.2
MET14	*YKL001C*	69.2	119	151.7	129.4
MET3	*YJR010W*	25.7	40.1	81.4	56.8
MMP1	*YLL061W*	17.1	22.8	43.6	34.9
MTH1	***YDR277C***	**6.8**	**14.3**	**18.8**	**16.6**
MVD1	*YNR043W*	202.2	242.2	333.8	252.7
NCA3	***YJL116C***	**10.1**	**24.4**	**28.4**	**25.8**
NDE1	*YMR145C*	204.4	523.2	487.4	351
NSG2	*YNL156C*	69.4	97.9	121.2	101
PAU4	***YLR461W***	**0.5**	**1.1**	**1.6**	**1.9**
PDH1	*YPR002W*	2.1	3.4	4.7	3.2
PET10	*YKR046C*	229.5	282.1	381.2	322.5
PRX1	*YBL064C*	32.5	39.7	46.3	54.7
PUT4	*YOR348C*	4.8	12.2	13.2	9.3
QCR10	*YHR001W-A*	72.4	103.2	222.3	142.1
QCR2	*YPR191W*	76.7	97.3	149.9	110.3
QCR6	*YFR033C*	149.3	247.8	247.8	233.7
QCR7	*YDR529C*	200.4	255.1	390.8	288
QCR8	*YJL166W*	193.6	289.7	396.2	318.6
QCR9	*YGR183C*	238.2	301	606	344.7
REX3	*YLR107W*	20.5	33.5	28.5	31.6
ROX1	*YPR065W*	20.5	35.1	95	57.5
RSB1	*YOR049C*	21.9	45.5	45.6	49.3
SER1	*YOR184W*	148.1	195.8	192.6	198.8
SER3	*YER081W*	102.3	135.7	131.3	160.3
SFC1	***YJR095W***	**0.8**	**1.6**	**1.4**	**1.8**

TGL2	*YDR058C*	9	12.4	13.5	15.4
THI5	***YFL058W***	**1.3**	**4.4**	**3.8**	**3.1**
UBX6	*YJL048C*	86.8	119.6	218.7	162.9
VBA3	***YCL069W***	**0.4**	**3.5**	**3.9**	**4.5**
YAR075W	***YAR075W***	**1.6**	**26**	**21.9**	**25**
YBR284W	*YBR284W*	2.1	3	3.7	4
YCL065W	***YCL065W***	**0**	**14.9**	**9.1**	**9.2**
YCL068C	***YCL068C***	**0.1**	**4.8**	**0.5**	**7.4**
YCL074W	***YCL074W***	**0**	**4.5**	**6.5**	**4.9**
YCL075W	***YCL075W***	**0**	**1.9**	**2.6**	**2.8**
YCL076W	***YCL076W***	**0**	**3.3**	**2.8**	**3.5**
YCR097W-A	*YCR097W-A*	0	8.8	5.6	6.2
YDR018C	*YDR018C*	2.2	4.2	4.1	4.5
YDR042C	***YDR042C***	**4.6**	**19.4**	**14.6**	**10.7**
YDR119W-A	***YDR119W-A***	**27**	**70.8**	**145.3**	**136.2**
YER053C-A	***YER053C-A***	**0**	**777.5**	**1640.7**	**371.2**
YFL063W	***YFL063W***	**0**	**1.7**	**1.2**	**0.4**
YFR057W	***YFR057W***	**0.2**	**12**	**9.7**	**10.8**
YGL258W-A	***YGL258W-A***	**3.4**	**13.1**	**27.8**	**29.7**
YGR182C	*YGR182C*	44.8	55.8	48.5	56.5
YIL014C-A	*YIL014C-A*	19.4	28.6	29	23.5
YJL047C-A	***YJL047C-A***	**0**	**39.2**	**9.5**	**11.8**
YJL133C-A	***YJL133C-A***	**67.2**	**183.8**	**152**	**303.5**
YJR115W	***YJR115W***	**11.2**	**20.9**	**21.3**	**24.5**
YKR075C	***YKR075C***	**8.1**	**24.6**	**36.1**	**38.5**
YLR312C	*YLR312C*	2	3.6	4.8	5.4
YLR460C	*YLR460C*	2	3.5	4.4	4.1
YMR206W	*YMR206W*	2.2	4.9	4.9	6
YNL337W	***YNL337W***	**0**	**2.2**	**0.4**	**0.6**
YNR064C	*YNR064C*	6.1	9.5	9.1	10.7
YPC1	*YBR183W*	53.8	101.6	150.1	130.5
YPS5	***YGL259W***	**0.2**	**2.9**	**3.3**	**2.7**

For the twenty-one subtelomeric genes that were upregulated in all three *sir* mutants, we evaluated whether proximity to Sir proteins influenced repression. First we determined whether the genes that increased expression in all three mutants were within peaks as defined by MACS. Most (15 of 21) of the genes whose expression changes in all three *sir* mutants (Table 2.5) were within MACS peaks (Table 2.4). For seventeen of these upregulated genes, the distance between the mid-point of the gene to the midpoint of the nearest prominent Sir-protein peak was less than two kilobase pairs (Table 2.5, last column). Four such examples of Sir-repressed coding genes adjacent to Sir peaks are shown (Figure 2.13). Another gene, *COS6*, displayed a significantly enriched peak for only Sir4, and the expression of this gene increased ~1.4-fold relative to wild type in the *sir4*Δ (because it did not increase in *sir2*Δ and *sir3*Δ, this gene is not included in

Table 2.5). Proximity to a Sir protein peak was not, however, predictive of whether or not a gene would be de-repressed in a *sir* mutant. There were many genes that either fell under a Sir-protein peak or fell within two kbp of a Sir-protein peak but did not change in expression in a *sir* mutant. Of the 101 coding genes that fell within two kilobases of Sir2 peaks, 84 (~83%) were not de-repressed in a *sir2*Δ strain. Additionally, there were three genes that MACS called as significantly enriched for at least one of the three Sir proteins, but whose expression did not change in the sir mutants: *IRC7*, *VBA5* and *PAU20*. *PAU20* was previously implicated as a secondary recruitment site for Sir3 (RADMAN-LIVAJA *et al.* 2011). Thus, Sir proteins can be recruited to a locus without repressing the adjacent gene.

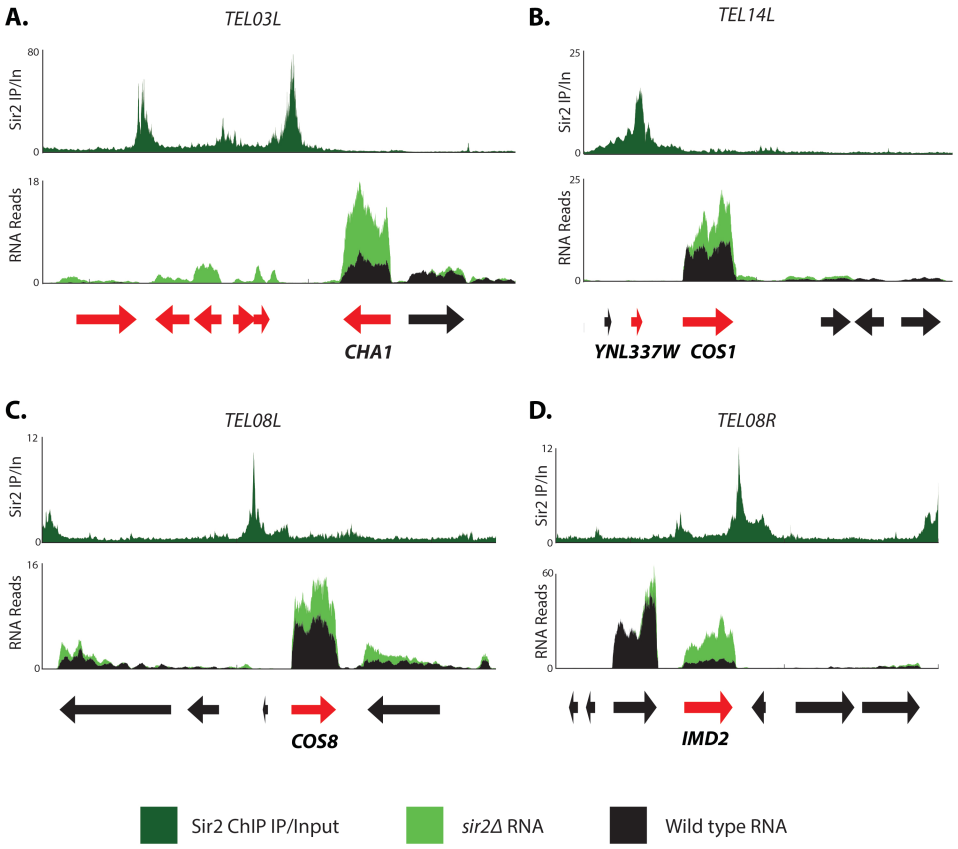

Figure 2.13. Genes that were de-repressed in *sir* mutants tended to be located near peaks of Sir binding. For each panel, the top horizontal axis shows Sir2 ChIP IP/input. The lower panel shows expression in the form of RNA read pileups in wild type (black) and *sir2Δ* (green). Genes that showed a statistically significant increase in expression in *sir2Δ* relative to wild type are colored in red. A) Left arm of chromosome III, *TEL03L*. *CHA1* is adjacent to a peak of Sir2 present at the *HML E* silencer. B) Left arm of chromosome XIV, *TEL14L*. Both *YNL337W* and *COS1* are adjacent to a peak of Sir2 and were de-repressed in the *sir2Δ* mutant. (C-D) Left and right arms of chromosome VIII, *TEL08L* and *TEL08R*, respectively. Both *COS8* and *IMD2* are adjacent to a peak of Sir2 and showed increased expression in the *sir2Δ* mutant.

2.4.6 At Least Thirteen Y' Elements Were Expressed

There are nineteen annotated Y' elements, all near the telomeres in the S288C genome. A small percentage (0.010-0.058%) of the total reads in each RNA-Seq library mapped to Y' elements (Table 2.7), corroborating previous work on the expression of Y' elements (PRYDE and LOUIS 1999). However, the high degree of sequence similarity among Y' elements precluded microarray experiments from being able to determine which of the Y' elements were expressed. Likewise, the majority of our reads from Y' elements, ~81%, did not map uniquely to specific Y' elements. Using the ~19% that mapped uniquely due to SNPs that distinguish Y' elements, we found that thirteen Y' elements were expressed. Absolute differences in read counts were difficult to interpret, as the number of uniquely-mapped reads per Y' element varies as a function of the number of unique SNPs within its sequence. Nevertheless, in no case was the level of expression significantly higher or lower in a *sir* mutant relative to wild type (Table 2.8). Six Y' elements (*TEL04R-YP*, *TEL16L-YP*, *TEL07R-YP*, *TEL12R-YP1*, *TEL14L-YP*, *TEL15R-YP*) contributed no uniquely mapped reads.

TABLE 2.7 Reads Mapped to Y' Elements

Average Percent Uniquely-Mapped Y' reads: 18.95%

Strain	Alias	% Reads Mapped to Y'	% Of Total Y' Reads Uniquely Mapped
JRY9316	Wild type	0.044	18.8
JRY9316	Wild type	0.055	17.3
JRY9316	Wild type	0.058	18.9
JRY9720	*sir2Δ*	0.053	20.0
JRY9721	*sir2Δ*	0.056	19.9
JRY9722	*sir2Δ*	0.052	19.4
JRY9723	*sir3Δ*	0.011	19.2
JRY9724	*sir3Δ*	0.010	19.2
JRY9725	*sir3Δ*	0.010	18.7
JRY9726	*sir4Δ*	0.048	18.8
JRY9727	*sir4Δ*	0.050	18.3
JRY9728	*sir4Δ*	0.056	18.9

TABLE 2.8 Normalized Read Counts Of Uniquely-Mapped Reads at Y' Elements.

Y' Element	Wild type	*sir2Δ*	*sir3Δ*	*sir4Δ*
TEL04R-YP	0.0	0.0	0.0	0.0
TEL16L-YP	0.0	0.0	0.0	0.0
TEL08L-YP	130.6	185.8	159.0	174.1
TEL07R-YP	0.0	0.0	0.0	0.0
TEL06L-YP	61.8	76.6	94.3	70.9
TEL05R-YP	23.7	17.4	24.6	22.4
TEL13L-YP	3.9	3.3	5.2	5.4
TEL05L-YP	209.6	199.5	206.2	203.1
TEL12R-YP2	16.0	20.6	17.3	15.8
TEL12-R YP1	0.0	0.0	0.0	0.0
TEL14L-YP	0.0	0.0	0.0	0.0
TEL15R-YP	0.0	0.0	0.0	0.0
TEL16R-YP	78.2	61.7	53.2	56.3
TEL08R-YP	4.3	6.5	13.1	8.4
TEL10L-YP	10.5	6.2	15.3	4.8
TEL12L-YP2	16.1	15.6	13.4	20.0
TEL09L-YP	0.5	0.0	0.0	0.0
TEL02L-YP	140.5	168.3	147.4	167.7
TEL12L-YP1	0.8	0.0	0.3	0.4

Others have detected telomere-repeat containing RNAs, or TERRAs, originating from the repeated sequences within X elements (IGLESIAS *et al.* 2011). We detected a small percentage of sequence reads that mapped to sufficiently polymorphic X elements and found that X elements present at *TEL02L, TEL06L, TEL06R, TEL07R,* and *TEL11R* increased in expression in all three *sir* mutants. However, the transcripts we detected originated from the core X, which contains the Abf1 and ORC binding sites, not the repeats within X elements.

2.4.7 Newly-Identified Haploid or Diploid-Regulated Genes

S. cerevisiae cell type is specified by the activity of transcription factors encoded by alleles of the *MAT* locus (HABER 2012). These transcription factors activate or repress transcriptional programs in each of the three cell types. Haploid yeast mutant for *SIR2, SIR3,* or *SIR4* simultaneously express the α2 and a1 proteins due to de-repression of *HMLα* and *HMRa*, respectively. Dimerization of a1 and α2 leads to the a1/α2 repressor complex, which represses haploid-specific genes by directly binding to their promoters. α2 also dimerizes with Mcm1 and represses **a**-specific genes. Our data provided an opportunity to use the enhanced resolving power and sensitivity of RNA-Seq to obtain a potentially full catalogue of haploid-specific genes and a/α -specific genes. Therefore, any previously undiscovered **a**-specific genes might also be included among the haploid specific genes due to their decreased expression in *sir* mutants relative to wild type.

We applied the following criteria to obtain a list of candidate cell-type specific genes: (1)

the gene increased or decreased in all three *sir* mutants compared to wild type; (2) the gene's expression level had a 2-fold or greater statistically significant change; and (3) the gene was not directly bound by Sir2, Sir3, or Sir4. Using these criteria, we identified sixteen genes with elevated expression in Sir- mutants (Table 2.9). Six of these genes have mitochondrial functions (*FMP43, SFC1, CYC7, CYC1, NCA3,* and *YJL133C-A*) and are clearly expressed in haploids as well. Hence these genes were more accurately interpreted as having a/α-enhanced expression. No common functions were found for the remaining eleven, nor have any diploid functions been attributed to these. To evaluate the dependence of these expression changes on the presence of the a1/α2 dimer, *HML*α was deleted in the *sir2Δ* background and expression changes were measured using qRT-PCR. The expression increase for *YJL133C-A* was dependent on the presence of α2 (Figure 2.14C), making it a candidate for indirect regulation by a1/α2 (perhaps through *RME1*, for example).

Thirty-five genes decreased in expression in *sir* mutants relative to wild type. We compared this list to known haploid-specific genes as found by chromatin immunoprecipitation of α2 in a/α diploids followed by hybridization of immunoprecipitated DNA to a genome-wide array (GALGOCZY *et al.* 2004). That study found twenty haploid-specific genes, all of which were reproduced in our dataset (un-starred genes, Table 2.9). *YGL193C* and the anti-sense transcript of *IME4,* which are positioned in tandem, are also known a1/α2 targets that were reproduced in our dataset (VALENCIA-BURTON *et al.* 2006; HONGAY *et al.* 2006). An additional known indirect a1/α2 target reproduced in our dataset was the G1 cyclin gene *CLN2. CLN2* is weakly activated by *RME1*, and therefore, as expected, decreased in expression in *sir* mutants presumably due to the repression of *RME1* itself (Table 2.9) (TOONE *et al.* 1995).

The remaining thirteen of thirty-five genes in the decreasing-genes list represented genes with previously unrecognized haploid specific or **a**-specific expression (starred genes, Table 2.9). To further evaluate if these genes were direct targets of a1/α2 or α2/Mcm1 repression, we performed two additional tests: (1) a scan of each gene's promoter sequences for the presence of annotated a1/α2 or α2/Mcm1 binding motifs using the motif discovery program MEME and the The Yeast Transcription Factor Specificity Compendium (YeTFaSpCo) (BAILEY *et al.* 2009; DE BOER and HUGHES 2012); and (2) measurement of the expression of each gene via qRT-PCR in a *sir2Δ hmlΔ* strain. If the observed expression change were in fact due to the presence of a1/α2, deleting α2 should abolish the effect. For both tests, known a1/α2 and α2/Mcm1 targets served as positive controls. Four genes with previously unrecognized haploid-specific expression were confirmed with these two tests: *STE14, TOS1, AXL2,* and *MHF2*. Interestingly, none of the four were under strong a1/α2 repression. Instead, they appeared to be weakly repressed by α2 (Figure 2.14A). Consistent with this observation, none possessed clear a1/α2 binding motifs of the kind found in the strongly repressed haploid specific genes *STE2* and *HO*. However, weak a1/α2 or α2 binding sites, as annotated in the Yeast Transcription Factor Specificity Compendium, were found for all four (Figure 2.14B).

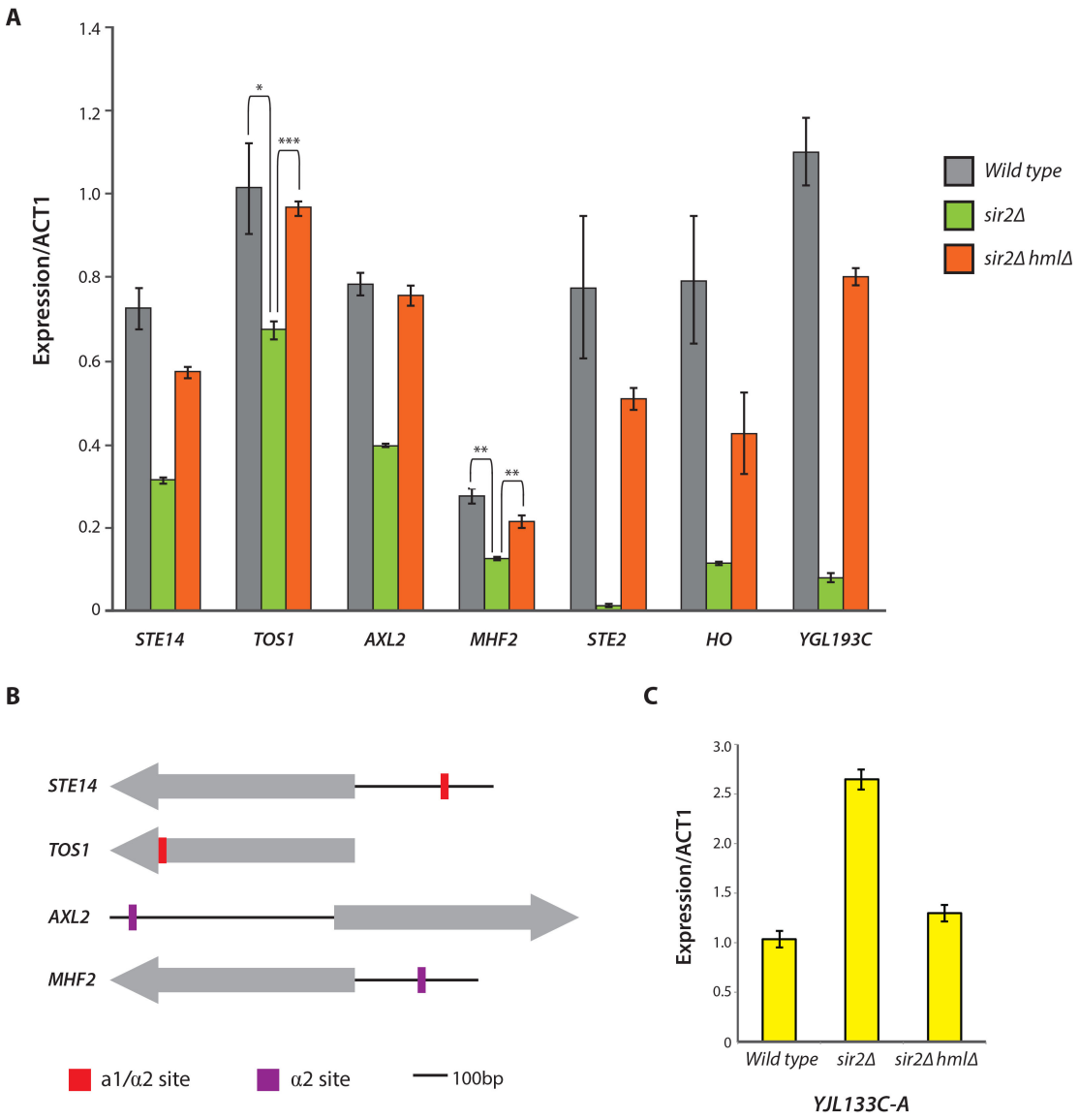

Figure 2.14. Expression confirmation via qRT-PCR and promoter analysis of candidate haploid-specific genes. A) *STE14*, *TOS1*, *AXL2*, and *MHF2* were weakly repressed in an α2-dependent manner. The strongly a1/α2-repressed genes *STE2*, *HO,* and *YGL193C* are shown for comparison. B) Annotated binding sites for the a1/α2 heterodimer and α2 itself are shown in relation to the protein-coding sequences (gray arrows) for *STE14*, *TOS1*, *AXL2*, and *MHF2* (coding regions are not drawn to scale). *STE14* contains a weak a1/α2 binding site 232 base pairs upstream from its coding sequence. *TOS1* contains a weak a1/α2 binding site within its gene body. Both *AXL2* and *MHF2* contain weak α2 binding sites 578 base pairs and 174 base pairs, respectively, upstream of their coding regions. C) *YJL133C-A*, a gene of unknown function, increases in expression in a α2-dependent manner.

TABLE 2.9 Mating-type Regulated Genes

All genes below: (i) changed significantly in expression in all three *sir* mutants relative to wild type, and (ii) are NOT located at *HML, HMR,* or subtelomeric regions. Seventeen genes increased in expression and thirty-five decreased in expression. Genes not found in previous lists of haploid-specific or haploid-enhanced genes are marked with an asterisk (*). Expression levels are in units of FPKM and genes are ordered by increasing FPKM levels in wild type. **The FPKM value for *MFA2* in the *sir3Δ,* though greater than 0, is not statistically different from the values of 0 FPKM seen in *sir2Δ* and *sir4Δ*. Similar numbers of raw reads mapped to the *MFA2* locus in all three mutants (18, 19, and 11 average reads for *sir2Δ*, *sir3Δ*, and *sir4Δ* respectively). The inflated FPKM value seen in the *sir3Δ* strain is likely a consequence of the FPKM normalization method used by Cufflinks, which due to the substantially larger library size of the *sir3Δ* strains (Table 2.2), may have overestimated the FPKM for the lowly-expressed *MFA2* gene.

Genes Increasing In Expression					
Gene	Systematic Name	Wild type	*sir2Δ*	*sir3Δ*	*sir4Δ*
*YJL047C-A**	*YJL047C-A*	0	39.2	9.5	11.8
*YER053C-A**	*YER053C-A*	0	777.5	1640.7	371.2
*SFC1**	*YJR095W*	0.8	1.6	1.4	1.8
*FMP43**	*YGR243W*	1.3	10.4	8.5	8.3
*JID1**	*YPR061C*	3.2	9.1	8.3	8.5
*GTO3**	*YMR251W*	3.7	7.6	8.5	10.6
*YDR042C**	*YDR042C*	4.6	19.4	14.6	10.7
HMX1	*YLR205C*	6.7	29.3	44	24.5
*MTH1**	*YDR277C*	6.8	14.3	18.8	16.6
*YKR075C**	*YKR075C*	8.1	24.6	36.1	38.5
*NCA3**	*YJL116C*	10.1	24.4	28.4	25.8
*YJR115W**	*YJR115W*	11.2	20.9	21.3	24.5
*CYC7**	*YEL039C*	11.2	26.8	99.7	62.9
*YDR119W-A**	*YDR119W-A*	27	70.8	145.3	136.2
*YJL133C-A**	*YJL133C-A*	67.2	183.8	152	303.5
*CYC1**	*YJR048W*	130.8	444.2	513.5	267.8
*AHP1**	*YLR109W*	218.2	480.6	438.6	526.6
Genes Decreasing In Expression					
Gene	Systematic Name	Wild type	*sir2Δ*	*sir3Δ*	*sir4Δ*
*SNO3**	*YFL060C*	7.8	2	2.4	3.1
*HUA2**	*YOR284W*	10	3.8	4.3	4.6
HO	*YDL227C*	10.7	1.7	0.8	1.1
AXL1	*YPR122W*	15	4.3	3.6	2.9
STE5	*YDR103W*	15.1	1.7	2.7	2.3

*YPR027C**	*YPR027C*	16.1	2.7	3.5	4.1
YDR170W-A	*YDR170W-A*	16.1	3.9	4.6	3.5
*SST2**	*YLR452C*	16.8	7	7.5	6.5
RDH54	*YBR073W*	16.9	3.3	3.7	2.7
NEJ1	*YLR265C*	19	2.4	2.1	1.6
*YDR034C-D**	*YDR034C-D*	25.8	6.1	15.4	12
STE6	*YKL209C*	25.9	2.9	4.1	3.6
GPA1	*YHR005C*	26.1	3.5	2.8	2.8
ICS2	*YBR157C*	31.4	5.8	4.6	5.1
*VBA2**	*YBR293W*	35.1	8.2	10	8
BAR1	*YIL015W*	44.7	4.3	3.2	3.2
FUS3	*YBL016W*	49.1	1.1	0.8	0.9
*MHF2**	*YDL160C-A*	49.7	19.9	13.5	18.6
*AXL2**	*YIL140W*	49.7	14.8	21.8	14.9
*CLN2**	*YPL256C*	50.3	21.9	20.6	19.6
IME4	*YGL192W*	53.8	6	8	7.4
*STE14**	*YDR410C*	75.6	23.5	21.5	17
STE4	*YOR212W*	75.8	8	7.3	5.8
YGL193C	*YGL193C*	79.2	2.6	3.3	4.2
STE18	*YJR086W*	82.8	10.8	10.7	5.3
AGA2	*YGL032C*	87.8	0.5	2	2.3
DDR2	*YOL052C-A*	97.3	39.2	41.2	29.8
AMN1	*YBR158W*	102.5	39.4	39.5	33.6
RME1	*YGR044C*	108.2	5.1	6.7	4.8
MFA1	*YDR461W*	227.3	0	0	0
*SUN4**	*YNL066W*	311.4	125.2	122.1	136.1
STE2	*YFL026W*	327.7	5.5	5.5	5.8
*ZRT1**	*YGL255W*	389.9	110.8	117.2	160.9
*TOS1**	*YBR162C*	1143.3	437.3	557.7	478.5
*MFA2***	*YNL145W*	3465.9	0	71.6	0

2.5 Discussion

This study provided a comprehensive evaluation of both the molecular topology of Sir-protein distribution at telomeres and subtelomeric regions, and of the extent of telomere position effects on gene expression mediated by Sir-based gene silencing. The *URA3* reporter gene, and other reporter genes, near truncated telomeres have served as an assay for telomere position effects for many years. Their use has enabled multiple discoveries including the gene for the RNA component of telomerase (SINGER and GOTTSCHLING 1994), and implicated many chromatin factors and histone modifications as key players in silencing genes near telomeres. However, because the repression of the *URA3* reporter at the truncated telomere of *TEL07L* is

robust, there exists a commonly held view that all natural telomeres of *Sacccharomyces cerevisiae* are transcriptionally silent, and that most, if not all, subtelomeric genes are strongly repressed by the Sir-protein complex. By measuring expression at native telomeres using the highly-sensitive RNA-Seq method, we found that many genes near telomeres are transcribed, albeit at lower levels compared to the rest of the genome, supporting and extending earlier data that expression of genes in subtelomeric regions of *S. cerevisiae* were largely uninfluenced by Sir proteins (TAKAHASHI *et al.* 2011). Moreover, we found that Sir-based silencing was not a widespread phenomenon at telomeres, despite strong enrichment of Sir proteins at telomeric repeats and core X elements. Twenty-one genes in the vicinity of Sir proteins are de-repressed, but most genes are not, resulting in only 6% of subtelomeric genes repressed by Sir proteins. Qualitatively, these data are in agreement with a high-density microarray-based genome-wide expression study of wild type and *sir2*Δ*, sir3*Δ and *sir4*Δ mutants (WYRICK *et al.* 1999).

2.5.1 Transcription Occurs Near Telomeres, But at Lower Levels Than at Non-Telomeric Regions

Although transcription does occur in subtelomeric regions, it produces fewer transcripts per gene compared to non-telomeric regions of the genome. This global observation was consistent with previous studies that found telomeres to be both gene poor and, for the genes present, having lower levels of transcription than is typical for the rest of the genome, as measured with hybridization studies with high density microarrays (LOUIS 1995; WYRICK *et al.* 1999). A limitation of all RNA based studies to date is their reliance on mRNA samples from a large population of cells. Hence high-level expression in a small fraction of cells, but no expression in the majority, would have been missed. Indeed the epigenetic inheritance of expression states observed for reporter genes at telomeres underscores the existence of such cell-to-cell variation.

Importantly, however, transcript levels at subtelomeric regions in *sir* mutants did not match transcript levels from non-subtelomeric regions. Therefore, Sir-protein binding at telomeres was not solely responsible for the low transcript levels from most genes in subtelomeric regions. Other factors potentially responsible for the lower expression of subtelomeric genes include: (1) other, non-Sir protein chromatin factors that might confer an additional tier of repression on subtelomeric genes; or (2) sequence-specific reasons for low subtelomeric expression, such as the use of intrinsically weak promoters. In support of the first possibility, histone H4 depletion increases expression of 15% of subtelomeric genes whereas *sir* mutations increase expression of only 7-9% of genes within subtelomeric regions (WYRICK *et al.* 1999; MARTIN *et al.* 2004). Our data show that a similar percentage, ~6%, of subtelomeric genes are repressed by Sir proteins. Perhaps other chromatin factors targeting histone H4 confer an additional repressive effect on subtelomeric regions. Silencing at different telomeres might also be more or less sensitive to distinct histone modifying enzymes. For example, the subtelomeric gene *FLO10*, which encodes a cell-wall glycoprotein, is repressed by the action of deacetylases Hst1 and Hst2, two paralogs of Sir2 (HALME *et al.* 2004). Additionally, there is almost no agreement in the identity of the genes repressed by *DOT1* (TAKAHASHI *et al.* 2011), the enzyme that catalyzes H3K79 methylation, and those repressed by *SIR2* (this study), which deacetylates H4K16-acetyl.

The second possible reason that subtelomeric domains exhibit lower levels of transcription could be that subtelomeric genes, on average, have weaker promoters than

centromere-proximal genes. If subtelomeric genes tend to have weaker promoters and lack of transcriptional activator binding sites, it would be expected that most are weakly expressed regardless of chromatin state. Interestingly, subtelomeric genes are among the most highly divergent genes in the yeast genome and are often upregulated under stressful conditions (HARRISON *et al.* 2002; TEYTELMAN *et al.* 2008). Previous studies show that part of the reason for this elevated rate of divergence is the ability of Sir proteins to interfere with certain types of DNA repair, highlighting a functional consequence of Sir protein association (TERLETH *et al.* 1989). Our data implied that this mechanism could not account for all of the enhanced divergence in these regions since the distribution of Sir proteins was focal rather than distributed throughout the region. However, given that some mechanisms of DNA repair are transcription coupled (SVEJSTRUP 2002), perhaps the low expression level of genes (or cell-to-cell variation in expression) in the subtelomeric regions leads to the absence of transcription-coupled repair and thereby contributes to their rapid divergence. If so, the higher mutation rate could, in turn, result in reduced functioning of promoter elements. Furthermore, a higher proportion of ORFs at telomeres are categorized as "Dubious" or "Uncharacterized," with ~56% of subtelomeric genes falling into these two categories as opposed to ~24% of non-subtelomeric genes. Thus, these ORFs may not be functional protein-coding genes whose expression is needed for general cellular function.

2.5.2 Only A Small Fraction of Subtelomeric Genes Were Repressed by Sir Proteins

Overall, we found that Sir proteins repressed only 6% of all subtelomeric genes. Why are some subtelomeric genes repressed by Sir proteins, whereas others are not? Certain strong transcription activators can efficiently escape Sir-based repression (Steakley and Rine, in preparation). Perhaps genes with increased expression in the absence of Sir proteins possess promoters with binding sites for weak transcriptional activators or weak binding sites for strong activators. In the absence of Sir proteins, these weakly-binding activators would gain access and promote transcription. If so, the promoters of these Sir-protein-sensitive genes might contain transcription factor binding sites that are distinct from binding sites present at genes that are not repressed by Sir proteins. To explore this possibility, we catalogued the transcription-factor binding profiles for the promoters of the twenty-one *SIR*-sensitive subtelomeric genes and compared them to each other as well as to the transcription factor binding profiles from all other subtelomeric genes. Overall, we found no differences in transcription factor binding profiles between *SIR*-sensitive and *SIR*-resistant subtelomeric genes, though the small number of genes involved limited any statistical power of the analysis (data not shown). Motifs for the Mot2 and Ash1 transcription factors were the most commonly found sequences in the dataset for all subtelomeric genes analyzed, regardless of whether they were Sir-repressed or not. Furthermore, thirteen of the twenty-one *SIR*-sensitive genes are annotated as "dubious" and the remaining seven shared no common functional annotations, consistent with an absence of common transcription factor binding sites. In sum, we were unable to find differences in promoter sequence or transcription factor binding sites between the genes that were repressed by Sir proteins and those that were not.

2.5.3 The Functional Significance of Sir Proteins At Telomeres

At present, one clear function of Sir proteins at telomeres is to repress, or at least lower, the expression of a small subset of genes in this part of the genome. But why would a cell want to simply lower the expression of genes that way, as opposed to simply having a weaker promoter for such genes? Perhaps subtelomeric genes regulated by Sir proteins in *S. cereivisiae*, like those in *C. glabrata* (PEÑAS *et al.* 2003; DOMERGUE *et al.* 2005; MA *et al.* 2009), are involved in regulating the transcription of genes necessary only under certain conditions. In support of this model, six genes encoding metabolic enzymes increased in expression in all three *sir* mutants: *CHA1, AAD15, IMD2, FDH1, THI5, VBA3* and *PAU4.* It is possible that *S. cerevisiae* encounters some condition in nature that would inhibit Sir-based silencing like nicotinamide does in the laboratory. If so, perhaps these enzymes are part of an as yet undiscovered response mechanism to such agents or conditions.

A second hypothesis is that Sir proteins at telomeres contribute to the suppression of recombination at telomeric repeats, much like Sir2 suppresses recombination at the rDNA repeats (GOTTLIEB and ESPOSITO 1989; SMITH and BOEKE 1997). While the yeast Ku proteins, which associate with Sir proteins at the subtelomeric core X sequences, do suppress recombination between telomeric repeats (MARVIN *et al.* 2009), so far, there is no direct evidence that Sir proteins are involved in this suppression. Additionally, a previous report that the association of Sir proteins with Ku70/Ku80 suggests a role for Sir proteins in preventing non-homologous end joining (TSUKAMOTO *et al.* 1997) has since been shown to be an artifact of the a/α state of *sir* mutants (ÅSTRÖM *et al.* 1999).

2.5.4 Discovery Of Novel Haploid-Specific Genes

Historically, elucidation of transcriptional regulatory circuits of *S. cerevisiae* has relied on microarray-based technologies, which are limited in sensitivity and dynamic range (GALGOCZY *et al.* 2004). The sensitivity of RNA-Seq and the "pseudodiploid" state of *sir* mutants allowed us to evaluate the "completeness" of the identification of cell-type-regulated genes, particularly those genes that are potential targets of a1/α2 and α2/Mcm1 regulation. We confirmed all previously identified genes of these classes. In addition, we found twenty-nine new candidate haploid-specific or a/α-specific genes. Of these twenty-nine, the expression of *YJL133C-A, STE14, TOS1, AXL2*, and *MHF2* were verified by qRT-PCR and found to be moderately repressed in an α2-dependent manner, thus revealing a new class of genes that were partially but not fully repressed in the a/α cell type. The remaining twenty-four were too low in expression to be verified by qRT-PCR. The cell-type regulation of these genes was likely missed in previous studies precisely because they are not strongly repressed and thus exhibit a less dramatic fold-change in expression as compared to other a/α regulated genes. At least three of the five genes verified by qRT-PCR function in processes unrelated to cell-type determination. For example, *STE14* encodes a methyltransferase that methylates a-factor in *MATa* cells and Ras proteins in all cell types (MARR *et al.* 1990; HRYCYNA *et al.* 1991). On a per cell basis, it is likely that more a-factor is produced in *MATa* cells than Ras proteins in all cell types, consistent with the partial reduction in *STE14* expression in cells that do not make a-factor due to the expression of α2. We speculate that the Tos1, Mfh2, and Axl1 proteins have functions in **a**/α diploids and other functions that are needed either in **a** cells or in haploid cells, leading to their modest repression in **a**/α diploids.

Chapter 3

Evolution and Functional Trajectory of Sir1 in Gene Silencing

3.1 Abstract

We used the budding yeast species *Saccharomyces cerevisiae* and *Torulaspora delbrueckii* to examine steps in the evolution of Sir-based silencing, focusing on Sir1, silencers, on the molecular topology of silenced chromatin, and on the relative roles of Sir proteins and RNAi protein orthologs in silencing in *T. delbrueckii*. Chromatin immunoprecipitation followed by deep sequencing (ChIP-Seq) on Sir proteins of *T. delbrueckii*, revealed a different topography of silencing proteins at the *HML* and *HMR* loci than seen previously in *S. cerevisiae*, suggestive of action of Sir proteins at a distance. In *S. cerevisiae* Sir1 was enriched primarily at the silencers of *HMLα* and *HMRa*, and at all but one centromere. Sir 1 was absent from telomeres, and did not contribute to repression of any subtelomeric genes. In contrast to *SIR1*'s partially dispensable role in gene silencing in *S. cerevisiae*, the Sir1 ortholog in *T. delbrueckii, Td-KOS3* was essential for silencing the *HML* and *HMR* loci of *T. delbrueckii*, was found at the telomeres of *T. delbrueckii* as a partner with Td-Sir2 and Td-Sir4, and was required for repression of multiple subtelomeric genes. Silencer mapping in *T. delbrueckii* revealed single silencers rather than pairs of silencers at *HML* and *HMR*, bound by TdKos3, Td-Sir2 and Td-Sir4. The *KOS3* gene mapped near one of these silencers, and its expression was regulated by Sir-based silencing, providing feedback regulation of a critical silencing protein by silencing. These results highlighted the shifting role of this rapidly diverging gene in the task of establishing and maintaining heterochromatin in budding yeasts as well as the diverse chromatin architectures that can underlie silenced chromatin.

3.2 Introduction

Heterochromatin-based gene silencing in *Saccharomyces cerevisiae* and its close relatives among the budding yeasts use the four Sir proteins to form complexes that bind to nucleosomes throughout specific regions on chromosomes and block accessibility of other DNA binding proteins in that region (GRUNSTEIN and GASSER 2013; THURTLE and RINE 2014b; STEAKLEY and RINE 2015). In these species, the Sir1 protein is perhaps most enigmatic. In contrast to Sir2, Sir3 and Sir4, which are the structural proteins of heterochromatin, necessary for its establishment, maintenance and inheritance, Sir1's main role in *S. cerevisiae* seems to be in the establishment of heterochromatin at *HML* and *HMR* (PILLUS and RINE 1989), though recent evidence indicates that it contributes somewhat to the maintenance of heterochromatin (DODSON and RINE 2015). *sir1*Δ causes between 50-80% of individual cells within the mutant population to completely lack silencing at *HMLα* and *HMRa,* whereas the remaining cells are fully silenced at these loci. The unsilenced *sir1*Δ cells express transcripts from the silent mating type loci to the same extent as *sir4*Δ mutants, are mating defective, and in the case of *MATa* haploids, lose sensitivity to α-factor (PILLUS and RINE 1989; DODSON and RINE 2015). Furthermore, individual *sir1*Δ cells can switch transcriptional states, switching from unsilenced to silenced once every 250 cell divisions, and somewhat slower in the reverse direction (PILLUS and RINE 1989).

In addition to its subtle mutant phenotype, *SIR1* has a dynamic evolutionary history. *SIR1* has been duplicated more than once among *Saccharomyces* yeasts, and some species have lost these paralogs, while others have retained them (GALLAGHER *et al.* 2009). As a result, *SIR1* paralogs vary widely among these species in number and in the level of protein sequence similarity between paralogs, which is low (typically < 50%). On one end of the spectrum,

S*accharomyces bayanus v. uvarum* has four *SIR1* paralogs: *SIR1* and three *Kin-Of-SIR1* (*KOS1-3*). All four paralogs contribute to silencing in this species (GALLAGHER *et al.* 2009). On the other end of the spectrum, in *K. lactis,* there is no identifiable *SIR1* paralog in the genome, and silencing is mediated by *SIR2*, *SIR4*, *ORC1*, and *SUM1* (HICKMAN and RUSCHE 2009, 2010). *Candida glabrata* is another yeast that lacks *SIR1*, yet like *S. cerevisiae,* has *SIR2, SIR3,* and *SIR4* orthologs that function in silencing (PEÑAS *et al.* 2003). Each yeast species seems to have innovated a unique solution to the problem of silencing, with some having no need for a *SIR1* gene, whereas others have employed up to four *SIR1* genes. Analyses of *SIR1* orthologs among the species of this clade indicate that the most ancestral form of Sir1 is Kos3 (Kin of Sir1-3) (GALLAGHER *et al.* 2009).

The most common mechanism by far of gene silencing by heterochromatin involves the function of the RNAi pathway. Key components of the RNAi machinery include Argonaut, and Dicer, and in most other organisms an RNA-dependent RNA polymerase (GREWAL 2010). RNAi mechanisms involve the production of double-stranded RNAs generated either by DNA-dependent RNA polymerases or the RNA-dependent RNA polymerase. These double-stranded RNAs are cleaved by Dicer and bound by Argonaute proteins, which use them to direct the modification of DNA and histones occupying sequences complementary to the RNAs bound by the Argonaute protein. RNAi is found widely in plants, animals and many fungi, including *Schizosaccharomyces pombe,* but is completely missing from *S. cerevisiae*.

Torulospora delbrueckii is a budding yeast evolutionarily well positioned to explore some of the most enigmatic questions concerning the origins of Sir-based silencing, and especially the role of Sir1/Kos3. This species diverged from *Saccharomyces* species before the whole-genome duplication, and has Kos3, the most ancestral form of Sir1. *T. delbrueckii* also has pre-whole genome duplication orthologs of *SIR2* and *SIR4*. *T. delbrueckii* has a single gene orthologous to the *ORC1/SIR3* gene pair of Saccharomyces, which we referred to as *ORC1/SIR3*. In addition, this species has orthologs of key RNAi components: a gene encoding Argonaute, *AGO1*, and a budding-yeast Dicer-like gene called *DCR1*. These RNAi-like genes are orthologous to the *AGO1* and *DCR1* present in *Naumovozyma castellii*, a species in which they repress transcription of repetitive Ty elements (DRINNENBERG *et al.* 2009b). *T. delbrueckii* thus offers a chance to explore possible connections between, or divergence of, the two major mechanisms of heterochromatic gene silencing.

This study began with a genome-wide analysis of the roles of Sir1 in *Saccharomyces* to set the stage for studies of Kos3 in *T. delbrueckii.* To date, no one has uncovered a sexual cycle for this species. However, genome sequences of wild isolates of *T. delbrueckii* identify two alleles of a *MAT* locus on *T. delbrueckii* chromosome III, a *HML* locus on the same chromosome, and two *HMR* loci (one on chromosome V and the other on chromosome VII). To explore the functions of *T. delbrueckii* silencing genes, we first created marked strains, protocols and vectors to allow molecular genetic investigations (Ellahi and Rine, manuscript in preparation). We then compared the functions of presumptive silencing genes of *T. delbrueckii* to the functions of their *S. cerevisiae* orthologs. These experiments offered an unbiased view of the genome-wide function of *T. delbrueckii SIR* genes, revealing a distinctly different molecular topology of silenced chromatin than seen in *S. cerevisiae*. Additionally, we constructed *ago1*Δ and *dcr1*Δ single mutants and an *ago1*Δ*dcr1*Δ double-mutant and performed deep-sequencing of mRNAs to uncover all loci that were possibly subject to transcriptional repression by the *T. delbrueckii* RNAi pathway. Collectively, these experiments lead to new conceptualization for the evolution of Sir1's role in silencing, and contribute to an expanded appreciation of the roles of

RNAi components. These data provide the most complete picture to date of how the earliest *SIR1*-containing *SIR* silencing complex functioned and the evolutionary trajectories it may have followed.

3.3 Materials and Methods

***Identification of SIR1 Paralogs*:** To identify *SIR1* paralogs, the *SIR1* protein sequence was used as a BLAST query against sequenced yeast genomes available on the Yeast Gene Order Browser (YGOB). Performing this blast generated a list of 26 hits, all with an e-value of < 0.5. This list included the *KOS3* gene in *T. delbrueckii* (TDEL0E00350), as well as all other previously found *SIR1* paralogs (GALLAGHER *et al.* 2009). *T. delbrueckii KOS3* itself, when used as a BLAST query against yeast genomes on YGOB, identified the *Zygosaccharomyces rouxii KOS3* gene and the *S. bayanus v. uvarum KOS3* gene as the two top matches. Other *SIR1* paralogs, including *S. cerevisiae SIR1*, were among the top 15 matches (all e-values < 0.5).

Yeast Strains and plasmids
Strains are listed in Table 3.1. *Saccharomyces cerevisiae* strains were generated in the W303 background. Deletion mutants and epitope-tagged alleles of *SIR* genes were made as previously described, using one-step integration of knockout cassettes (LONGTINE *et al.* 1998). *Torulaspora delbrueckii* strains were grown in rich medium (YPD) at 30°C. Gene disruption in *T. delbrueckii* required ~500 base pairs of sequence identity to the target region. Therefore, knockout cassettes and other tagging constructs were first cloned into plasmids containing 500 base pairs of sequence identical to the sequences flanking the genomic target, then amplified via PCR and transformed into strains. Transformations for *T. delbrueckii* were performed using the same lithium acetate-PEG method used for *S. cerevisiae* (GEITZ 2014).

Table 3.1: Yeast Strains Used In Chapter 3

Name	Species	Genotype	Source
JRY10152	*S. cerevisiae*	*matΔ::HygMX can1-100 his3-11 leu2-3,112 lys2- trp1-1 ura3-52 SIR1-3xV5-KanMX*	This study
JRY9316	*S. cerevisiae*	*matΔ::HygMX can1-100 his3-11 leu2-3,112 lys2- trp1-1 ura3-52*	Teytelman et al. 2013
JRY9319	*S. cerevisiae*	*matΔ*::HygMX lys2 his3-11 leu2-3,112 trp1-1 ura3-52 can1-100 SIR2-13xMyc::KanMX	Teytelman et al. 2003
JRY10153	*S. cerevisiae*	*matΔ::HygMX can1-100 his3-11 leu2-3,112 lys2- trp1-1 ura3-52 sir1Δ::KanMX*	This study
JRY10154	*S. cerevisiae*	*matΔ::HygMX can1-100 his3-11 leu2-3,112 lys2- trp1-1 ura3-52 sir1Δ::KanMX*	This study
JRY10155	*S. cerevisiae*	*matΔ::HygMX can1-100 his3-11 leu2-3,112 lys2- trp1-1 ura3-52 sir1Δ::KanMX*	This study
JRY9720	*S. cerevisiae*	*matΔ::HygMX can1-100 his3-11 leu2-3,112 lys2- trp1-1 ura3-52 sir2Δ::KanMX*	Ellahi et al. 2015
JRY9721	*S. cerevisiae*	*matΔ::HygMX can1-100 his3-11 leu2-3,112 lys2- trp1-1 ura3-52 sir2Δ::KanMX*	Ellahi et al. 2015
JRY9722	*S. cerevisiae*	*matΔ::HygMX can1-100 his3-11 leu2-3,112 lys2- trp1-1 ura3-52 sir2Δ::KanMX*	Ellahi et al. 2015

JRY9723	*S. cerevisiae*	*matΔ::HygMX can1-100 his3-11 leu2-3,112 lys2- trp1-1 ura3-52 sir3Δ::KanMX*	Ellahi et al. 2015
JRY9724	*S. cerevisiae*	*matΔ::HygMX can1-100 his3-11 leu2-3,112 lys2- trp1-1 ura3-52 sir3Δ::KanMX*	Ellahi et al. 2015
JRY9725	*S. cerevisiae*	*matΔ::HygMX can1-100 his3-11 leu2-3,112 lys2- trp1-1 ura3-52 sir3Δ::KanMX*	Ellahi et al. 2015
JRY9726	*S. cerevisiae*	*matΔ::HygMX can1-100 his3-11 leu2-3,112 lys2- trp1-1 ura3-52 sir4Δ::KanMX*	Ellahi et al. 2015
JRY9727	*S. cerevisiae*	*matΔ::HygMX can1-100 his3-11 leu2-3,112 lys2- trp1-1 ura3-52 sir4Δ::KanMX*	Ellahi et al. 2015
JRY9728	*S. cerevisiae*	*matΔ::HygMX can1-100 his3-11 leu2-3,112 lys2- trp1-1 ura3-52 sir4Δ::KanMX*	Ellahi et al. 2015
JRY10156	*T. delbrueckii*	*MATα ura3Δ0 trp3-1*	This study
JRY10157	*T. delbrueckii*	*MATα ura3Δ0 trp3-1 kos3Δ::KanMX*	This study
JRY10158	*T. delbrueckii*	*MATα ura3Δ0 trp3-1 sir2Δ::KanMX*	This study
JRY10159	*T. delbrueckii*	*MATα ura3Δ0 trp3-1 sir4Δ::KanMX*	This study
JRY10160	*T. delbrueckii*	*MATα ura3Δ0 trp3-1 KOS3-3xV5-NatMX*	This study
JRY10161	*T. delbrueckii*	*MATα ura3Δ0 trp3-1 SIR2-3xV5-NatMX*	This study
JRY10162	*T. delbrueckii*	*MATα ura3Δ0 trp3-1 SIR4-3xV5-NatMX*	This study
JRY10163	*T. delbrueckii*	*MATα ura3Δ0 trp3-1 ago1Δ::NatMX*	This study
JRY10164	*T. delbrueckii*	*MATα ura3Δ0 trp3-1 dcr1Δ::NatMX*	This study
JRY10165	*T. delbrueckii*	*MATα ura3Δ0 trp3-1 ago1Δ::NatMX dcr1Δ::KanMX*	This study
JRY10166	*T. delbrueckii*	*MATα ura3Δ0 trp3-1 pRS41H-TdCEN3-Tdhmlα2Δ::K. lactis URA3*	This study
JRY10167	*T. delbrueckii*	*MATα ura3Δ0 trp3-1 kos3Δ::NatMX [pRS41H-TdCEN3-Tdhmlα2Δ::K. lactis URA3]*	This study
JRY10168	*T. delbrueckii*	*MATα ura3Δ0 trp3-1 sir2Δ::NatMX [pRS41H-TdCEN3-Tdhmlα2Δ::K. lactis URA3]*	This study
JRY10169	*T. delbrueckii*	*MATα ura3Δ0 trp3-1 [pRS41H-TdCEN3-Tdhmlα2Δ::K. lactis URA3] sir4Δ::NatMX*	This study
JRY10170	*T. delbrueckii*	*MATα ura3Δ0 trp3-1 [pRS41H-TdCEN3]*	This study
JRY10171	*T. delbrueckii*	*MATα ura3Δ0 trp3-1 [pRS41H-TdCEN3-Tdhmlα2Δ::K. lactis URA3_regionAΔ]*	This study
JRY10172	*T. delbrueckii*	*MATα ura3Δ0 trp3-1 [pRS41H-TdCEN3-Tdhmlα2Δ::K. lactis URA3_regionBΔ]*	This study
JRY10173	*T. delbrueckii*	*MATα ura3Δ0 trp3-1[pRS41H-TdCEN3-Tdhmlα2Δ::K. lactis URA3_regionCΔ]*	This study
JRY10174	*T. delbrueckii*	*MATα ura3Δ0 trp3-1 [pRS41H-TdCEN3-Tdhmlα2Δ::K. lactis URA3_rap1-site-mutant]*	This study
JRY10175	*T. delbrueckii*	*MATα ura3Δ0 trp3-1 [pRS41H-TdCEN3-Tdhmra1Δ::K. lactis URA3]*	This study
JRY10176	*T. delbrueckii*	*MATα ura3Δ0 trp3-1 kos3Δ::NatMX [pRS41H-TdCEN3-Tdhmra1Δ::K. lactis URA3]*	This study
JRY10177	*T. delbrueckii*	*MATα ura3Δ0 trp3-1 sir2Δ::NatMX [pRS41H-TdCEN3-Tdhmra1Δ::K. lactis URA3]*	This study
JRY10178	*T. delbrueckii*	*MATα ura3Δ0 trp3-1 sir4Δ::NatMX [pRS41H-TdCEN3-Tdhmra1Δ::K. lactis URA3]*	This study
JRY10179	*T. delbrueckii*	*MATα ura3Δ0 trp3-1 [pRS41H-TdCEN3-Tdhmra1Δ::K.*	This study

		lactis URA3_regionCΔ]	
JRY10180	*T. delbrueckii*	*MATα ura3Δ0 trp3-1 [pRS41H-TdCEN3-Tdhmra1Δ::K. lactis URA3_regionAΔ]*	This study
JRY10181	*T. delbrueckii*	*MATα ura3Δ0 trp3-1 [pRS41H-TdCEN3-Tdhmra1Δ::K. lactis URA3_regionBΔ]*	This study
JRY10182	*T. delbrueckii*	*MATα ura3Δ0 trp3-1 [pRS41H-TdCEN3-Tdhmra1Δ::K. lactis URA3_rap1-siteΔ]*	This study
JRY10183	*T. delbrueckii*	*MATα ura3Δ0 trp3-1 [pRS41H-TdCEN3-Tdhmra1Δ::K. lactis URA3_rap1-site-mutant]*	This study
JRY10184	*T. delbrueckii*	*MATα ura3Δ0 trp3-1 kos3Δ::KanMX SIR2-3xV5-NatMX*	This study
JRY10185	*T. delbrueckii*	*MATα ura3Δ0 trp3-1 kos3Δ::KanMX SIR4-3xV5-NatMX*	This study

RNA Isolation

Strains of both *S. cerevisiae* and *T. delbrueckii* were grown to an A600 of 0.8-1.0 at 30°C in YPD. RNA was extracted as described previously using the hot acid-phenol method (COLLART and OLIVIERO 2001; ELLAHI *et al.* 2015).

Table 3.2 RNA-Seq Reads Per Data Set

Strain	Alias	Total Reads	Reads Mapped	% Reads Mapped	% Mapped Non-Uniquely
JRY9316	wildTypeA	15747860	14480231	92	6.9
JRY9316	wildTypeB	20204590	18636063	92.2	6.8
JRY9316	wildTypeC	19988764	18323263	91.7	9
JRY10153	sir1_A	16667732	15105456	90.6	7.1
JRY10154	sir1_B	21854922	20320743	93	6.9
JRY10155	sir1_C	25010370	23014267	92	7.1
JRY10156	td_Wildtype_A	15286600	14186364	92.8	2.2
JRY10156	td_Wildtype_B	19561586	17479536	89.4	3.8
JRY10156	td_Wildtype_C	15787518	14440572	91.5	2.7
JRY10157	kos3_A	18855860	16598907	88	2.4
JRY10157	kos3_B	12373772	10960974	88.6	2.4
JRY10157	kos3_C	9463160	8657370	91.5	2.1
JRY10158	td_sir2_A	22461150	19501160	86.8	1.9
JRY10158	td_sir2_B	34093000	30790506	90.3	2.7
JRY10158	td_sir2_C	17313930	15385654	88.9	2.3
JRY10159	td_sir4_A	34504902	31345497	90.8	2.3
JRY10159	td_sir4_B	19359522	17642827	91.1	2.7
JRY10159	td_sir4_C	22980378	20541732	89.4	2.3
JRY10163	td_ago1_A	20246704	18125537	89.5	1.8
JRY10163	td_ago1_B	17229086	15783662	91.6	2.3
JRY10163	td_ago1_C	25218810	22352227	88.6	1.8
JRY10164	td_dcr1_A	26475104	24049831	90.8	2.9

JRY10164	td_dcr1_B	26475104	24049831	90.8	2.9
JRY10164	td_dcr1_C	18018972	15589654	86.5	2.5
JRY10165	ago1dcr1_A	17995398	15313261	85.1	2
JRY10165	ago1dcr1_B	24626138	23131252	93.9	2.4
JRY10165	ago1dcr1_C	17013842	16058396	94.4	3.3

Chromatin Isolation and Immunoprecipitation

All strains were grown in 100ml YPD and harvested in log phase at an A_{600} of ~0.7. Cross-linking was performed at 25°C in 1% formaldehyde for 45 minutes. Chromatin was prepared as previously described (APARICIO *et al.* 2005). Sonication was performed to an average genomic fragment size of 300-400 base pairs. Immunoprecipitation of V5 epitope-tagged ScSir1, TdKos3, TdSir2, and TdSir4 was performed overnight at 4°C using 800µl of chromatin and 75µl of anti-V5 resin from Sigma (A7345). After several washes, protein and DNA was eluted from beads in TE buffer + 1% SDS at 65°C, followed by reverse crosslinking, followed by protease treatment. DNA was purified using Qiagen DNA spin columns prior to library preparation. Functions of epitope-tagged *SIR* alleles in *T. delbrueckii* were assayed by measuring repression at the silent *HMRa1* gene; function of V5-tagged ScSir1 was measured by mating.

Table 3.3: ChIP-Seq Reads Per Data Set

Strain	Alias	Sample	Total_Reads	Reads_Mapped	Genome-wide_Median
JRY10152	scSir1_IP	IP	38416222	20135820	132
JRY10152	scSir1_in	input	24223214	13916174	91
JRY9316	scNoTag_IP	IP	41359126	33887088	211
JRY9316	scNoTag_in	input	30951676	22488089	143
JRY10160	kos3_IP	IP	30692204	28180256	208
JRY10160	kos3_in	input	37857090	23046669	83
JRY10161	tdSir2_IP	IP	64772046	61078532	283
JRY10161	tdSir2_in	input	33789380	26576719	253
JRY10162	tdSir4_IP	IP	34959374	26516814	198
JRY10162	tdSir4_in	input	49459360	35696614	267
JRY10156	td_NoTag_IP	IP	34902818	30961776	271
JRY10156	td_NoTag_in	input	53648772	46344215	431
JRY10185	td_sir4_kos3Δ_IP	IP	33347158	23556275	39
JRY10184	td_sir2_kos3Δ_IP	IP	42035285	31642374	152
JRY10184	td_sir2_kos3Δ_in	input	42467510	8631392	30

Library Preparation and Sequencing

ChIP libraries were prepared using the Illumina TruSeq DNA Sample Prep kit. RNA-Seq libraries were prepared using the Illumina TruSeq mRNA Sample Prep kit. 100-bp paired-end libraries were used to accurately assign reads. A Bioanalyzer instrument (Agilent) was used to quantify all libraries. Libraries were sequenced on an Illumina HiSeq 2000 machine. Reads were

deposited in the NCBI Sequence Read Archive (SRA) at http://www.ncbi.nlm.nih.gov/sra under accession numbers SRP055208, SRP065348, SRP065349, SRP065572, and SRP065573.

URA3 Reporter-Gene Assay for Silencing

Cells were grown to saturation overnight in 2ml of YPD containing hygromycin B drug (to select for plasmids). Cells were then pinned onto plates with three different media: CSM containing hygromycin B (to assay overall growth), CSM medium containing hygromycin B and lacking uracil (to select for cells expressing *URA3*), and CSM containing uracil and 5-fluoroorotic acid (5FOA) to select for cells lacking URA3 function (BOEKE *et al.* 1987). Cells were pinned in a 5-fold dilution series, and plates were imaged on day three of growth.

Data Analysis

ChIP-Seq. Reads were mapped using Bowtie2 to either the *Saccharomyces cerevisiae* S288C reference genome or the *T. delbrueckii* reference genome sequence (GORDON *et al.* 2011). Duplicate reads were discarded using Picard and pileup files were generated using Samtools (LI *et al.* 2009). Data was plotted and visualized using custom python scripts. Statistically significant peaks of enrichment in IP samples were found by using the MACS peak calling software (ZHANG *et al.* 2008).

RNA-Seq. Data were analyzed as previously described (ELLAHI *et al.* 2015). Briefly, Tophat2 was used to map reads. Transcript quantification was performed using Cufflinks (TRAPNELL *et al.* 2012). DESeq was used to perform tests for differential gene expression (ANDERS and HUBER 2010). Results were filtered for genes that showed differences in expression greater than two-fold relative to Wild type, with p-value of <0.05 and a false-discovery rate of $< 10\%$. Weighted Venn diagrams detailing overlap in gene sets were made using the Matplotlib_venn package in Python.

Transcription Factor Binding Site Analysis. Putative transcription factor binding sites were identified by the motif scanning algorithm in MochiView (HOMANN and JOHNSON 2010).

GO-Term Analysis. Gene sets were subject to GO term analysis on the *Saccharomyces Genome Database* website using the "Go Term Finder" tool using default settings and background sets of genes . All significant GO terms with p-value < 0.05 and false discovery rate of $< 10\%$ were noted.

3.4 Results

3.4.1 *S. cerevisiae* Sir1 Localized To The Autonomous Silencers of *HML* and *HMR-E*

Previous studies of genome-wide Sir protein localization in *S. cerevisiae* have focused on Sir2, Sir3, and Sir4 (THURTLE and RINE 2014b; ELLAHI *et al.* 2015). To study Sir1's evolution, we first established the molecular topography of Sir1 across the *S. cerevisiae* genome. Chromatin immunoprecipitation of tagged ScSir1-V5 followed by deep sequencing (ChIP-Seq) revealed

several important features of Sir1's genome-wide binding profile. First, ScSir1 displayed a sharp, narrow, largely silencer-restricted binding profile at *HML-E*, *HML-I*, and *HMR-E* (Figure 3.1; No Tag control shown in Figure 3.2). This distribution was in agreement with previous ChIP-PCR data suggesting that Sir1 is restricted to the *HMR-E* silencer (RUSCHE *et al.* 2002). Sir1's binding profile was strikingly different from previous data on Sir2, Sir3, and Sir4. Those proteins exhibit strong co-enrichment in discrete peaks both at the pair of silencers blanking both *HML* and *HMR* as well as within the *HMLα* and *HMRa* loci (THURTLE and RINE 2014b). ScSir1 enrichment overlapped with Sir2, Sir3, and Sir4 enrichment at three of the silencers and at a smaller peak located in the promoter region of *HMLα* but not within *HMRa* (Figure 3.1A). No Sir1 enrichment was detected at the *HMR-I* silencer. Each silencer at *HML* is sufficient, on its own, for silencing *HML* (MAHONEY and BROACH 1989). At *HMR,* the *E* silencer is required for *HMR* silencing. The *HMR-I* contributes to silencing when the locus is carried on a plasmid, but on its own is insufficient to silence *HMR* and can be deleted from the chromosome with no obvious impact on silencing (ABRAHAM *et al.* 1984; BRAND *et al.* 1985).

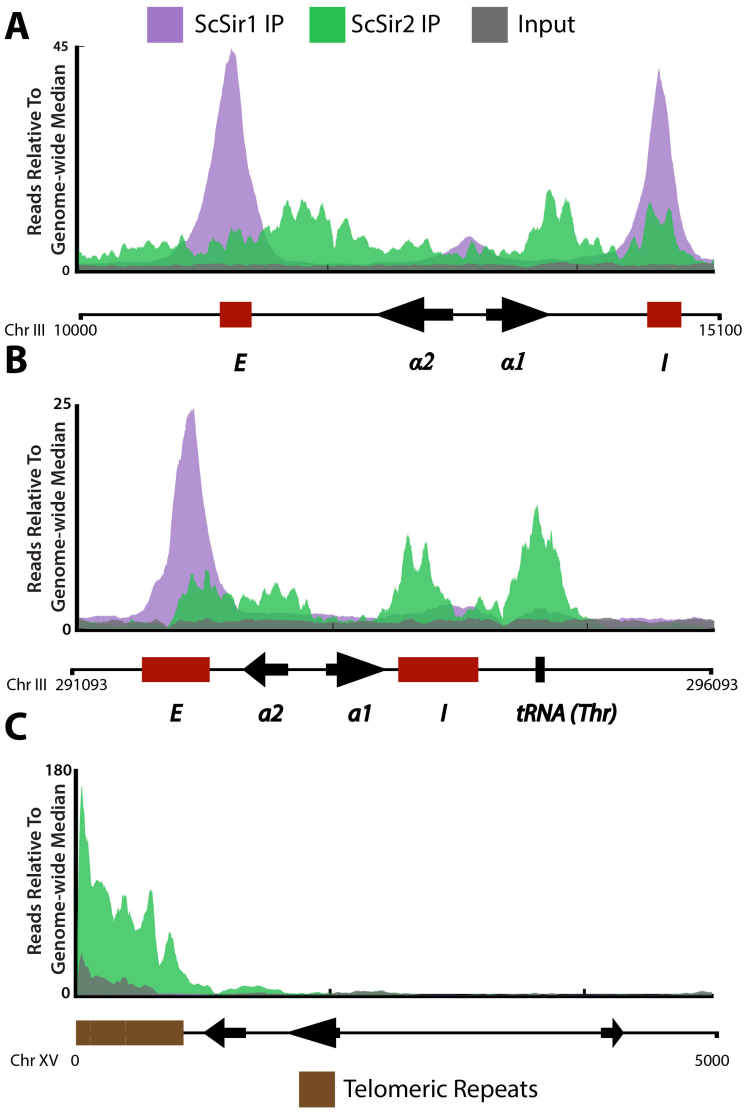

Figure 3.1. ScSir1 associates with the silencers of *HMLα* and *HMR-E* in *S. cerevisiae*. Chromatin immunoprecipitation following by deep-sequencing was performed on V5-tagged ScSir1 protein. Shown are the ScSir1-3xV5 IP enrichment patterns (purple) at various genomic loci, with chromosomal coordinates shown on bottom axis of each panel. Input shown in gray. (A) ScSir1 at *HMLα*. *HMRa* is shown in (B). For comparison, binding of ScSir2 is shown in green. The *E* and *I* silencers are depicted by red boxes and coding genes by black arrows. (C) ScSir2 enrichment (green) at the left arm of chromosome XV, *TEL15*-L. ScSir1 was not enriched at this locus. By contrast, ScSir2 enrichment was high.

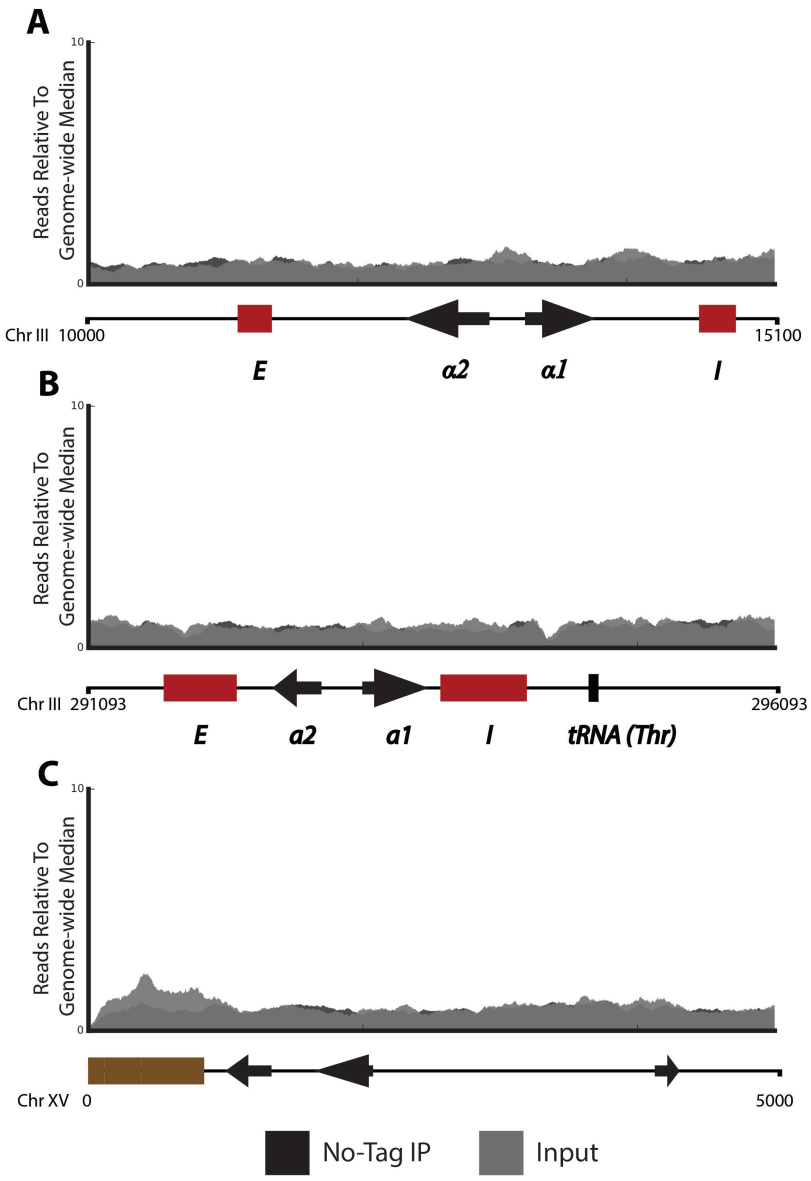

Figure 3.2. No tag IP and input enrichment in *S. cerevisiae.* No tag IP and input tracks shown for *S. cerevisiae* at *HMLα* (A), *HMRa* (B), and *TEL15L* (C). IP shown in black, input in gray, in terms of reads relative to genome-wide median.

3.4.2 *S. cerevisiae* Sir1 Was Absent From Telomeres

Telomeres in *S. cerevisiae* recruit the Sir2, Sir3, and Sir4 proteins through interactions with Rap1 (MORETTI *et al.* 1994). Mutations in *SIR2, SIR3,* and *SIR4*, but not *SIR1*, disrupt transcriptional repression of reporter genes placed adjacent to artificially truncated telomeres (APARICIO *et al.* 1991; THURTLE and RINE 2014b). These early studies suggested *SIR1* has no

role in gene silencing near artificial telomeres. However, one study of a *URA3* reporter gene at a native telomere (*TEL11L*) indicated a role for Sir1 in repressing genes at native telomeres (PRYDE and LOUIS 1999). Thus, *SIR1*'s role in telomeric and subtelomeric silencing warranted further genome-wide evaluation.

Strikingly, our results showed that the Sir1 protein was undetectable at all telomeres and subtelomeric regions (*TEL15L* shown in Figure 3.1C; see Figure 3.3 for all 32 telomeres). The sole exceptions to this rule are the Sir1 peaks at the silencers of *HML*α, which fall within 20 kbp of chromosome III (Figure 3.1A and Figure 3.3). In contrast, ScSir2, ScSir3, and ScSir4 are all highly enriched at the telomeres, where they repress ~6% of subtelomeric genes (Figure 3.1C and (THURTLE and RINE 2014b; ELLAHI *et al.* 2015)). To test the possibility that Sir1 might bind telomeres transiently, long enough to repress genes but not long enough to be detectably enriched, we performed deep-sequencing of mRNAs from wild-type and *sir1Δ* strains. Genes at *HML*α and *HMRa* were de-repressed in the *sir1Δ* strain, as expected, as were genes under a/a control (Table 3.4). However, consistent with a lack of Sir1 binding at and/or near telomeres, no subtelomeric genes were de-repressed in the *sir1Δ* mutant.

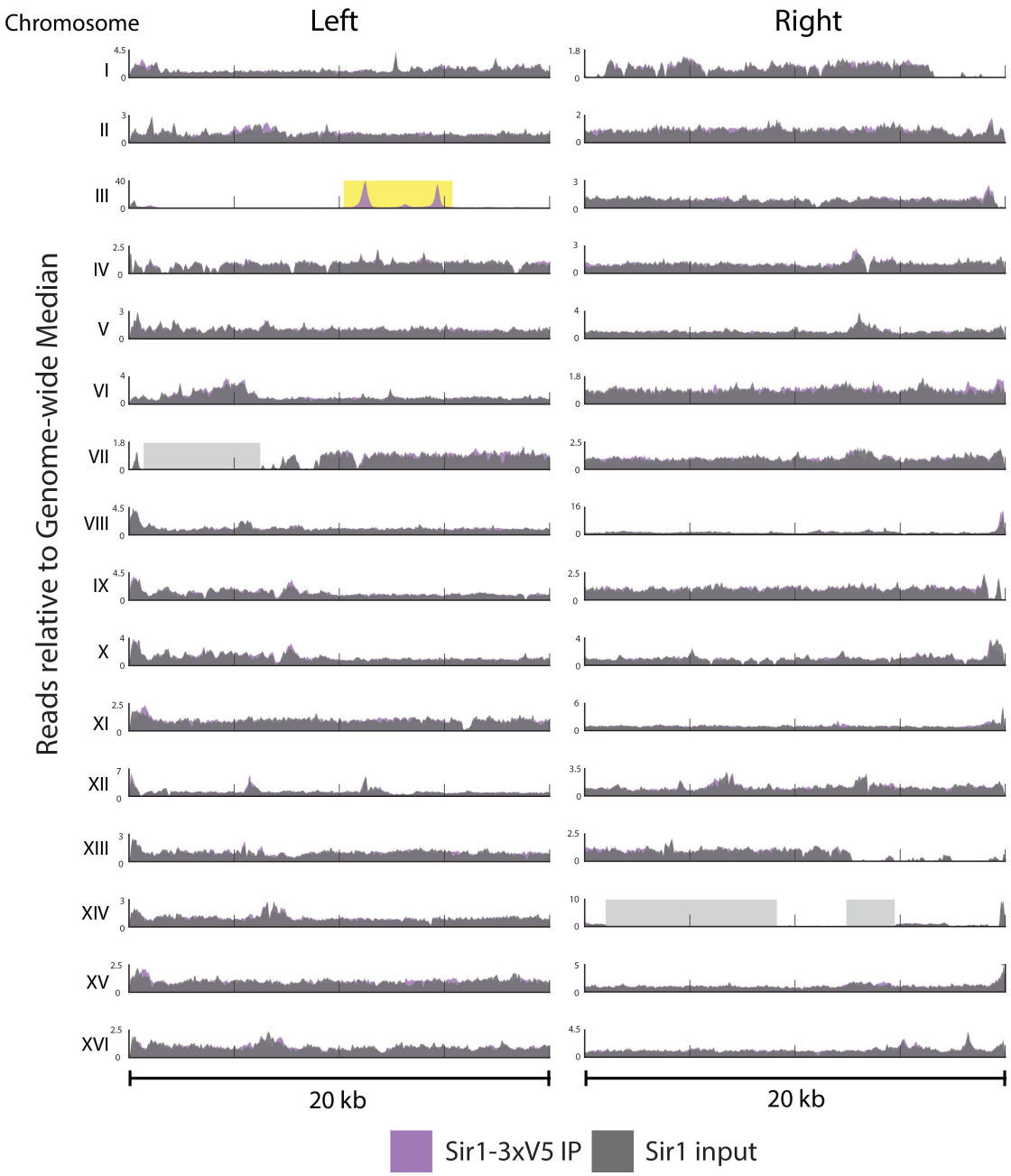

Figure 3.3. Lack of Sir1 enrichment at 31 out of 32 *S. cerevisiae* telomeres. Sir1 IP shown in purple, input shown in gray. Sir1 enrichment is seen at *HMLα* on *TEL03L* (yellow box). 20kb inward from the left and right ends of each chromosome is shown. Regions deleted in the W303 strain relative to S288C shown in gray.

Table 3.4: Genes Increasing and Decreasing in Expression in *sir1Δ*

Shown below is the list of genes that statistically significantly increased or decreased in expression by 2-fold or greater in the *sir1*Δ mutant relative to Wild type. Expression is shown in units of Fragments per Kilobase per Million reads (FPKM).

Genes Increasing				
Gene	Systematic Name	Wild type FPKM	*sir1Δ*	Log_2 Fold-Change
HMRA1	*YCR097W*	0.02	21.62	Inf
HMLALPHA1	*YCL066W*	0	2.14	Inf
YCL065W	*YCL065W*	0	3.37015	Inf
HMLALPHA2	*YCL067C*	0.02	11.17	Inf
FUS1	*YCL027W*	2.80	13.0	2.17
HMX1	*YLR205C*	6.71	28.62	2.16
YDR426C	*YDR426C*	3.95	12.82	2.02
AGA1	*YNR044W*	18.81	75.23	2.01
AGA2	*YGL032C*	87.78	300.10	1.76
GPM2	*YDL021W*	6.54	17.01	1.39
TMA10	*YLR327C*	48.23	99.15	1.28
KAR4	*YCL055W*	12.85	30.56	1.27
CYC7	*YEL039C*	11.21	25.88	1.22
BAR1	*YIL015W*	44.74	101.48	1.19
SPO11	*YHL022C*	0.99	2.81	1.19
SCM4	*YGR049W*	51.79	110.81	1.16
YNL155W	*YNL155W*	22.01	47.49	1.07
STR3	*YGL184C*	11.73	24.72	1.07
GPG1	*YGL121C*	22.92	46.69	1.02
Genes Decreasing				
YLR413W	*YLR413W*	389.82	194.19	-1.00
PHO5	*YBR093C*	915.81	453.48	-1.00
PHO89	*YBR296C*	73.89	36.65	-1.10
ZRT1	*YGL255W*	389.91	184.98	-1.10
TOS6	*YNL300W*	340.12	172.12	-1.10
PHO12	*YHR215W*	400.97	151.36	-1.34
PHO11	*YAR071W*	244.35	81.25	-1.66

3.4.3 The *Torulaspora delbrueckii* Genome Contains *KOS3,* an Ancestral *SIR1* Paralog

A reconstruction of the evolutionary history of the *SIR1* gene (GALLAGHER *et al.* 2009) yielded two important findings: (1) *SIR1* has undergone at least two to three gene duplications among post-whole-genome-duplication yeast species; and (2) *SIR1* may itself may also be the product of an internal duplication of a shorter *SIR1* paralog called *KOS3 (Kin of Sir1),* first recognized in *S. bayanus v. uvarnum*. This paralog dates back to pre-whole genome duplication yeast species (GALLAGHER *et al.* 2009). *Torulaspora delbrueckii*, like *Zygosaccharomyces rouxii*, also has a *KOS3* ortholog as its only Sir1-related gene (Figure 3.4). *TdKOS3* is approximately half the sequence length of *SIR1* and best aligns to the C-terminal Orc1-interacting region of Sir1. *S. bayanus v. uvarum*, *N. castellii*, and *N. diarenesis* also have *KOS3* paralogs of similar size (Figure 3.4). The *KOS3* paralog in *S. bayanus v uvarum* participates in silencing, though its function is partially shared with the other three paralogs in that species (GALLAGHER *et al.* 2009). All identified *SIR1* paralogs are highly divergent at the protein sequence level (GALLAGHER *et al.* 2009). Similarly, ScSir1 and TdKos3 share only 16% protein similarity.

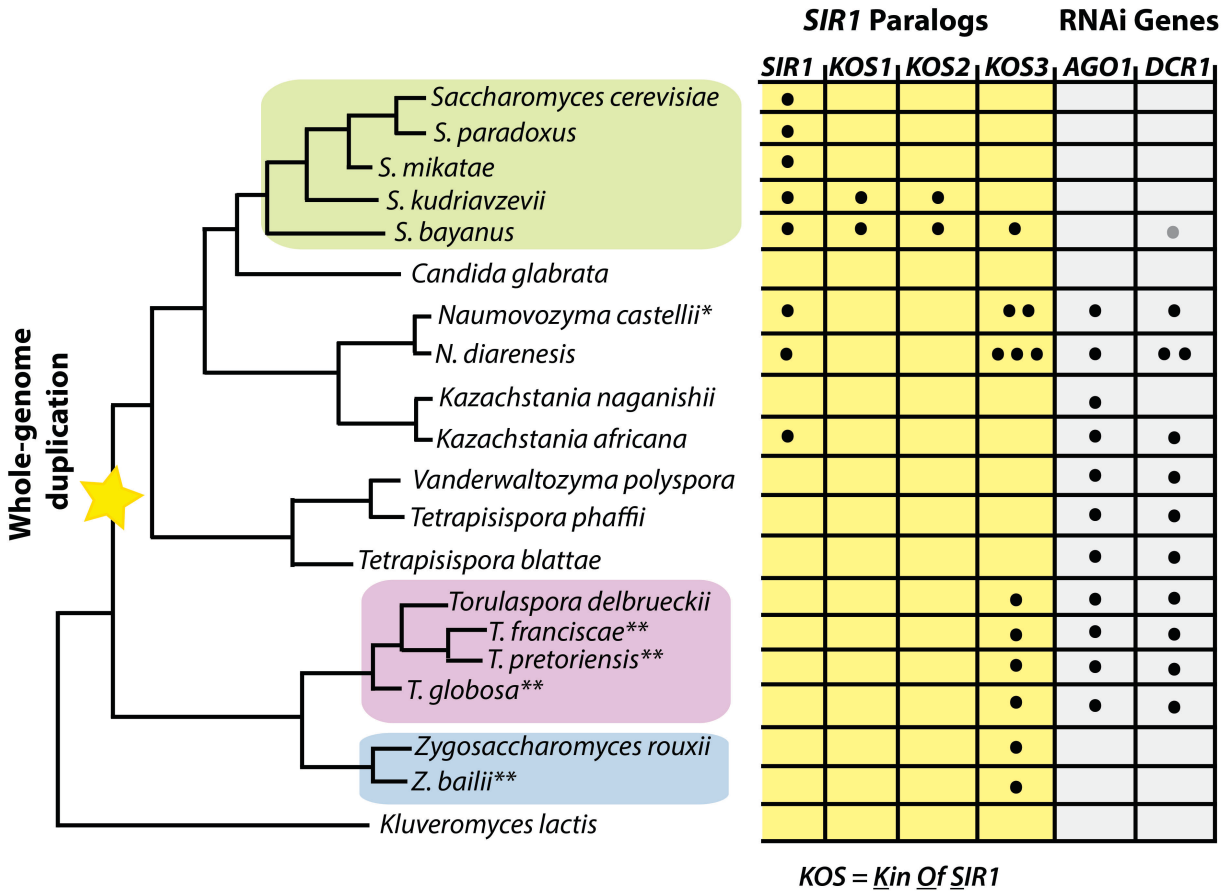

Figure 3.4. *SIR1* Paralogs and RNAi Genes In The *Saccharomycetaceae* Family. Depicted is a phylogenetic tree of budding yeast species in the *Saccharomycetacae* family along with the *SIR1* paralogs and RNAi gene paralogs (where applicable; some species that do not have *SIR1* or RNAi genes *AGO1* and *DCR1*; e.g. *K. lactis*). The number of dots within each box indicates the number of copies of that particular paralog in the genome (e.g., *N. castellii* has two highly similar *KOS3* paralogs). *S. cerevisiae* contains the defining *SIR1* gene, whereas *S. bayanus* contains four *SIR1* genes: *SIR1* and three kin-of-Sir1 (*KOS*) paralogs. *KOS3* is the earliest *SIR1* paralog, deduced to have occurred prior to the whole-genome duplication. *T. delbrueckii* also has the budding yeast orthologs of *AGO1* and *DCR1*. All sequenced species in the *Zygosaccharomyces* and *Torulaspora* clades have a *KOS3* paralog in their genomes. **N. castellii* also has a fourth *SIR1* paralog, *KOS4*, specific to that species; not shown for simplicity. **Results from additional species (*Z. baillii, T. francisiae, T. pretoriensis, T. globosa*) are unpublished (Devin Scannell, personal communication). Note: the gray dot in the *DCR1* gene column for *S. bayanus var. uvarum* indicates that its *DCR1* is a pseudogene.

3.4.4 *KOS3* was Indispensible For Silencing in *T. delbrueckii*

In *S. cerevisiae*, deletion of *SIR1* causes a partial loss of silencing at *HMLα* and *HMRa* when evaluated at the population level. At the single-cell level, 50-80% of *sir1*Δ cells lack silencing at *HMLα* and *HMRa*, whereas these loci are fully silenced in the remaining cells (DODSON and RINE 2015). Thus, expression of *HMRa1* in a *sir1Δ* strain, as measured in bulk RNA from a population of cells, is less than the expression seen in *Scsir2Δ*, *Scsir3Δ,* or *Scsir4Δ* cells (Figure 3.5A).

To evaluate whether *KOS3* was also only partially required for silencing in *T. delbrueckii,* or played a more prominent role, we measured expression of the *HMRa1* locus in a *MATα* strain containing deletion alleles of *KOS3, SIR2,* or *SIR4* (the *SIR3* ortholog in *T. delbrueckii* is *ORC1*, which appears to be essential; unpublished observation). In contrast to the partial de-repression of *HMRa1* seen in *S. cerevisiae sir1Δ*, In *T. delbrueckii kos3Δ* cells showed complete de-repression of *HMRa1*, indistinguishable from that in *sir2Δ* and *sir4Δ* (Figure 3.5B). Thus, *KOS3* played a more central role in silencing in *T. delbrueckii* as compared to *S. cerevisiae's SIR1*.

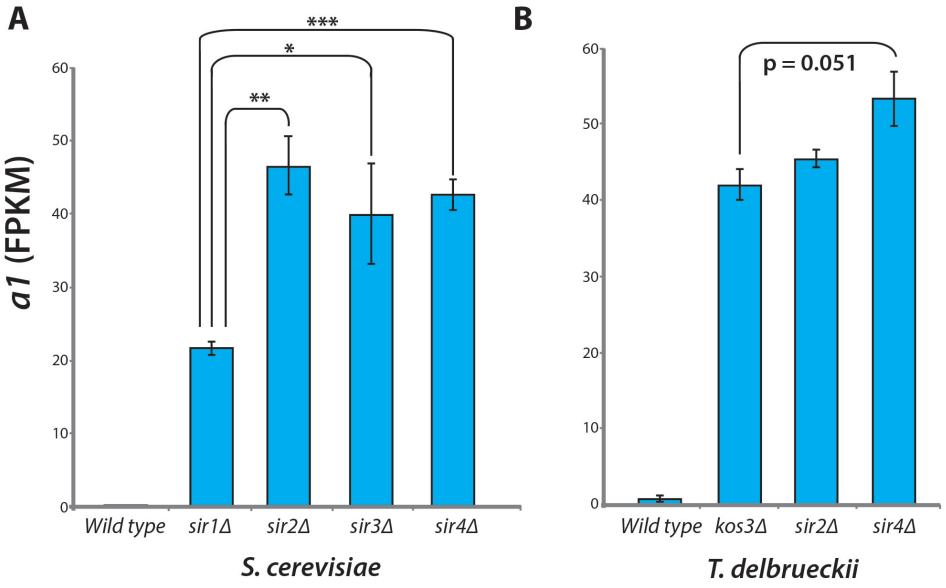

Figure 3.5. *T. delbrueckii kos3*Δ Mutants Exhibit a Complete Lack of Silencing at *HMRa*. (A) *HMRa1* expression in wild type and four *S. cerevisiae* silencing mutants: *sir1*Δ, *sir2*Δ, *sir3*Δ, and *sir4*Δ. Expression was measured from deep sequencing of mRNAs and quantified as Fragments per Kilobase per Million reads (FPKM). Because *sir1*Δ mutants in *S. cerevisiae* are able to inefficiently re-establish heritable silencing, the total extent of *a1* de-repression measured in a population of *sir1*Δ cells is ~50% that of the de-repression measured in *sir2*Δ, *sir3*Δ, and *sir4*Δ mutants, which completely lack the ability to silence the *HML* and *HMR*. Students t-test was performed to calculate the significance in the difference in mean FPKM values for comparisons shown. p-values: * < 0.01 to 0.05, ** 0.001 to 0.01, *** < 0.001. (B) *HMRa1* expression in *T. delbrueckii* in four genetic conditions: wild type, *kos3*Δ, *sir2*Δ, and *sir4*Δ. In contrast to the more modest effect of deleting *ScSIR1,* deletion of *TdKOS3* leads to as great of a silencing defect as deleting *TdSIR2* or *TdSIR4*.

3.4.5 *T. delbrueckii* Kos3 Co-localized With Sir2 and Sir4 at all Heterochromatic Locations

The genome-wide binding profiles of Kos3, Sir2, and Sir4, in *T. delbrueckii* were striking with respect to the differences with Sir protein distributions in *S. cerevisiae*. At *HMR* TdKos3 was most enriched in a pair of close but discrete peaks beginning approximately 670 base pairs and 3' of *HMRa1,* which were also the positions most enriched for Sir2 and Sir4. The first of these peaks corresponded to a tRNA-Val gene. Remarkably the enrichment of all three proteins over the promoter regions of *HMR* was modest at best, and was difficult to reconcile with spreading of Sir protein complexes, as envisioned for Sir proteins in *S. cerevisiae*. The distribution of Kos3, Sir2 and Sir4 at *HML*α echoed the theme from *HMR* but with only a single prominent peak of enrichment 770 base pairs from the 3' end of *HML*α*1* (Figure 3.6A and 3.6B). In contrast to *HMR*, all three silencing proteins showed some enrichment within *HML*, and with a minor peak corresponding to the promoter regions between *HML*α*1* and *HML*α*2*. At neither *HML* nor *HMR* of *T. delbrueckii* was there evidence of two sites of enrichment peaks analogous to the two silencers flanking *HML* in *S. cerevisiae*.

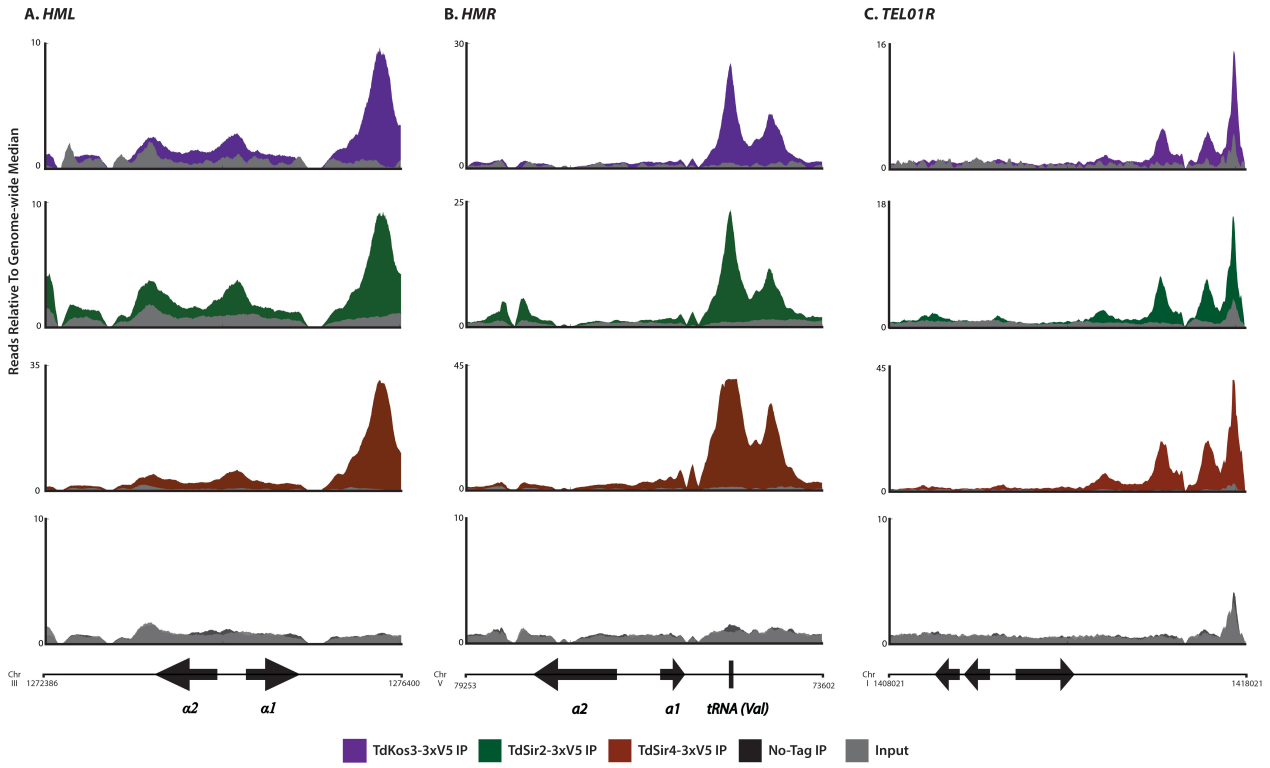

Figure 3.6. Enrichment of Kos3, Sir2, and Sir4 at heterochromatic regions in *T. delbrueckii*. Chromatin immunoprecipitation and deep sequencing of V5-tagged TdKos3, TdSir2, and TdSir4, and a control strain with no V5 tagged genes. Shown are the enrichment patterns of the three proteins at (A) *HML,* (B) *HMR*, and (C) a representative telomere: *TEL01R*. The binding pattern of TdKos3 (dark purple) mirrored the binding pattern of TdSir2 (dark green) and TdSir4 (brown) at these loci. The No-tag control immunoprecipitation is shown in black. Black arrows without labels depict nearby coding genes. Input values for each sample are shown in gray.

In addition to examining Kos3 binding at *HML* and *HMR*, we also interrogated Kos3 enrichment at presumptive telomeres in *T. delbrueckii* to determine whether TdKos3 was absent from telomeres, as Sir1 was in *S. cerevisiae*. Kos3, Sir2, and Sir4 were enriched at eleven telomeres: *TEL01L*, *TEL02L*, *TEL04L*, *TEL07L*, *TEL08L*, *TEL01R*, *TEL04R*, *TEL05R*, *TEL06R*, and *TEL08R* (Figure 3.6C shows *TEL01R*; see Figure 3.7 for all 16 telomeres). Kos3's presence at telomeric sequences in *T. delbrueckii* was a marked difference to ScSir1's absence from telomeres in *S. cerevisiae*. Likewise, many genes within 20 kilobases of chromosome ends increased in expression in all three *T. delbrueckii sir* mutants examined (*kos3Δ, sir2Δ,* and *sir4Δ*) (Table 3.5 and Figure 3.10). Thus, similar to its more extensive role in silencing at *T. delbrueckii HML* and *HMR*, Kos3 also repressed expression of subtelomeric genes.

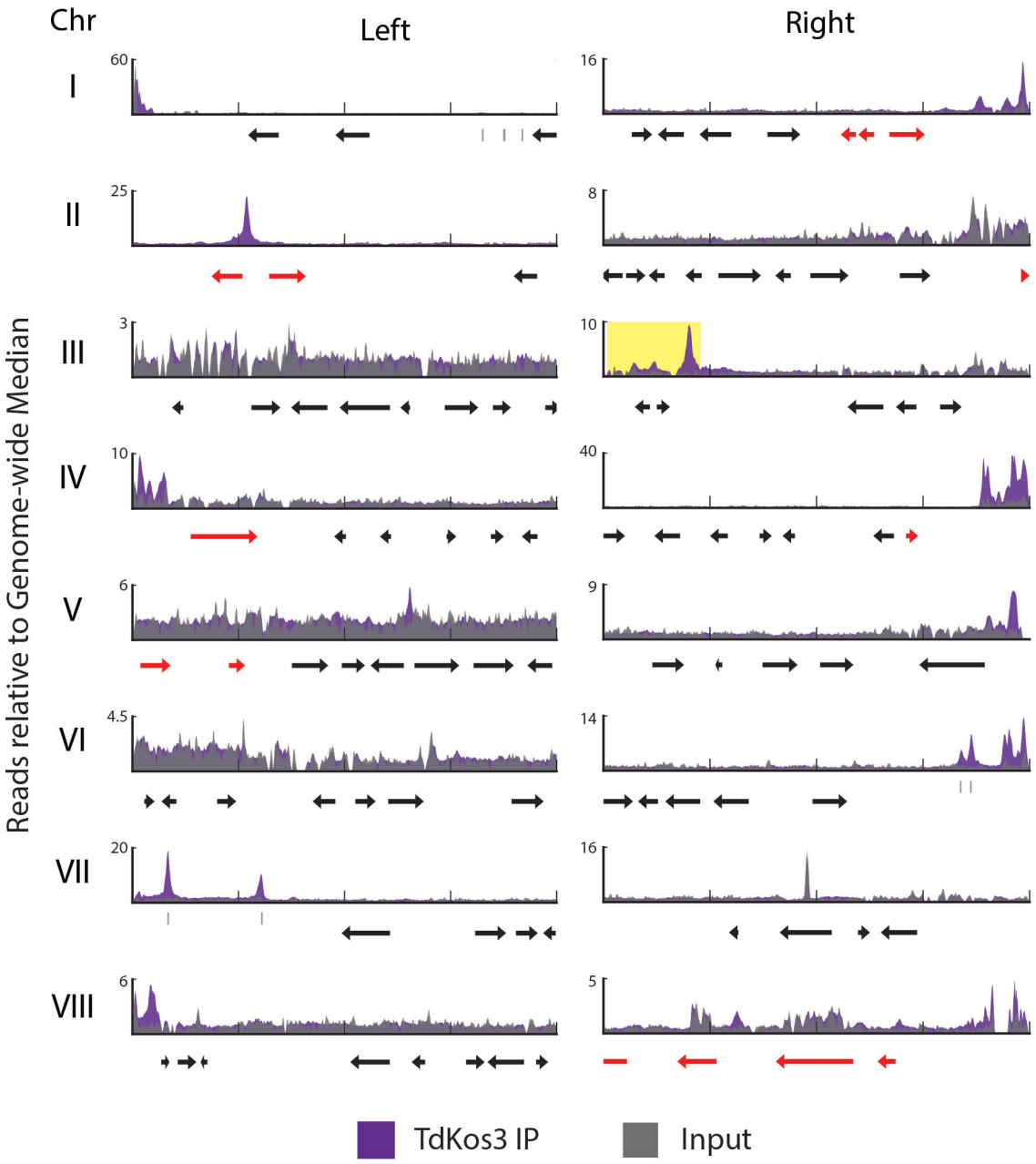

Figure 3.7. Enrichment of Kos3 telomeres in *T. delbrueckii.* Shown is Kos3 enrichment (dark purple) at eleven telomeres in *T. delbrueckii*: *TEL01L, TEL01R, TEL02L, TEL03R, TEL04L, TEL04R, TEL05R, TEL06R, TEL07L, TEL08L,* and *TEL08R*. Open reading frames (ORFs) depicted in black arrows and tRNA genes depicted in gray boxes. *HML* on *TEL03R* boxed in yellow. Subtelomeric genes that significantly increased in expression in all three *sir* mutants relative to Wild type are shown in red arrows.

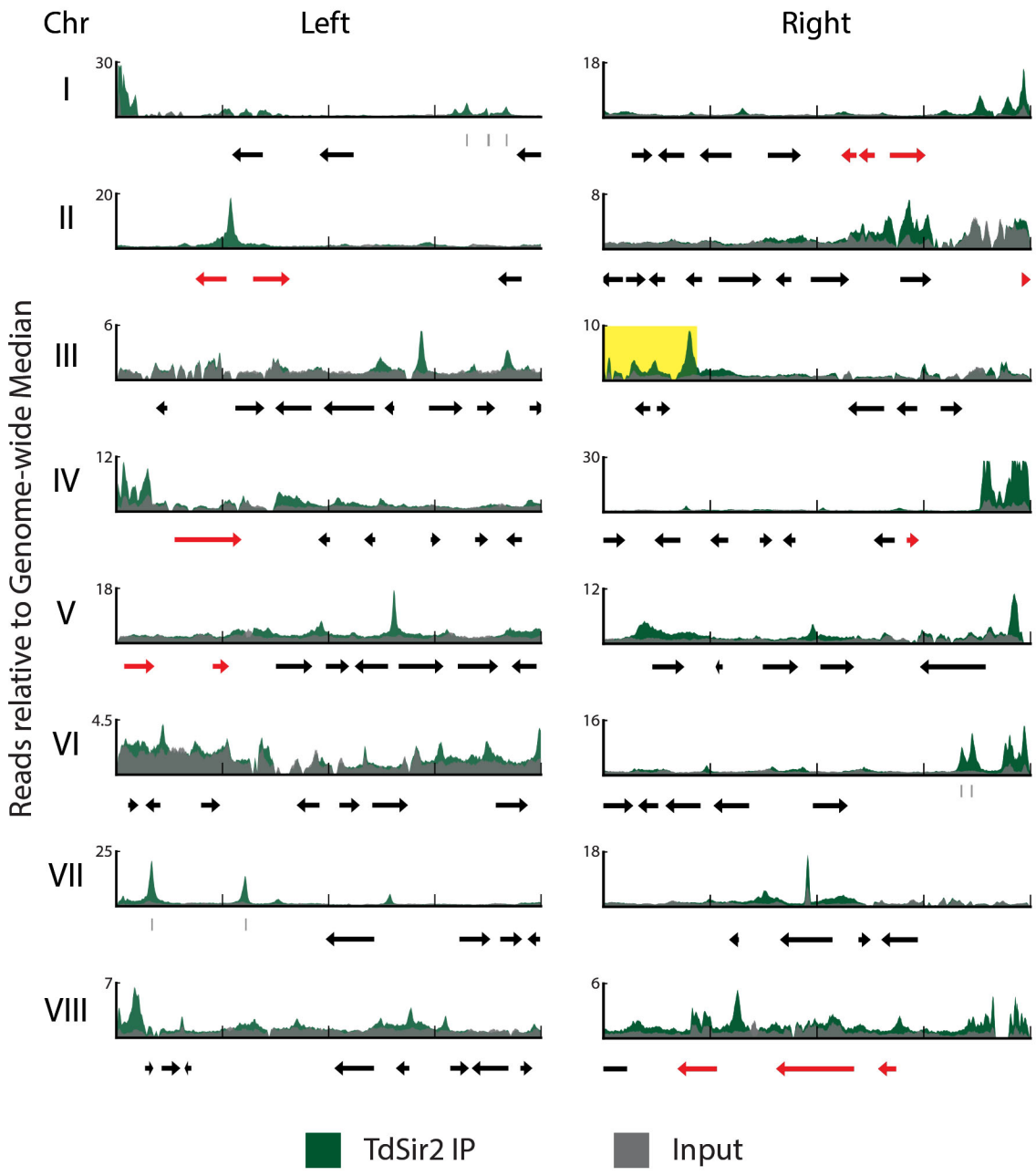

Figure 3.8. Enrichment of Sir2 at telomeres in *T. delbrueckii*. Genome features marked as in Figure 3.7. *HML* on *TEL03R* boxed in yellow. Subtelomeric genes that significantly increased in expression in all three *sir* mutants relative to Wild type are shown in red arrows.

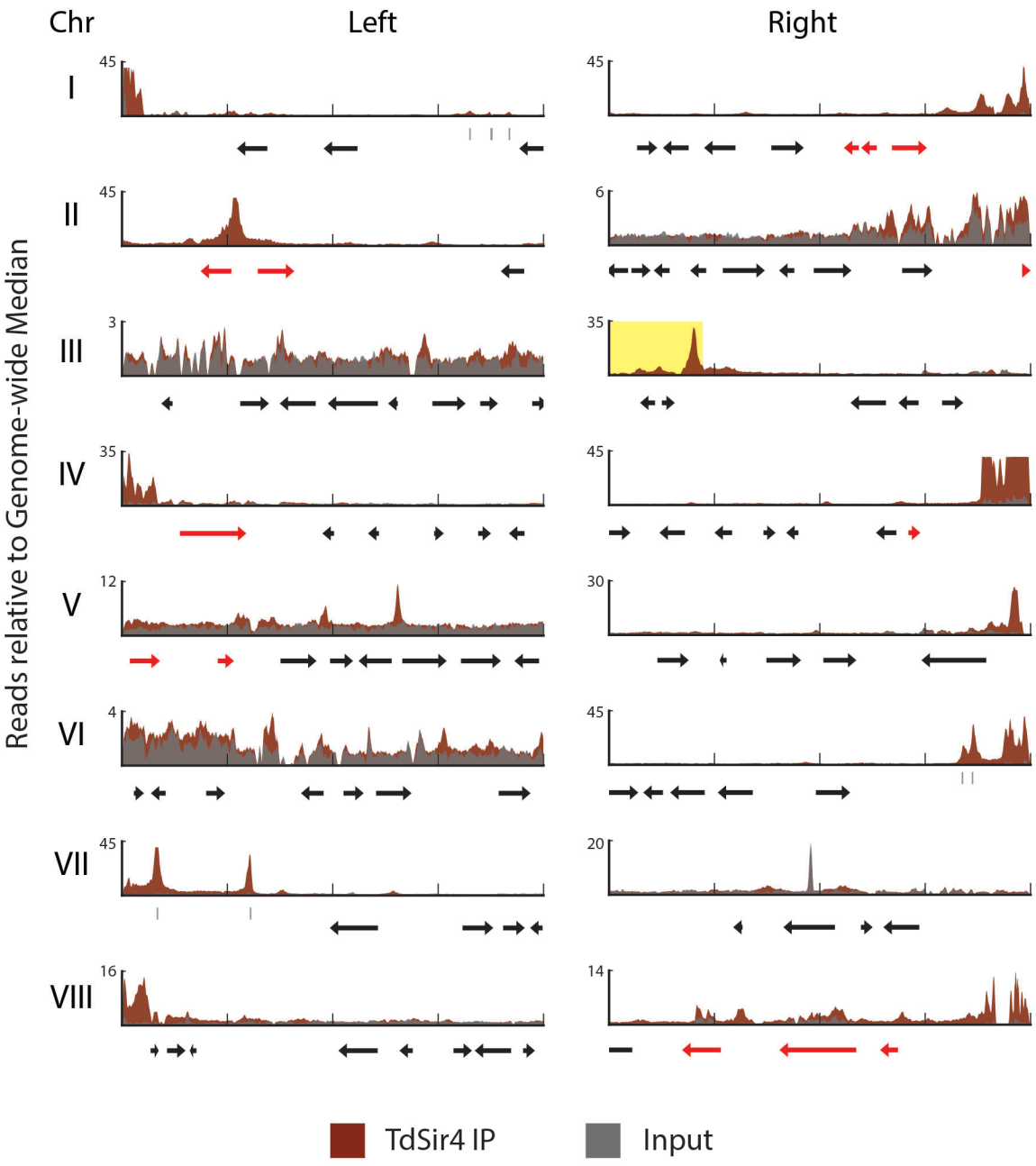

Figure 3.9. Enrichment of Td Sir4 at telomeres in *T. delbrueckii*. Genome features marked as in Figure 3.7. *HML* on *TEL03R* boxed in yellow. Subtelomeric genes that significantly increased in expression in all three *sir* mutants relative to Wild type are shown in red arrows.

3.4.6 *T. delbrueckii SIR2* Had Roles Outside of Its Functions with *KOS3* and *SIR4*

We interrogated genome-wide functions for *T. delbrueckii KOS3*, *SIR2*, and *SIR4* by performing mRNA-Seq in *kos3*Δ, *sir2*Δ, and *sir4*Δ mutants. Overall, twenty-two genes increased in expression across all three mutants (Table 3.5). These twenty-two genes were all genes either at the silenced mating type loci, adjacent to the silent mating type loci, or were subtelomeric genes within 20kb of a chromosome end. No centromere-adjacent genes changed expression among this set of mutants. When comparing the overlap between genes across all three *sir* mutants, we found that the majority of the changes in expression in the *kos3*Δ and *sir4*Δ mutants completely overlapped with the *sir2*Δ mutant, suggesting that *KOS3* and *SIR4* did not have any function outside of their role in the Sir complex (Figure 3.10B). There were 124 genes that increased specifically in the *sir2*Δ mutant, however, indicating that like *SIR2* in *S. cerevisiae, T. delbrueckii SIR2* has roles beyond heterochromatin.

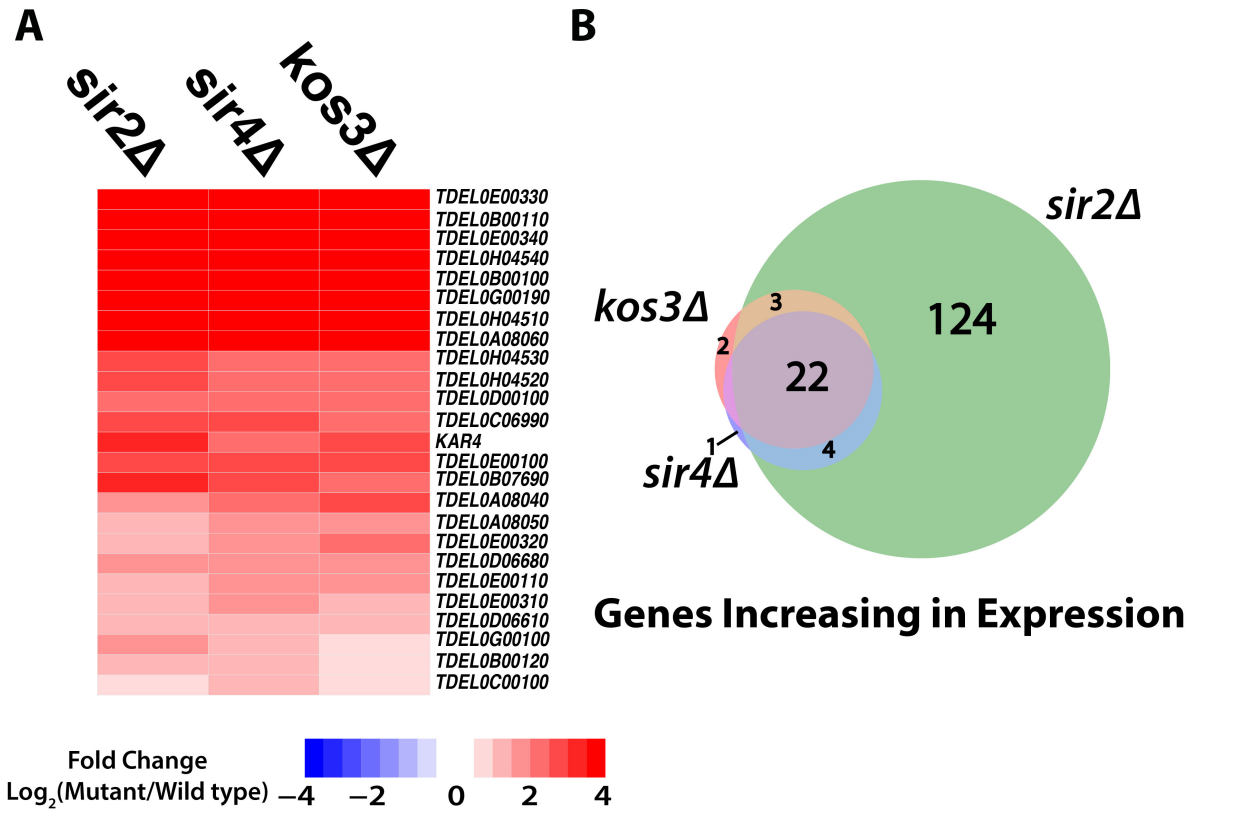

Figure 3.10. Summary of genes that significantly increased in expression in all three *sir* mutants in *T. delbrueckii* (*kos3*Δ, *sir2*Δ, and *sir4*Δ). (A) Heatmap of all genes that increased significantly relative to Wild type (red boxes) across all three mutants. (B) Venn diagram showing overlap of all genes that significantly increased in *kos3*Δ, *sir2*Δ, and *sir4*Δ. Genes specific to *kos3*Δ and *sir4*Δ are contained within the set specific to *sir2*Δ; many genes specifically increased in the *sir2*Δ only, suggesting that *SIR2* regulates many other genes in addition to the genes at *HML* and the two *HMR*s in *T. delbrueckii*.

Table 3.5: Genes Increasing In Expression in *T. delbrueckii sir* Mutants

Listed below are twenty-two subtelomeric genes and silent mating type loci genes that were de-repressed in all three *T. delbrueckii sir* mutants. Some of the subtelomeric genes on the same telomeric arm are adjacent to each other (for example, *TDEL0B00100* and *TDEL0B00110*). For those genes that have *S. cerevisiae* orthologs, the *S. cerevisiae* systematic name and three-letter name is provided.

T. delbrueckii Gene	*S. cerevisiae ortholog*	Wild type FPKM	*kos3*Δ FPKM	*sir2*Δ FPKM	*sir4*Δ FPKM	Description
TDEL0E00330	a1 gene at T. delbrueckii Chr V HMR	0.67	40.95	44.37	53.57	Silent mating type locus
TDEL0E00340	a2 gene at Chr V HMR	4.91	30.53	28.16	29.11	Silent mating type locus
TDEL0G00190	a1 gene at T. delbrueckii Chr VII HMR	0.67	39.07	43.35	52.26	Silent mating type locus
TDEL0E00310	N/A	14.29	37.15	37.41	48.66	Adjacent to silent mating type locus
TDEL0E00320	N/A	8.39	33.06	20.1	28.03	Adjacent to silent mating type locus
TDEL0A08040	N/A	10.44	61.2	37.98	46.64	Subtelomeric *(TEL01R)*
TDEL0A08050	N/A	3.05	10.85	6.85	8.77	Subtelomeric *(TEL01R)*
TDEL0A08060	N/A	1.49	26.46	21.86	24.12	Subtelomeric *(TEL01R)*
TDEL0B00100	N/A	2.28	503.74	402.2	608.34	Subtelomeric (*TEL02L)*
TDEL0B00110	N/A	2.77	192.53	190.95	168.79	Subtelomeric (*TEL02L)*
TDEL0B07690	N/A	101.14	503.52	1056.35	683.41	Subtelomeric (*TEL02R)*
TDEL0C06910	*YCL055W (KAR4)*	1.85	14.01	16.53	10.11	Subtelomeric (*TEL03R*)
TDEL0C06990	*DIC1* copy in X-region of *HML*	77.04	166.36	131.33	171.66	Subtelomeric (*TEL03R*)
TDEL0D00100	N/A	26.89	46.74	59.84	48.29	Subtelomeric *(TEL04L*)
TDEL0D06610	N/A	25.19	60.31	54.86	57.05	Subtelomeric *(TEL04R*)
TDEL0D06680	N/A	5.78	22.74	17.81	18.5	Subtelomeric *(TEL04R*)
TDEL0E00100	N/A	5.86	33.8	40.74	34.04	Subtelomeric (*TEL05L*)
TDEL0E00110	N/A	9.01	32.16	21.11	28.72	Subtelomeric (*TEL05L*)

TDEL0H04510	N/A	2.62	51.31	53.12	43.62	Subtelomeric (*TEL08R*)
TDEL0H04520	N/A	32.92	80.85	121.08	83.02	Subtelomeric (*TEL08R*)
TDEL0H04530	N/A	26.32	96.68	123.82	96.46	Subtelomeric (*TEL08R*)
TDEL0H04540	N/A	3.31	284.53	430.43	211.64	Subtelomeric (*TEL08R*)

To examine additional roles that *T. delbrueckii SIR2* may have, we performed GO term analysis on the 85 *sir2*Δ-specific genes that had orthologs in *S. cerevisiae*. Using the *S. cerevisiae* functional annotations for these genes, we found 21 genes that were associated with meiosis and sporulation, and 9 genes that were associated with carbohydrate metabolism (starred genes, Table 3.7).

Table 3.6 Genes Increasing and Decreasing in Expression Relative to Wild Type in *T. delbrueckii kos3*Δ Mutant

Shown below are the two-fold or greater statistically significant expression changes that occurred in the *kos3*Δ mutant relative to Wild type.

Gene Name	Description/S.cerevisiae ortholog	Wild Type Read Counts	Mutant Counts	Log_2 Fold-Change
TDEL0E00330	*silenced copy of a1 gene at T. delbrueckii HMR-2 locus*	0	23.34	inf
TDEL0B00100	*N/A*	23.54	5151.5	7.77
TDEL0G00190	*silenced copy of a1 gene at T. delbrueckii HMR-1 locus*	0.3	41.67	7.12
TDEL0H04540	*N/A*	20.37	1855.18	6.51
TDEL0B00110	*N/A*	31.5	2304.93	6.19
TDEL0E00340	*silenced copy of a2 gene at T. delbrueckii HMR-2 locus*	0.56	33.59	5.91
TDEL0H04510	*N/A*	34.31	650.35	4.24
TDEL0A08060	*N/A*	19.43	329.58	4.08
TDEL0C06910	*Anc_1.12 YCL055W KAR4*	14.82	103.18	2.8
TDEL0E00100	*N/A*	66.67	389.42	2.55
TDEL0A08040	*N/A*	46.49	269.21	2.53

TDEL0B07690	*N/A*	240.6	1216.89	2.34
TDEL0H04530	*N/A*	358.29	1763.19	2.3
TDEL0H04520	*N/A*	99.47	464.31	2.22
TDEL0D00100	*N/A*	33.22	151.71	2.19
TDEL0C06990	*additional copy of DIC1 in X region of T. delbrueckii HML locus*	3.66	15.83	2.11
TDEL0E00320	*N/A*	44.16	178.34	2.01
TDEL0E00110	*Possible pseudogene*	52.84	202.37	1.94
TDEL0A08050	*N/A*	15.63	59.74	1.93
TDEL0D06680	*N/A*	31.31	110.8	1.82
TDEL0E00270	*N/A*	110.71	305.47	1.46
TDEL0E00310	*N/A*	166.41	432.48	1.38
TDEL0E05490	*Anc_6.240 YGL138C YGL138C*	9.42	24.41	1.37
TDEL0D06610	*N/A*	266.07	644.94	1.28
TDEL0A08020	*N/A*	197.16	429.64	1.12
TDEL0A07280	*Anc_6.313 YCR045C RRT12*	94.62	205.37	1.12
TDEL0A07990	*Anc_1.194 YKR066C CCP1*	424.18	876.8	1.05
TDEL0E00350	*KOS3*	187.66	2.46	-6.25

Table 3.7: Genes Increasing and Decreasing in Expression Relative to Wild Type in *T. delbrueckii sir2*Δ mutant

Shown below are the two-fold or greater statistically significant expression changes that occurred in the *sir2*Δ mutant relative to Wild type. GO term analysis revealed some genes that function in meiosis (*) and carbohydrate metabolism (**).

Tdel Gene Name	Description/S.cerevisiae ortholog	Wild type Read Counts	Mutant Counts	Log_2 Fold-Change
TDEL0E00330	*silenced copy of a1 gene at T. delbrueckii HMR-2 locus*	0	30.34	inf
TDEL0B00100	*N/A*	28.56	5030.33	7.46
TDEL0H04540	*N/A*	24.73	3376.62	7.09
TDEL0G00190	*silenced copy of a1 gene at T. delbrueckii HMR-1 locus*	0.36	42.41	6.88
TDEL0B00110	*N/A*	38.16	2754.24	6.17
TDEL0E05490	*Anc_6.240 YGL138C YGL138C*	11.42	579.83	5.67
TDEL0D03040	*N/A*	6.42	275.89	5.43
TDEL0E00340	*silenced copy of a2 gene at T. delbrueckii HMR-2 locus*	0.67	27.74	5.36
TDEL0H03220	*N/A*	21.89	573.92	4.71
TDEL0C02460	*Anc_7.301 YDL186W YDL186W*	6.76	159.44	4.56
TDEL0H04510	*N/A*	41.63	830.98	4.32

*TDEL0A03570**	*Anc_5.493 YDR402C DIT2*	66.44	1280.49	4.27
*TDEL0A05800**	*Anc_8.634 YPL130W SPO19 YOR214C YOR214C*	326.1	4960.5	3.93
TDEL0A08060	*N/A*	23.54	355.85	3.92
TDEL0D02390	*N/A*	7.06	105.6	3.9
TDEL0G02080	*Anc_1.169 YJL170C ASG7*	11.47	124.36	3.44
TDEL0B07690	*N/A*	291.82	3152.53	3.43
TDEL0C06230	*Anc_1.78*	21.03	196.88	3.23
TDEL0G00740	*Anc_5.50 YGR260W TNA1*	760.16	6641.08	3.13
*TDEL0A03580**	*Anc_5.494 YDR403W DIT1**	305.27	2584.58	3.08
TDEL0C06910	*Anc_1.12 YCL055W KAR4*	18	145.73	3.02
TDEL0A00420	*Anc_3.23 YNL318C HXT14*	63.73	494.54	2.96
TDEL0G01600	*Anc_6.185 YGL089C MF(ALPHA)2 YPL187W MF(ALPHA)1*	39.76	297.07	2.9
*TDEL0D02770**	*Anc_4.174 YLR343W GAS2*	45.12	315.62	2.81
*TDEL0A06450**	*Anc_8.700 YOR255W OSW1*	35.61	247.62	2.8
TDEL0B03880	*N/A*	62.55	431.69	2.79
TDEL0E00100	*probable pseudogene*	80.85	540.34	2.74
*TDEL0A00530**	*Anc_3.34 YOL132W GAS4*	85.16	547.68	2.69
TDEL0H04530	*N/A*	434.83	2760.86	2.67
TDEL0C06990	*additional copy of DIC1 in X region of T. delbrueckii HML locus*	4.44	27.27	2.62
TDEL0H04520	*N/A*	120.74	717.27	2.57
*TDEL0D02810**	*Anc_4.171 YLR341W SPO77*	69.47	405.68	2.55
TDEL0D04700	*Anc_3.152 YOL067C RTG1*	110.74	633.36	2.52
*TDEL0A05130**	*Anc_8.570 YBR180W DTR1*	62.24	352.79	2.5
TDEL0D00830	*Anc_4.335*	109.78	619.08	2.5
TDEL0A04250	*YBR298C MAL31*	368.48	2063.52	2.49
TDEL0G03030	*Anc_2.371 YPL033C SRL4*	52.91	295.22	2.48
*TDEL0E01490***	*Anc_4.223 YDL049C KNH1*	99.52	518.7	2.38
*TDEL0G00780**	*Anc_5.54 YHR184W SSP1*	176.73	918.42	2.38
TDEL0D00100	*N/A*	40.36	209.06	2.37
*TDEL0B03420**	*Anc_8.768 YOR298W MUM3*	60.68	306.94	2.34
TDEL0E00260	*N/A*	2566.61	12859.78	2.32
TDEL0H03650	*N/A*	97.84	483.86	2.31
*TDEL0C06770**	*Anc_1.25 YCL048W*	121.68	595.33	2.29

	SPS22 YDR522C SPS2			
TDEL0B07410	*N/A*	37.16	178.54	2.26
TDEL0H03270	*N/A*	422.23	1923.48	2.19
*TDEL0B01080**	*Anc_8.790 YOR313C SPS4*	75.47	330.11	2.13
TDEL0C01450	*Anc_7.402 YER106W MAM1*	85.7	374.03	2.13
TDEL0H02150	*Anc_7.229 YER053C-A YER053C-A*	278.61	1212.99	2.12
TDEL0A07280	*Anc_6.313 YCR045C RRT12*	114.78	495.69	2.11
*TDEL0A02610**	*Anc_2.485 YKL096W CWP1**	418.19	1720.12	2.04
TDEL0D01720	*N/A*	148.46	589.36	1.99
TDEL0A06900	*Anc_6.277 YMR189W GCV2*	5122.21	20210.34	1.98
TDEL0H00530	*N/A*	491.32	1927.45	1.97
TDEL0H02590	*Anc_7.188 YFR032C RRT5*	59.24	229.4	1.95
TDEL0D06570	*N/A*	984.99	3787.33	1.94
TDEL0G02530	*Anc_2.323 YDL114W YDL114W*	76.26	289.63	1.93
TDEL0A08040	*N/A*	56.36	211.62	1.91
*TDEL0C00760**	*Anc_8.50 YLR054C OSW2*	222.35	818.13	1.88
TDEL0D03790	*Anc_3.246 YDR019C GCV1*	1394.09	5092.1	1.87
TDEL0F00170	*N/A*	514.16	1840.41	1.84
TDEL0D04720	*Anc_3.150 YDL043C PRP11*	169.35	603.95	1.83
TDEL0B06100	*Anc_1.396 YLR174W IDP2 YNL009W IDP3*	1408.31	5002.87	1.83
TDEL0A05020	*Anc_5.636 YDR270W CCC2*	651.52	2274.87	1.8
TDEL0A07980	*N/A*	278.86	972.97	1.8
TDEL0A02410	*Anc_2.465 YMR096W SNZ1*	1800.5	6156.83	1.77
TDEL0A02420	*Anc_2.466 YMR095C SNO1*	383.86	1300.79	1.76
TDEL0C00160	*N/A*	38.7	121.52	1.65
TDEL0B01290	*Anc_8.508 YBR157C ICS2*	16.04	50.17	1.64
TDEL0G04960	*no start codon apparent*	2339.73	7093.07	1.6
TDEL0D02340	*N/A*	316.47	953.87	1.59
TDEL0B06220	*Anc_1.385*	127.12	380.25	1.58
TDEL0G00100	*N/A*	401.9	1199.81	1.58
TDEL0E01760	*Anc_4.197 YLR359W ADE13*	4490.51	13391.34	1.58
TDEL0D05600	*Anc_3.492 YGR130C YGR130C*	2352.85	6992.01	1.57
TDEL0D06680	*N/A*	38.03	112.78	1.57
TDEL0D05330	*N/A*	104.35	308.51	1.56
TDEL0E02790	*Anc_5.348 YDR317W HIM1*	64.76	191.21	1.56

TDEL0E04950	*Anc_5.134 YGR204W ADE3*	3636.91	10599.18	1.54
*TDEL0A00960**	*Anc_2.55 YDL222C FMP45 YNL194C YNL194C*	1683.93	4875.4	1.53
TDEL0A02500	*Anc_2.474 YMR087W YMR087W*	201.34	579.65	1.53
*TDEL0G00760**	*Anc_5.52 YHR185C PFS1*	196	563.98	1.52
TDEL0D05160	*Anc_3.108 YBR149W ARA1*	1852.55	5329.9	1.52
TDEL0C05600	*Anc_3.424 YGR088W CTT1*	6793.72	19384.26	1.51
TDEL0H04480	*N/A*	7320.05	20813.2	1.51
TDEL0G01610	*Anc_6.184 YPL186C UIP4*	136.95	389.23	1.51
*TDEL0B06310***	*Anc_1.375 YFR015C GSY1 YLR258W GSY2*	1267.26	3569.67	1.49
TDEL0H03660	*N/A*	37.04	102.96	1.47
TDEL0A08050	*N/A*	18.95	51.66	1.45
TDEL0C01830	*N/A*	1567.76	4262.27	1.44
TDEL0B05440	*N/A*	45.96	124.44	1.44
TDEL0C00840	*Anc_8.58 YFL017C GNA1*	340.96	906.62	1.41
*TDEL0C04590**	*Anc_2.242 YNL065W AQR1 YIL120W QDR1*	1794.04	4734.42	1.4
TDEL0C00630	*Anc_8.38 YLR058C SHM2*	8025.37	20980.43	1.39
TDEL0C00170	*Anc_2.89 YNL165W YNL165W*	43.18	112.8	1.39
TDEL0C02500	*Anc_1.489 YEL046C GLY1*	3378.27	8801.43	1.38
TDEL0E00310	*N/A*	202	522.53	1.37
TDEL0A00140	*N/A*	109.36	282.47	1.37
TDEL0E00350	*N/A*	227.73	587.63	1.37
TDEL0G00210	*N/A*	449.42	1158.59	1.37
TDEL0E00850	*Anc_4.285 YKL187C YKL187C YLR413W YLR413W*	2873.13	7339.53	1.35
TDEL0B05780	*N/A*	102.69	260.58	1.34
TDEL0D05040	*Anc_3.119 YOL084W PHM7*	5727.35	14415.9	1.33
TDEL0E00320	*N/A*	53.58	133.94	1.32
TDEL0A05760	*Anc_8.630 YPL128C TBF1*	139.06	346.38	1.32
TDEL0H00120	*N/A*	90.65	222.93	1.3
TDEL0D05750	*Anc_3.507*	495.87	1215.55	1.29
TDEL0C00210	*N/A*	641.94	1543.38	1.27
TDEL0D03430	*Anc_3.281 YBR066C NRG2 YDR043C NRG1*	300.95	717.87	1.25
TDEL0C04620	*Anc_2.245 YNL063W MTQ1*	416.43	983	1.24
*TDEL0B04150***	*Anc_8.195 YDR074W TPS2*	2150.3	5060.38	1.23
TDEL0B02500	*Anc_5.673 YKR080W MTD1*	2761.04	6492.77	1.23

TDEL0D06610	*possible pseudogene; N added at two sites to avoid frameshifts*	322.84	758.48	1.23
TDEL0E00110	*possible pseudogene; N added to avoid frameshift*	64.14	149.43	1.22
TDEL0E00270	*N/A*	134.39	312.28	1.22
TDEL0F01320	*Anc_2.177 YNL101W AVT4*	1132.4	2618.17	1.21
TDEL0D05430	*Anc_3.81 YNL280C ERG24*	1549.78	3578.89	1.21
TDEL0E03600	*Anc_5.266 YHR022C YHR022C*	839.36	1936.88	1.21
TDEL0F03380	*N/A*	54.95	126.65	1.2
TDEL0D00650	*N/A*	389.91	880.46	1.18
TDEL0C01310	*N/A*	2145.74	4806.19	1.16
TDEL0G01510	*Anc_6.195 YGL082W YGL082W YPL191C YPL191C*	407.25	908.44	1.16
TDEL0A07230	*Anc_6.309 YMR206W YMR206W YNR014W YNR014W*	518.47	1152.23	1.15
TDEL0B00120	*N/A*	169.29	374.84	1.15
TDEL0H01710	*Anc_7.273 YER081W SER3 YIL074C SER33*	6936.33	15341.48	1.15
TDEL0B00960	*Anc_8.801 YMR250W GAD1*	953.92	2108.67	1.14
*TDEL0B05680***	*Anc_1.435 YEL011W GLC3*	809.34	1762.59	1.12
TDEL0C00140	*N/A*	85.09	184.53	1.12
TDEL0D02250	*Anc_1.357 YFR023W PES4 YHR015W MIP6*	308.62	668.74	1.12
TDEL0G01710	*Anc_4.20 YHL028W WSC4*	695.11	1506.14	1.12
TDEL0D02460	*Anc_5.455 YOR128C ADE2*	2232	4829.7	1.11
TDEL0E00280	*N/A*	376.24	806.8	1.1
TDEL0B03240	*Anc_8.525 YPL061W ALD6*	994.1	2127.76	1.1
TDEL0C02550	*Anc_1.484 YEL041W YEF1 YJR049C UTR1*	690.63	1476.64	1.1
TDEL0H04260	*Anc_7.25 YAL044C GCV3*	2743.83	5814.64	1.08
TDEL0C05340	*Anc_3.397 YBR132C AGP2*	596.01	1262.57	1.08
*TDEL0C05240***	*Anc_3.386 YBR126C TPS1*	2205.2	4663.53	1.08
TDEL0C00450	*Anc_8.22 YFL040W YFL040W*	80.29	169.32	1.08
TDEL0A02400	*Anc_2.464 YKL109W HAP4*	1447.85	3053.05	1.08
TDEL0G00200	*silenced copy of a2 gene at T. delbrueckii HMR-1 locus*	80.13	168.35	1.07
*TDEL0E03690***	*Anc_5.257 YKL152C GPM1*	53511.14	111819.2	1.06
TDEL0C00130	*N/A*	718.82	1499.25	1.06

*TDEL0D03730**	*Anc_3.252 YBR045C GIP1*	180.07	372.7	1.05
TDEL0D03300	*Anc_3.296*	3786.42	7762.59	1.04
TDEL0A00130	*N/A*	312.57	639.12	1.03
TDEL0H02310	*Anc_7.215 YER047C SAP1*	463.53	947.02	1.03
*TDEL0E00210***	*Anc_2.445 YKL127W PGM1 YMR105C PGM2*	7533.93	15266.2	1.02
*TDEL0G03220**	*Anc_2.391 YDL079C MRK1 YMR139W RIM11*	1715.92	3476.54	1.02
TDEL0C03290	*Anc_7.465 YJR094C IME1*	31.65	64.13	1.02
TDEL0B00340	*Anc_8.865 YML091C RPM2*	2336.03	4731.25	1.02
TDEL0B00830	*Anc_8.814 YMR262W YMR262W*	412.6	834.55	1.02
TDEL0A02430	*Anc_2.467 YMR094W CTF13*	103.45	208.01	1.01
TDEL0D01220	*Anc_1.255 YJL106W IME2*	86.48	173.31	1
TDEL0D04710	*Anc_3.151 YDL042C SIR2 YOL068C HST1*	1073.99	9.22	-6.86
TDEL0D06630	*YFR055W IRC7*	1735.47	356.24	-2.28
TDEL0F02930	*Anc_4.59 YGR161C RTS3*	3158.93	941.4	-1.75
TDEL0H00860	*YGR286C BIO2*	526.47	185.53	-1.5
TDEL0F04600	*Anc_8.336 YDR155C CPR1*	10592.71	3790.99	-1.48
TDEL0G03300	*N/A*	869.19	319.86	-1.44
TDEL0B04040	*Anc_6.150 YBR238C YBR238C YGL107C RMD9*	5774.79	2164.77	-1.42
TDEL0C02270	*Anc_7.319 YLR214W FRE1*	8103.25	3287.34	-1.3
TDEL0H02760	*Anc_7.169*	136.54	58.79	-1.22
TDEL0C01030	*N/A*	2182.98	941.75	-1.21
TDEL0E03870	*Anc_5.239 YJL034W KAR2*	6060.81	2660.19	-1.19
TDEL0E02290	*Anc_5.395 YDR343C HXT6 YHR094C HXT1*	2305.49	1013	-1.19
TDEL0F05620	*YKL216W URA1*	2366.8	1054.72	-1.17
TDEL0B04210	*Anc_8.189 YDR070C FMP16*	681.14	311.42	-1.13
TDEL0F01940	*Anc_6.244 YMR173W DDR48*	3659.39	1681.12	-1.12
TDEL0B02690	*Anc_5.654 YKR071C DRE2*	921.33	425.21	-1.12
TDEL0B01220	*Anc_8.516 YBR162W-A YSY6*	532.41	253.33	-1.07
TDEL0G04350	*Anc_6.34 YMR002W MIC17*	792.64	378.4	-1.07
TDEL0H01600	*N/A*	1848.38	892.09	-1.05
TDEL0F00720	*Anc_2.84 YHR144C DCD1*	262.29	129.14	-1.02
TDEL0A01990	*Anc_4.186 YGR041W*	394.24	195.73	-1.01

	BUD9 YLR353W BUD8			
TDEL0B00270	*Anc_8.858 YML123C PHO84*	7365.58	3679.29	-1

Table 3.8: Genes Increasing and Decreasing in Expression Relative to Wild Type in *T. delbrueckii sir4*Δ Mutant

Shown below are the two-fold or greater statistically significant expression changes that occurred in the *sir4*Δ mutant relative to Wild type.

Tdel Gene Name	Description/S.cerevisiae ortholog	Wild type Read Counts	Mutant Counts	Log_2 Fold-Change
TDEL0E00330	silenced copy of a1 gene at T. delbrueckii HMR-2 locus	0	32.67	inf
TDEL0B00100	N/A	31.67	8351.03	8.04
TDEL0G00190	silenced copy of a1 gene at T. delbrueckii HMR-1 locus	0.4	63.04	7.3
TDEL0H04540	N/A	27.41	1842.8	6.07
TDEL0B00110	N/A	42.34	2713.53	6
TDEL0E00340	silenced copy of a2 gene at T. delbrueckii HMR-2 locus	0.75	38.91	5.7
TDEL0H04510	N/A	46.16	745.75	4.01
TDEL0A08060	N/A	26.12	401.23	3.94
TDEL0B07690	N/A	323.59	2190.76	2.76
TDEL0C06990	additional copy of DIC1 in X region of T. delbrueckii HML locus	4.92	29.95	2.61
TDEL0E00100	probable pseudogene; NNN added at 2 sites to avoid internal stop codons	89.67	518.29	2.53
TDEL0C06910	Anc_1.12 YCL055W KAR4	19.95	101.29	2.34
TDEL0D00100	N/A	44.73	214.92	2.26
TDEL0H04530	N/A	482.14	2313.94	2.26
TDEL0H04520	N/A	133.86	606.11	2.18
TDEL0A08040	N/A	62.52	273.11	2.13
TDEL0A08050	N/A	21.02	75.4	1.84
TDEL0E00320	N/A	59.4	204.09	1.78
TDEL0D06680	N/A	42.15	144.07	1.77
TDEL0E00310	N/A	223.93	716.54	1.68
TDEL0E00110	possible pseudogene; N added to avoid frameshift	71.11	213.67	1.59
TDEL0G00100	N/A	445.66	1243.04	1.48
TDEL0E00350	N/A	252.49	659.05	1.38
TDEL0D06610	possible pseudogene; N added at two sites to avoid frameshifts	357.97	842.67	1.24
TDEL0B00120	N/A	187.69	426.62	1.18
TDEL0E00260	N/A	2845.36	6178.25	1.12
TDEL0C00100	N/A	58.85	120.26	1.03
TDEL0B01940	Anc_8.442 YDR227W SIR4	775.97	1.07	-9.5

3.4.7 *T. delbrueckii* Kos3 Bound to the Silencers of *HMLα* and *HMRa*

The largely silencer-restricted binding profile of ScSir1 correlated with ScSir1's importance in establishing silencing. To determine whether or not the regions bound by TdKos3 corresponded to the silencers of *T. delbrueckii*, we created a reporter-based silencing assay using a plasmid containing the entire *T. delbrueckii HMLα* locus plus 1000 base pairs on either side. In this plasmid the *α2* coding region was replaced with *K. lactis URA3*. Strains auxotrophic for uracil yet containing this plasmid were unable to grow on medium lacking uracil due to silencing of the *K. lactis URA3* gene (Figure 3.11A). Deletion of *TdKOS3, TdSIR2*, or *TdSIR4* relieved this repression, leading to *URA3* expression and growth on media lacking uracil (Figure 3.11A).

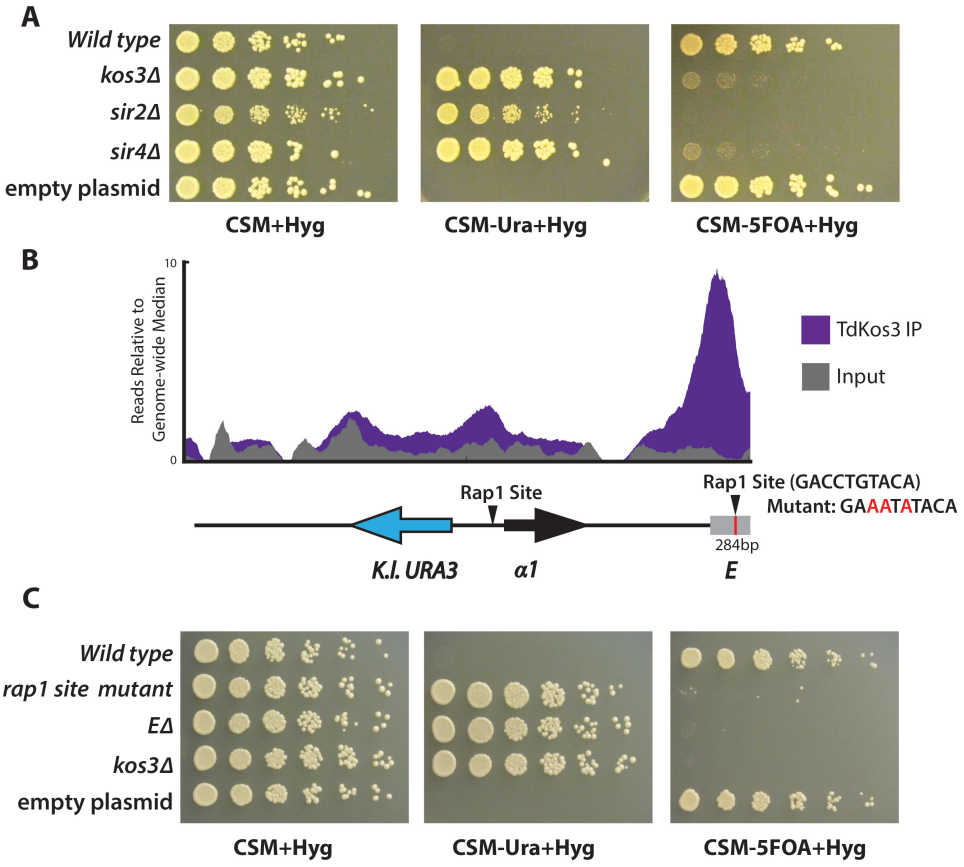

Figure 3.11. Kos3 Bound To the Silencer of *HMLα*. (A) A plasmid bearing the Hygromycin B resistance gene as a selectable marker and a ~5kb fragment of *TdHMLα* in which the *α2*-coding gene had been replaced with the *K. lactis URA3* gene was transformed into wild-type, *kos3*Δ, *sir2*Δ, and *sir4*Δ strains. *T. delbrueckii* silencing mutants were able to grow on medium lacking uracil and unable to grow on medium containing 5FOA. (B) A single region (labeled E, gray box) was deleted and found to be critical for silencing, as deleting it resulted in robust growth on medium lacking uracil (to approximately the same extent as deletion of *TdKOS3*). TdKos3 was highly enriched (purple) over region C. (C) A putative Rap1 binding site (red line in region E, 5B) was mutated at three positions and silencing was assayed via growth on media lacking uracil. These mutations resulted in a total loss of silencing, equivalent to the loss seen by deleting region C.

To map the silencers at *Td HMLα*, we deleted a 284 base-pair fragment (region E) corresponding to the major Kos3, Sir2 and Sir4 binding peak adjacent to the coding genes and evaluated its impact on *URA3* silencing. This deletion completely abolished silencing at *HMLα* when deleted and hence contained an *HML* silencer (Figure 3.11C). Formally, silencers are defined as cis-acting regulatory sites. Because of the nature of the assay, there was an intact copy of the E-region in the chromosome, which nevertheless could not maintain silencing in cells with a deletion of this region on a plasmid-borne *HML* locus. Therefore the deleted region contained a silencer for *HML*, or at least a critical component of one.

A similar assay was developed to map silencer elements at *HMRa* by cloning a ~5 kb fragment from the *HMR* on *T. delbrueckii* chromosome V and replacing the *a1* coding with the *K. lactis URA3* gene. Silencing of this reporter was also dependent on *KOS3, SIR2,* and *SIR4* (Figure 3.12A). The binding profile of Kos3 at *HMRa* at the putative silencer region showed two peaks, corresponding to regions A and B. Region C included regions A plus B and some surrounding sequence (Figure 3.12B). Region A was centered on the first peak and contained a valine tRNA gene. Deletion of region A had a modest effect on silencing, resulting in weak growth on medium lacking uracil, but not to the extent as in the *kos3*Δ mutant. Deletion of region B had a slight to almost no effect on silencing. Deletion region C led to a complete loss of silencing (Figure 3.12C). For the reasoning described above, the deletion of the C region must have removed all or a critical part of a silencer for *HMR*.

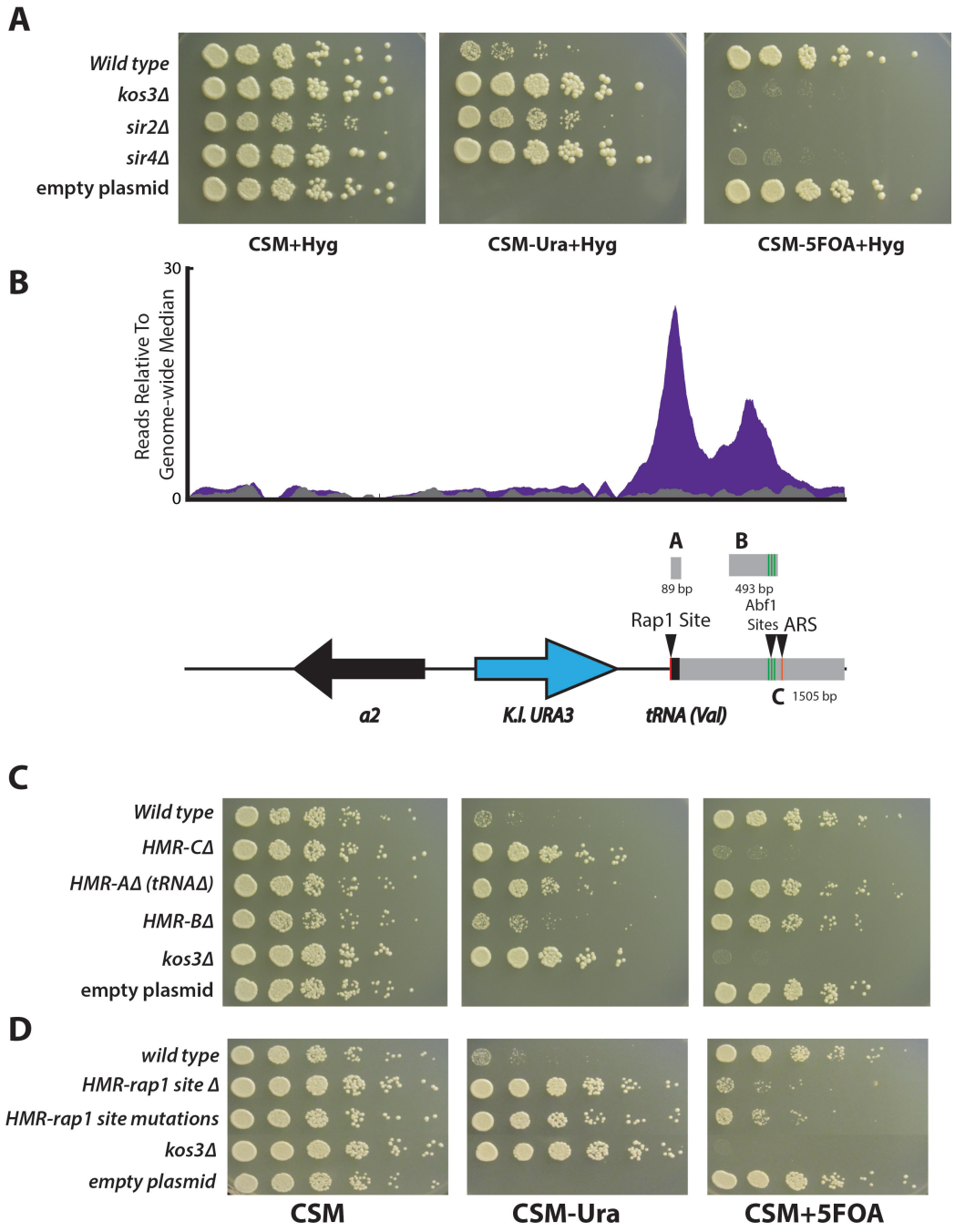

Figure 3.12. Kos3 Bound To The Silencer of *HMRa*. A plasmid-based *URA3* reporter construct developed to map silencers at *HMRa*. (A) Silencing (or lack of growth on CSM-URA) was dependent on *T. delbrueckii SIR* genes. (B) Depiction of the fragment of *TdHMRa* tested when cloned in a plasmid with the Hyg resistance gene, along with TdKos3 binding (purple). Regions A (89 base pairs), B (493 base pairs), and C (1505 base pairs), shown in gray boxes, were individually deleted and silencing was assayed by growth on CSM + Hyg, CSM-Ura+Hyg, and CSM+5FOA +HYG +Uracil. Region A included the valine tRNA (black box). Immediately adjacent to the valine tRNA (but not within region A) was a putative Rap1 site (red line). A cluster of three putative Abf1 binding sites was present in region B (green lines), as well as a

putative ARS consensus sequence (black arrow and red line adjacent to green lines). (C) Silencing as measured by growth on medium lacking uracil in each of the deletion constructs depicted in part (B). Deletion of region C resulted in a complete disruption of silencing, equivalent to that seen in a *kos3*Δ mutant. Deletion of region B resulted in little-to-no extra growth as compared to wild type, and deletion of region A resulted in a modest but not complete disruption of silencing. (D) The Rap1 binding site outside of region A was mutated in two ways: a clean deletion (growth in row 2), and by mutating two key cytosine residues to adenine (row 3; see text for exact mutations). Both of these mutations disrupted silencing to almost equivalent levels as that seen in a *kos3*Δ mutant.

3.4.8 *T. delbrueckii* Silencers Contained Rap1 Binding Sites That Were Important for Silencing

In *S. cerevisiae,* the *E* and *I* silencers contained combinations of binding sites for Rap1, Abf1, and the Origin Recognition Complex (ORC). The silencers of *K. lactis* contain binding sites for Reb1, Ume6, as well as an additional "C-box" sequence (BARSOUM *et al.* 2010). Since *T. delbrueckii* and *S. cerevisiae* are more closely related than *S. cerevisiae* is to *K. lactis*, we evaluated whether *T. delbrueckii* silencers contained binding sites that resembled those of *K. lactis* or *S. cerevisiae*, potentially illuminating how this major evolutionary transition of transcription-factor binding sites occurred. The DNA-binding domain of *S. cerevisiae* Rap1 has been mapped to amino acid residues 358-602 (KÖNIG *et al.* 1996; FELDMANN *et al.* 2015). Alignment of the *S. cerevisiae* Rap1 and *T. delbrueckii* Rap1 protein sequences revealed that this region of the protein is highly conserved between both species, displaying 81% sequence identity, providing further evidence that Rap1 may bind to the silencers of *T. delbrueckii*. The *T. delbrueckii* silencer regions defined by the deletion at *HML* contained a high-scoring Rap1 DNA binding motif within region E, 797 base pairs away from the 3' end of the $\alpha 1$ gene: GACCTGTACA. A high-scoring Rap1 site was also found in the promoter region of *Td HML*, between the $\alpha 2$ and $\alpha 1$ genes, reminiscent of the Rap1 binding site in the promoter region of *HML* in *S. cerevisiae.* To test the importance of the Rap1 binding site within the silencer for silencing, a triple mutant affecting three base pairs of this Rap1 motif was evaluated (Figure 3.11C, second row from top). This mutant site diminished silencing to the same extent as deleting the entire *E* region, suggesting that this Rap1 binding site was a key component of the silencer. A Rap1 binding site was also found in the *T. delbrueckii HMR* region immediately adjacent to the valine tRNA, residing just outside of region A. Disrupting this Rap1 binding site via a complete deletion, or mutating it from CATCCATACA to CATAAATACA, also greatly reduced silencing at *HMRa* (Figure 3.12D).

In addition to Rap1 binding sites, a motif search also revealed the presence of three putative Abf1 binding sites clustered within region B of *TdHMR* (green lines under black arrow, Figure 3.12B), as well as one site within the promoter region of *HML* (overlapping the putative Rap1 site). Mutating the highest scoring of these putative binding sites in the B region had no effect on silencing. Deletion of all three also had no effect (Figure 3.13A). A search for ARS consensus sequences revealed a potential candidate AT-rich sequence of 13 base pairs in length in the C region of *HMR* (Figure 3.12B, black arrow marked "ARS"). This C region was also found to have a functional ARS (Figure 3.14). Deleting the sequence that may represent this functional ARS had no effect on, at least on its own, on silencing (Figure 3.13B).

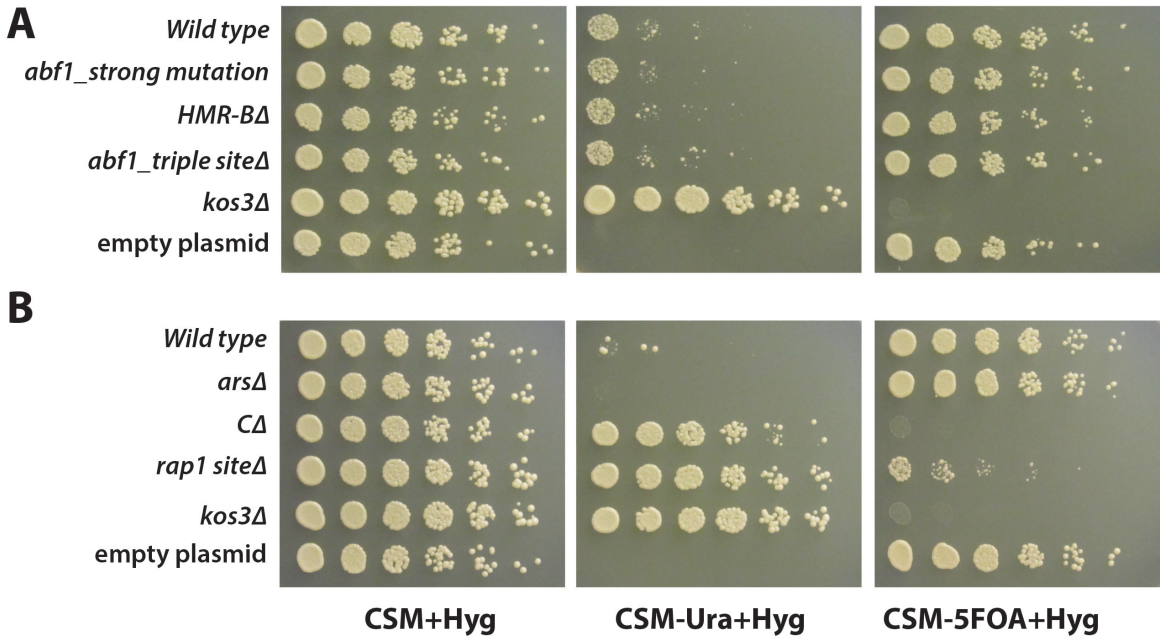

Figure 3.13. Mutations in putative Abf1 binding sites and a putative ARS consensus sequence do not have an effect on silencing at the chromosome V *HMR* in *T. delbrueckii*. (A) Of the three putative Abf1 sites, mutating the strongest one (second row from top) had no effect, as did deleting all three (fourth row from top). (B) Deleting a 13-base pair AT-sequence in the C region had no effect on silencing (second row from top). Silencing in the *kos3*Δ mutant is shown for comparison. Strains containing an empty plasmid are shown as a negative control.

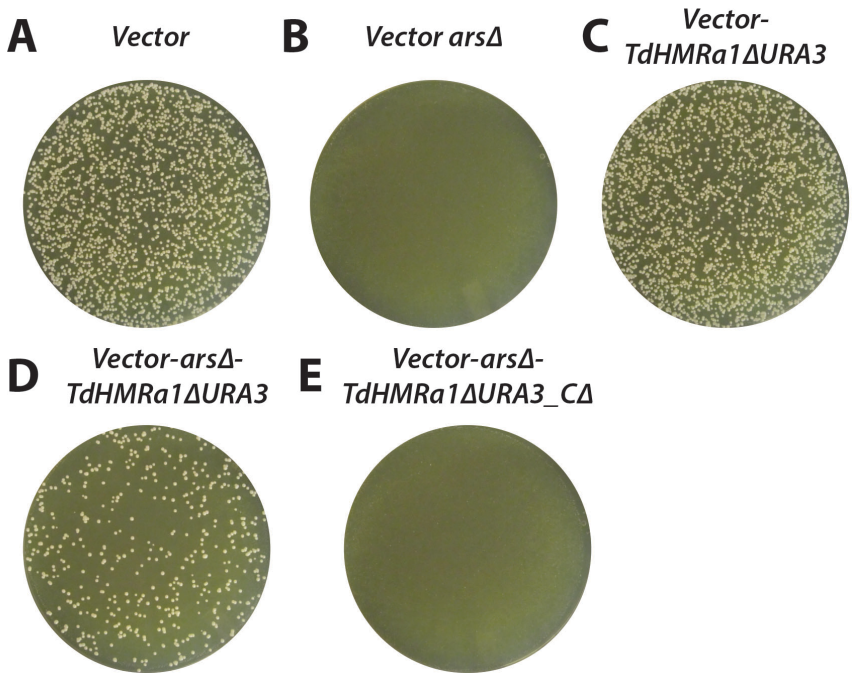

Figure 3.14. The *T. delbrueckii* chromosome V *HMR* C-region contains a functional ARS. (A) Transformation of *T. delbrueckii* strains with a backbone vector that contains a *T. delbrueckii CEN* and *S. cerevisiae ARS*. (B) Transformation with the same backbone vector after deleting the *S. cerevisiae ARS*. The cells can no longer maintain the plasmid. (C) Transformation with the vector from part B containing the full fragment of *HMR* from Figure 3.12B (with region C and with *a1* replaced with *K.l. URA3*. (D) Transformation of vector from part C with backbone *ARS* deleted. The cells can still maintain the plasmid, despite the deletion of the plasmid *ARS*. (E) Transformation of vector with both plasmid *ARS* and region C deleted. Cells can no longer maintain the plasmid without region C.

3.4.9 *KOS3* Expression Was Autoregulated By De-Repression at *Td HMRa*

The *KOS3* gene itself is located ~1kb away from the copy of *HMR* carried on chromosome V (Figure 3.15A). Interestingly, in *sir2*Δ and *sir4*Δ mutants, the expression of *KOS3* itself doubled (Figure 3.15B). Neither Sir2 nor Sir4 enrich at the promoter of the *KOS3* gene, indicating that these proteins do not directly repress it. Genes adjacent to silent mating type cassettes are often de-repressed when losses in silencing occur, presumably because repressive chromatin at the silent locus exerts transcriptional repression on nearby genes (for example, the *CHA1* gene in *S. cerevisiae*, located adjacent to *HML*, increases in expression in *sir* mutants (ELLAHI *et al.* 2015)). The location of the *KOS3* gene and the fact that its expression increases when *HMR* is de-repressed suggests that in a wild type strain, occasional lapses in silencing at *HMR* might increase the expression of its repressor, *KOS3*, providing an autoregulatory method of maintaining silencing.

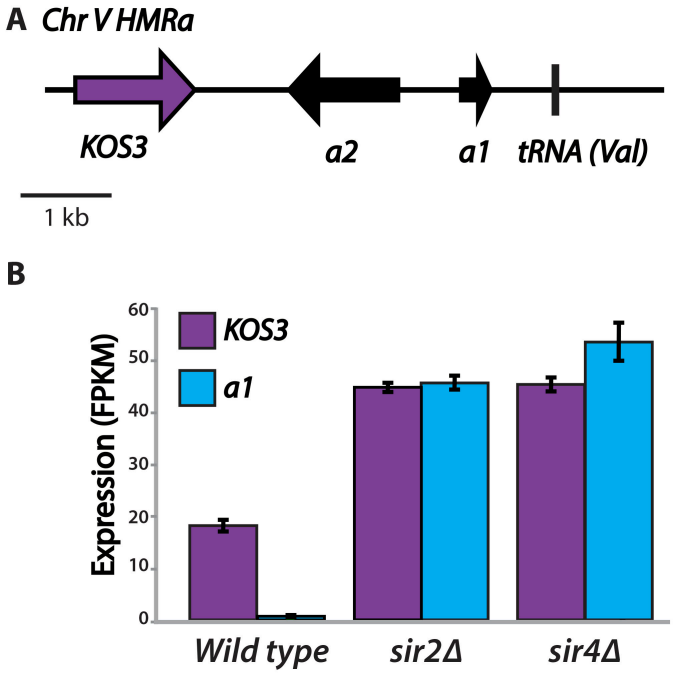

Figure 3.15. *KOS3* Expression is Autoregulated by The Expression State of the *HMR* on Chr V. (A) The *KOS3* gene is located ~1 kb away from the *HMRa2* gene of the Chr V *HMR*. (B) De-repression at the Chr V *HMRa1* gene in the *sir2*Δ and *sir4*Δ mutants leads to a doubling in *KOS3* expression. Sir2 and Sir4 do not enrich at the promoter of *KOS3*, but do enrich at a silencer adjacent to *HMRa1*.

3.4.10 *KOS3* Was Necessary For The Recruitment of *SIR2* and *SIR4* To Silenced Loci

In *S. cerevisiae,* Sir2, Sir3, and Sir4 can be recruited to the silencers of *HMR* in the absence of ScSir1 (RUSCHE *et al.* 2002), presumably due to the interactions between Rap1 at the silencer and a Sir4-Sir2 dimer, which, in turn, recruits Sir2 and Sir3. These interactions do not require Sir1 and allow silencing to be re-established, albeit inefficiently, in a *sir1*Δ strain. ChIP-seq of V5-tagged alleles of *TdSIR2* and *TdSIR4* in *kos3Δ* strains showed that *TdKOS3* was required for enrichment of TdSir2 and TdSir4 at *HML* and *HMR* and at telomeres (*TdHMRa* shown in Figure 3.16; see Figure 3.17 for *TdHMLα* and *TEL01R*).

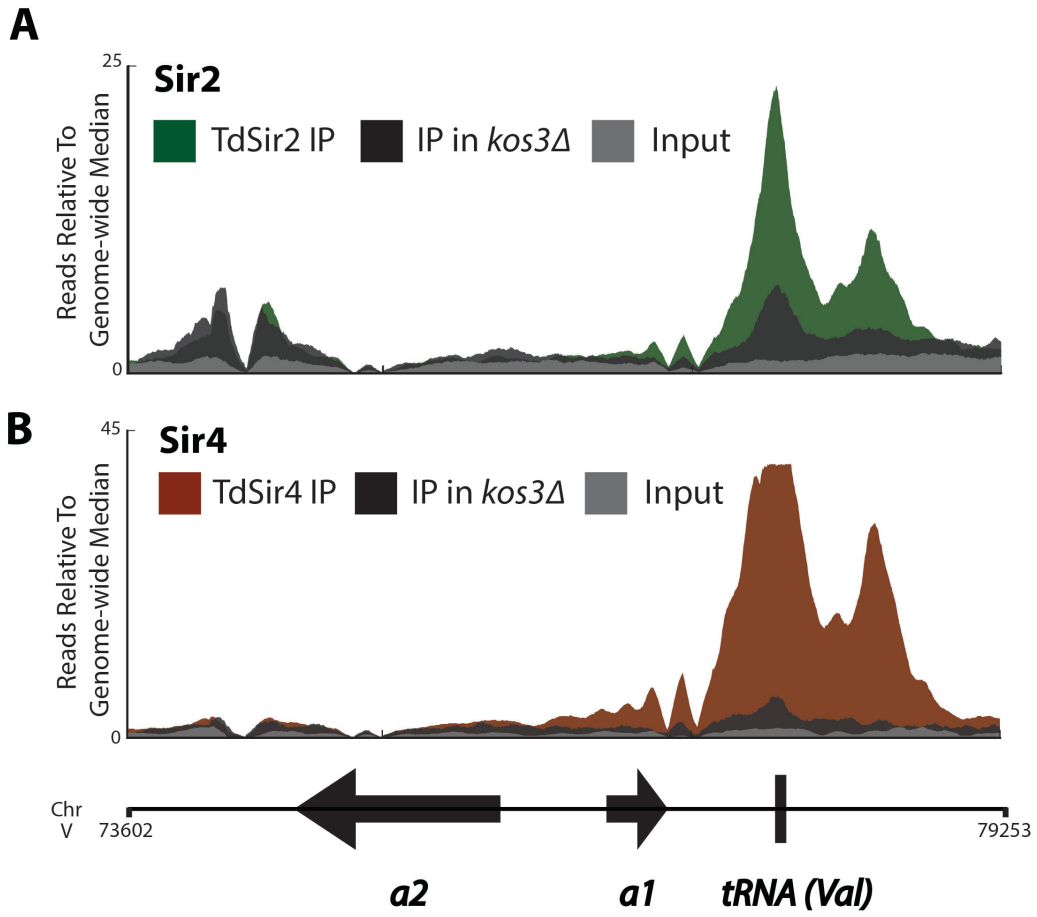

Figure 3.16. ***T. delbrueckii KOS3*** **was required to recruit TdSir2 and TdSir4 to** ***HMRa***. Chromatin immunoprecipitation followed by deep sequencing was carried out for V5-tagged TdSir2 and TdSir4 in *kos3*Δ strains. The enrichment of TdSir2 and TdSir4 was compared to strains wild type for *TdKOS3*. (A) Enrichment of TdSir2 (top) at *TdHMRa* in wild type (green) and *kos3*Δ (black). Bottom panel (B) depicts enrichment of TdSir4 at the same locus in wild type (brown) and *kos3*Δ (black). Sample input is shown in gray.

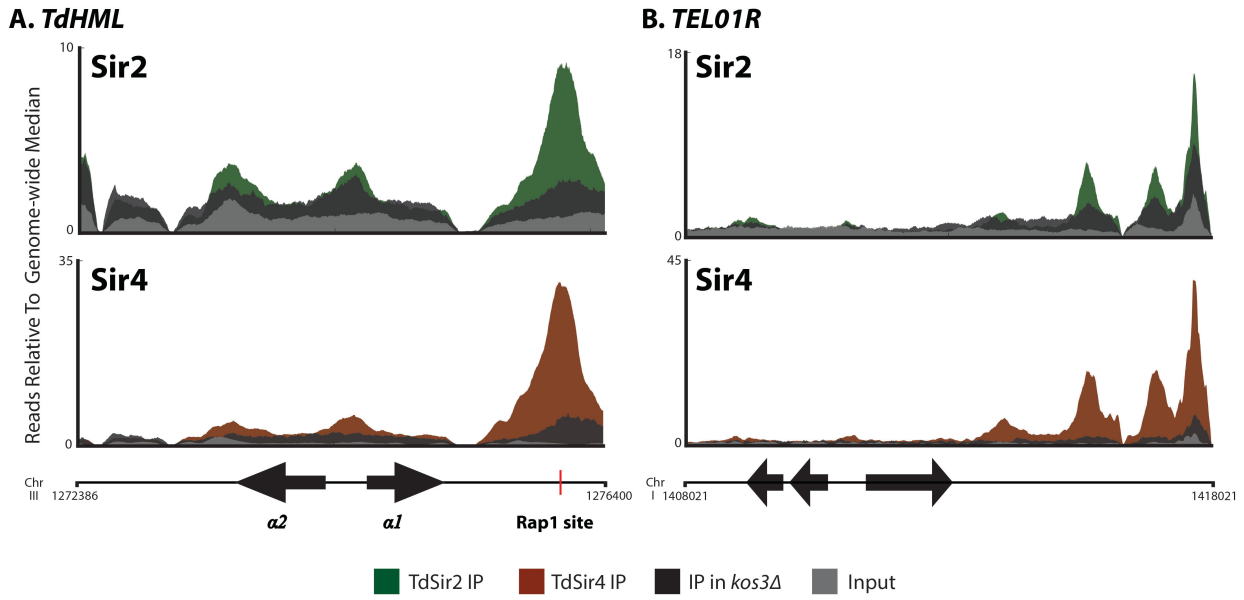

Figure 3.17. Td Sir2 and Sir4 display reduced enrichment at *HML* and *TEL01R*. Shown is enrichment of Sir2 (green) and Sir4 (brown) at *HML* (A) and a representative telomere, *TEL01R* (B) in *kos3*Δ strains. Enrichment in *KOS3* Wild type strains for Td Sir2 and Td Sir4 shown in green and brown respectively. Enrichment of Td Sir2 and Td Sir4 in the *kos3*Δ strain is shown in black. Input shown in gray. Genes marked with black arrows; Rap1 site at *HML* marked with red line.

3.4.11 Sir1 and *T. delbrueckii* Kos3, Sir2, and Sir4 Enriched at Centromeres

Sir1 had previously been found at six centromeres by locus specific ChIP (*CEN1*, *CEN2*, *CEN3*, *CEN4*, *CEN11*, and *CEN16*), and *sir1Δcac1Δ* mutants show elevated rates of nondisjunction (SHARP *et al.* 2003). When examining the Sir1 IP track separately from the input track, we saw a consistent under-representation of centromere sequences, hinting that centromere DNA was systematically under-recovered in our IP samples (representative example shown in Figure 3.18A). To account for this under-recovery, we plotted Sir1 enrichment in terms of IP/ input and compared those values to the IP/ input of the no-tag control. This analysis revealed Sir1 enrichment at all sixteen *S. cerevisiae* centromeres (Figure 3.19). However, none of these peaks were statistically significant as indicated by analysis with MACs, a peak-calling software. Furthermore, ChIP-Seq datasets have been shown to contain certain reproducible but artifactual signals, implying the association of proteins to sequences that they do not actually bind in vivo (PARK *et al.* 2013; TEYTELMAN *et al.* 2013). To test as rigorously as possible whether these Sir1 peaks at centromeres represented ChIP-Seq artifacts, we compared Sir1 enrichment to enrichment of GFP-NLS at centromeres (data from (TEYTELMAN *et al.* 2013)). GFP is not expected to bind in a meaningful way to any portion of the yeast genome, yet control experiments show that it co-localizes with multiple common ChIP-seq artifacts. Only one centromere, *CEN13*, showed GFP-NLS IP over input enrichment. Thus, the Sir1 signal present at that centromere is likely to be spurious (Figure 3.19, panel marked with *). While there were

smaller GFP-NLS peaks adjacent to some other centromeres, none directly overlapped with the centromere sequence except for the peak at *CEN13*. Additionally, despite the presence of Sir1 at centromere sequences, there was no indication of any Sir-dependent gene silencing adjacent to any centromere (see also (ELLAHI *et al.* 2015)).

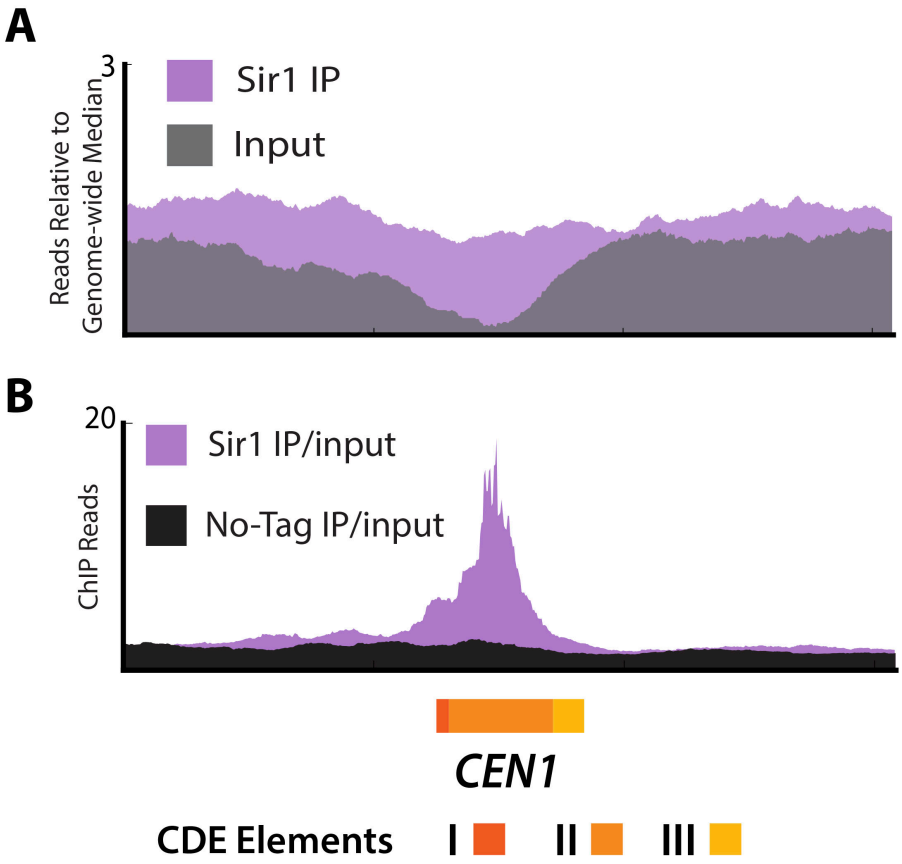

Figure 3.18. Under-enrichment of IP and input at *S. cerevisiae* centromeres. (A) Enrichment of Sir1 IP and input shown separately at *CEN1*. The input appears under-enriched. (B) Enrichment of Sir1 at *CEN1* viewed in terms of IP over input. The No tag negative control IP over input is shown in black.

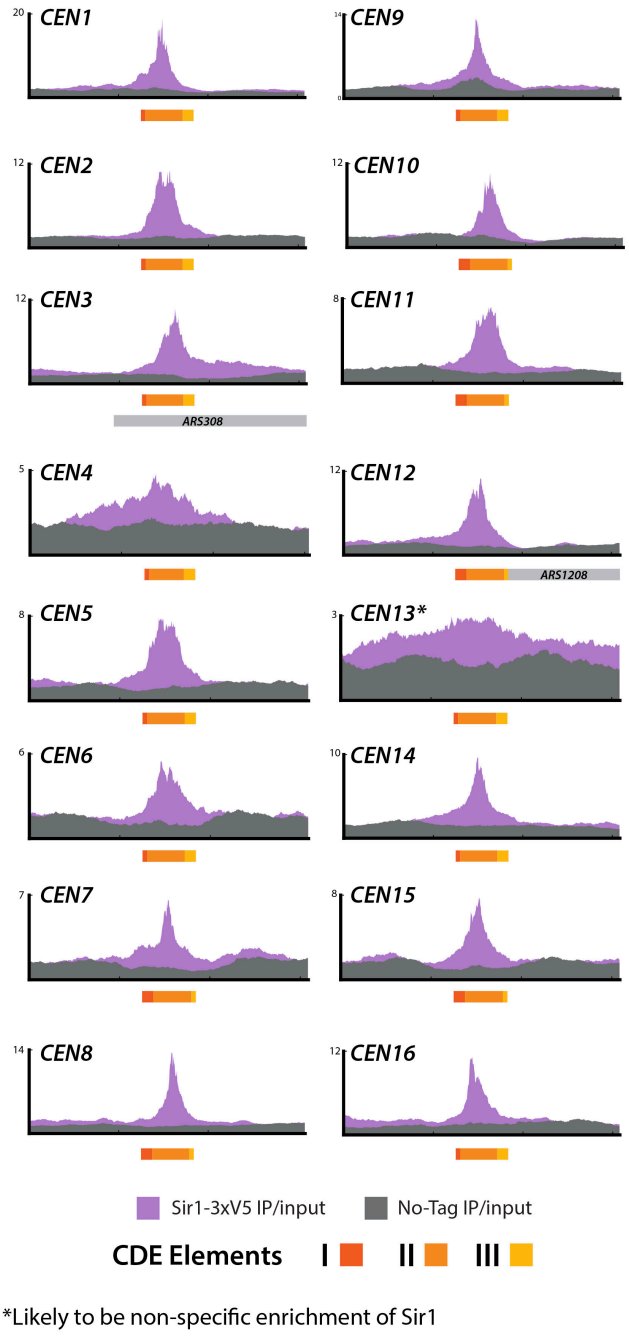

Figure 3.19. Sir1 enrichment at all 16 centromeres in *S. cerevisiae*. Enrichment is shown in terms of IP over input. IP over input of the no-tag control is shown in gray. *The enrichment seen at *CEN13* is likely to be non-specific, as its enrichment was not greater than the IP over input of GFP-NLS, a protein expected to non-specifically bind in the genome. Centromere sequence elements, CDE I, CDE II, and CDE III are marked with red orange, orange, and yellow boxes, respectively.

Because we saw Sir1 enrichment at *S. cerevisiae* centromeres, we evaluated whether Kos3 and *T. delbrueckii* Sir2 and Sir4 were present at centromeres in that species. *T. delbrueckii*,

like *S. cerevisiae*, has point centromeres that have been annotated based on conservation of the centromere DNA elements (CDEI, CDEII, and CDEIII) and by synteny (BYRNE and WOLFE 2005). We confirmed function for two of these centromeres (*Tdel* CEN1 and *Tdel CEN3*) by observing their ability to functionally replace *S. cerevisiae CEN6* in the pRS316 vector, allowing strains to maintain the plasmid in the absence of selection. We then examined Kos3, Sir2, and Sir4 enrichment at presumptive *T. delbrueckii* centromeres in terms of IP/ input and detected enrichment of all three proteins at centromeres (Figure 3.20). Kos3 exhibited a single peak of enrichment coincident with the annotated centromere sequence at 7 of the 8 centromeres. *CEN5* had a broader zone of enrichment, but otherwise Kos3 enrichment at centromeres was similar to Sir1's enrichment at centromeres of *S. cerevisiae*. The enrichment of Sir4 at the centromeres of *T. delbrueckii* was qualitatively similar to the enrichment distribution of Kos3. Sir2 was noteworthy in that it was enriched at all centromeres but at a low level, and the enrichment was spread out over a wider region outside the annotated *CEN* sequence. As in *S. cerevisiae*, we observed no evidence of gene silencing of genes adjacent to the centromeres.

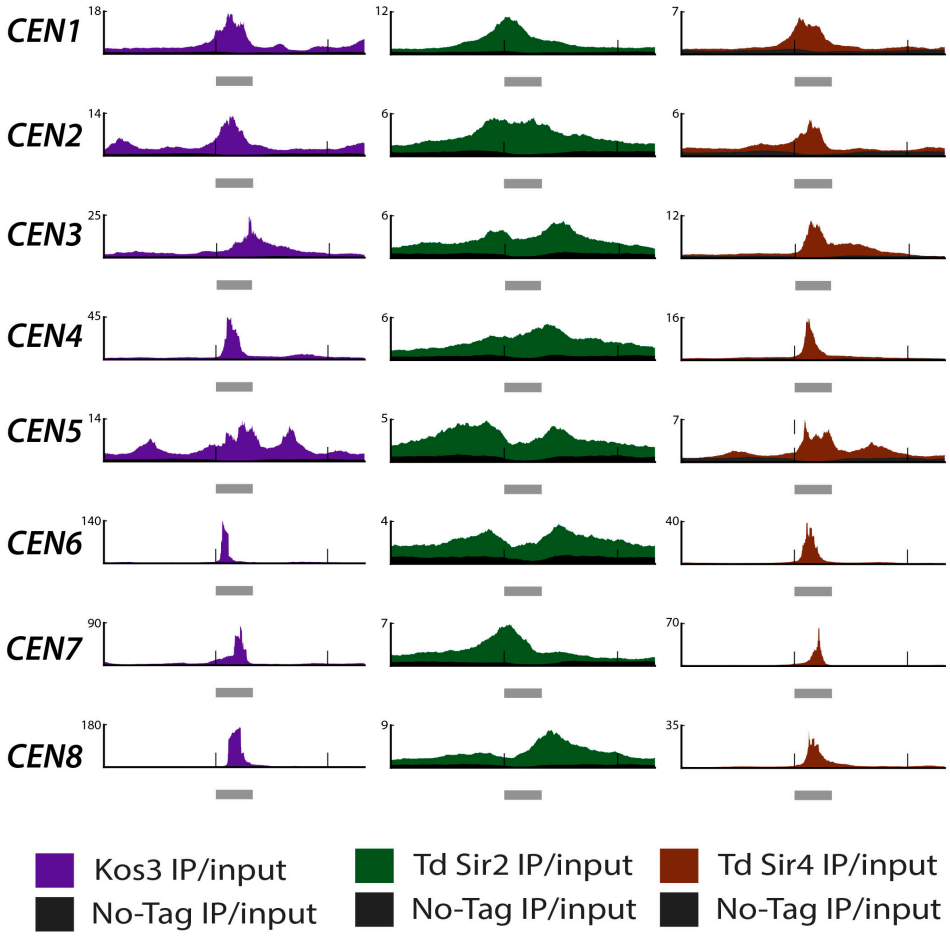

Figure 3.20. Enrichment of Kos3, Sir2, and Sir4 at *T. delbrueckii* centromeres. Enrichment is shown in terms of IP/input. Centromeres marked with gray boxes. Functionality of two centromeres, *CEN1* and *CEN3*, was confirmed experimentally.

3.4.12 *T. delbrueckii AGO1* and *DCR1* Had No Function in Silencing

Most *Saccharomyces* yeast lack the machinery for RNAi, a mechanism of gene silencing found in *Schizosaccharomyces pombe* and many other organisms, including plants and animals. The Argonaut and Dicer proteins are required for heterochromatin formation in *S. pombe*, and presumably in all organisms using the RNAi mechanism. Ago1 is a necessary component of the RNA-induced initiation of transcriptional gene silencing (RITS) complex, and Dcr1 cleaves double-stranded RNA into small interfering RNAs (siRNAs) that serve as guide RNAs, directing the heterochromatin machinery to the locus targeted for silencing (REYES-TURCU and GREWAL 2011). The *Naumovozyma castellii* genome contains an *AGO1* ortholog and a *DCR1*-like gene (*DCR1*-like because it is not directly orthologous to the *S. pombe DCR1*, but rather a duplicate of

RNT1, a ribonuclease specific for double-stranded RNA), which together degrade Ty transcripts in this species (DRINNENBERG *et al.* 2009b).

The *T. delbrueckii* genome also contains an *AGO1* and a *DCR1*-like gene, orthologous to those of *N. castellii*. Given that *AGO1* and *DCR1* repress Ty elements in *N. castellii*, we tested whether the *AGO1* and *DCR1* genes functioned in silencing in *T. delbrueckii* by deep sequencing of mRNAs in *T. delbrueckii ago1*Δ, *dcr1*Δ, and *ago1*Δ*dcr1*Δ double-mutants. These mutants displayed no defect in transcriptional repression of *HML, HMR*, or of any genes near telomeres (Figure 3.21A-B), and thus, these genes displayed no overlap in function with the *SIR* genes. Additionally, no genes showed a clear signal of de-repression in the RNAi mutants—i.e., no genes went from 0 FPKM in Wild type to an FPKM > 0 in the mutant. Overall, fifteen genes significantly changed in expression in the *ago1*Δ mutant, nine in the *dcr1*Δ mutant, and 53 in the *ago1*Δ*dcr1*Δ double mutant (Figure 3.21B and Tables 3.9, 3.10, and 3.11). Among the genes changing within RNAi mutants, little to no overlap was seen among these gene sets (Figure 3.21C and 3.21D). Perhaps the most striking observation is the much bigger impact that the double mutant has on expression of genes than either of the single mutants, discussed below. For the genes that had *S. cerevisiae* orthologs, we performed GO term analysis for the *ago1*Δ*dcr1*Δ double-mutant and found that several genes were associated with oxidation-reduction processes and/or small molecule metabolism, indicating a possible coordinating role in metabolic function (genes marked with black and orange dots, Figure 3.21B).

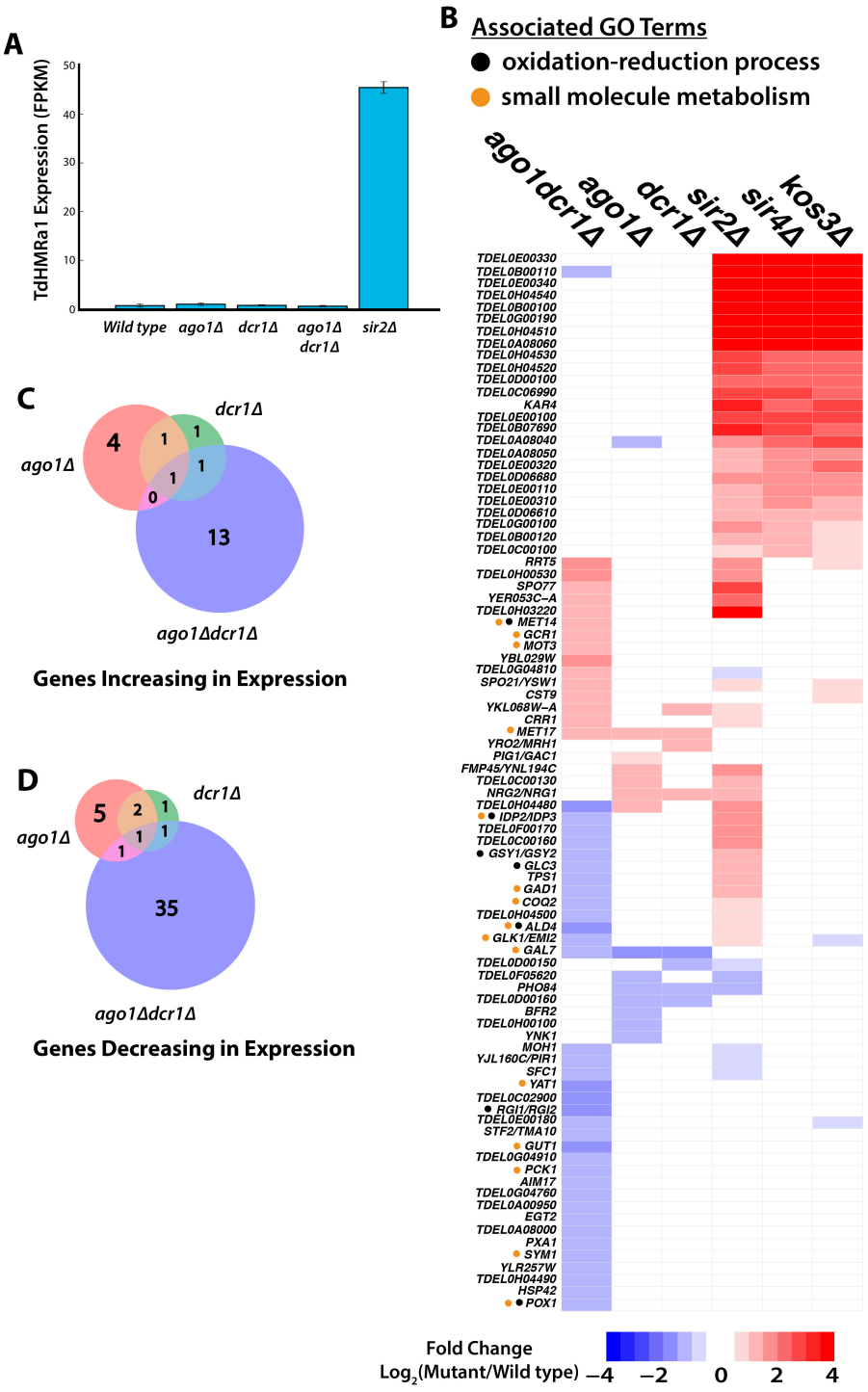

Figure 3.21. RNAi Did Not Function In Silencing In *T. delbrueckii.* (A) Expression of *TdHMRa1* in wild type, *ago1*Δ, *dcr1*Δ, and an *ago1*Δ*dcr1*Δ double mutant. Also shown for comparison is expression of *a1* in a *sir2*Δ mutant. Repression of *a1* is maintained in all three RNAi mutants. (B) A heatmap displaying significant changes in expression for genes across the three RNAi mutants (*ago1*Δ, *dcr1*Δ, and *ago1*Δ*dcr1*Δ), as well as the twenty-two genes that

increased in expression across all three *sir* mutants (*kos3*Δ, *sir2*Δ, and *sir4*Δ). All expression changes were filtered for genes that increased or decreased in expression greater than 2-fold relative to Wild type and showed a False-discovery rate (FDR) of < 10%. For genes with orthologs in *S. cerevisiae*, the three-letter gene name is shown. Whole-genome duplicates are named with the names of both *S. cerevisiae* duplicates (e.g., "*RGI1*/*RGI2"* represents the pre-whole genome duplication ancestor of these two genes in *T. delbrueckii*). (C) and (D) show weighted Venn diagrams of overlapping genes increasing (C) and decreasing (D) in expression relative to wild type in each of the single RNAi mutants and the double mutant.

Table 3.9 Genes Increasing and Decreasing in Expression Relative to Wild Type in *T. delbrueckii ago1*Δ Mutant

T. delbrueckii Gene Name	Description and *S. cerevisiae* ortholog	Wild type Read Counts	Mutant Counts	Log_2 Fold-Change
TDEL0E05620	*Anc_4.53_YLR303W_MET17*	1282.81	2605.93	1.02
TDEL0D03430	*Anc_3.281_YBR066C_NRG2_YDR043C_NRG1*	313.05	686.07	1.13
TDEL0C00130	*None*	747.86	1511.21	1.01
TDEL0A00960	*Anc_2.55_YDL222C_FMP45_YNL194C_YNL194C*	1753.09	3807.72	1.12
TDEL0G04020	*Anc_6.70_YLR273C_PIG1_YOR178C_GAC1*	782.76	1570.67	1
TDEL0H04480	*None*	7605.79	16321.03	1.1
TDEL0D00760	*AGO1*	4105.13	18.85	-7.77
TDEL0D00160	*None*	2316.09	1132.09	-1.03
TDEL0H00100	*None*	180.65	89.78	-1.01
TDEL0B00270	*Anc_8.858_YML123C_PHO84*	7680.71	3103.39	-1.31
TDEL0F05620	*YKL216W_URA1*	2471.09	1104.82	-1.16
TDEL0E03110	*Anc_5.316_YDR299W_BFR2*	848.82	367.55	-1.21
TDEL0E00130	*Anc_3.217_YBR018C_GAL7*	5447.66	1847.84	-1.56
TDEL0B06990	*Anc_2.606_YKL067W_YNK1*	1149.35	551.91	-1.06
TDEL0A08040	*None*	58.8	27.88	-1.08

Table 3.10 Genes Increasing and Decreasing in Expression Relative to Wild Type in *T. delbrueckii dcr1*Δ Mutant

T. delbrueckii Gene Name	Description and *S. cerevisiae* ortholog	Wild type Counts	Mutant Counts	Log_2 Fold-Change
TDEL0E05620	*YLR303W (MET17)*	1282.81	2919.77	1.19
TDEL0B07040	*YKL068W-A*	115.16	253.29	1.14
TDEL0D03430	*Anc_3.281_YBR066C_NRG2_YDR043C_NRG1*	313.05	640.28	1.03
TDEL0D03620	*Anc_3.263_YBR054W_YRO2_YDR033W_MRH1*	1143.57	2645.5	1.21
TDEL0B00490	*TdDCR1*	527.95	0.49	-10.09
TDEL0D00150	*None*	2483.46	1224.75	-1.02
TDEL0D00160	*None*	2316.09	1156.62	-1
TDEL0B00270	*Anc_8.858_YML123C_PHO84*	7680.71	3726.61	-1.04
TDEL0E00130	*Anc_3.217_YBR018C_GAL7*	5447.66	1831.02	-1.57

Table 3.11 Genes Increasing and Decreasing in Expression Relative to Wild Type in *T. delbrueckii ago1Δdcr1Δ* Mutant

A total of 15 genes increased in expression, while 36 genes decreased in expression (excluding *AGO1* and *DCR1* themselves, which were deleted). Statistically significant associated GO terms are starred: *oxidation-reduction process and **small molecule metabolism.

Tdel Gene Name	Gene Description and *S. cerevisiae* ortholog	Wild type Counts	Mutant Counts	Log_2 Fold-Change
TDEL0D05180	*Anc_3.106_YOL091W_SPO21_YBR148W_YSW1*	315.93	818.69	1.37
TDEL0H02150	*Anc_7.229_YER053C-A_YER053C-A*	290.62	638.93	1.14
*TDEL0E05620***	*Anc_4.53_YLR303W_MET17*	1282.81	3371.21	1.39
TDEL0A02860,***	*Anc_2.510_YKL001C_MET14*	500.72	1049.28	1.07
TDEL0B07040	*Anc_2.611_YKL068W-A_YKL068W-A*	115.16	293.26	1.35
TDEL0C02250	*Anc_7.321_YLR213C_CRR1*	393.95	872.25	1.15
TDEL0H00530	*None*	511.71	1924.72	1.91
*TDEL0A03070***	*Anc_2.533_YMR070W_MOT3*	531.53	1184.55	1.16
TDEL0D02810	*Anc_4.171_YLR341W_SPO77*	72.41	165.49	1.19
TDEL0G04810	*Anc_5.225_YJR004C_possible_pseudogene;_NNN_added_to_avoid_internal_stop_codon_SAG1*	2856.36	8065.96	1.5
TDEL0H02590	*Anc_7.188_YFR032C_RRT5*	61.8	177.97	1.53
*TDEL0B03030***	*Anc_8.543_YPL075W_GCR1*	3043.67	6173.95	1.02
TDEL0H03220	*None*	22.84	50.38	1.14
TDEL0E01150	*Anc_4.255_YLR394W_CST9*	151.86	386.56	1.35
TDEL0F02030	*Anc_3.314_YBL029W_YBL029W*	1882.73	5733.91	1.61
TDEL0D00760	*DCR1*	4105.13	15.95	-8.01
TDEL0B00490	*AGO1*	527.95	0.93	-9.15
TDEL0F04930	*Anc_8.369_YDR171W_HSP42*	2110.06	942.43	-1.16
*TDEL0C06700***	*Anc_1.33_YCL040W_GLK1_YDR516C_EMI2*	5278.83	2026.37	-1.38
TDEL0C03660	*Anc_1.187_YJL160C_YJL160C_YKL164C_PIR1*	9328.27	4467.78	-1.06
TDEL0C03310	*Anc_7.467_YJR095W_SFC1*	760.01	293.07	-1.37
*TDEL0A07760***	*Anc_6.361_YNR041C_COQ2*	1513.9	745.09	-1.02
TDEL0B06100,***	*Anc_1.396_YLR174W_IDP2_YNL009W_IDP3*	1468.89	674.28	-1.12
TDEL0A08000	*None*	1015.03	494.25	-1.04
TDEL0C03550	*Anc_7.492_YBL049W_MOH1*	189.09	89.77	-1.07
TDEL0H04450,***	*Anc_7.6_YOR374W_ALD4*	2790.18	883.98	-1.66
TDEL0H04500	*None*	505.82	239.16	-1.08
TDEL0C05240	*Anc_3.386_YBR126C_TPS1*	2297.85	1130.33	-1.02
TDEL0A00300	*Anc_3.11_YNL327W_EGT2*	1436.95	705.1	-1.03
*TDEL0B02120***	*Anc_5.708_YKR097W_PCK1*	142.3	57.36	-1.31
TDEL0G04910	*None*	2657.68	1038.52	-1.36
TDEL0H04490	*None*	417.79	192.3	-1.12
*TDEL0B00960***	*Anc_8.801_YMR250W_GAD1*	993.32	465.26	-1.09
*TDEL0G01820***	*Anc_4.9_YHL032C_GUT1*	1450.81	509.11	-1.51
*TDEL0H01960**	*Anc_7.248_YER067W_RGI1_YIL057C_RGI2*	615.46	183.96	-1.74
TDEL0H03410	*Anc_7.110_YHL021C_AIM17*	1713.68	693.58	-1.3
TDEL0G04760	*None*	9784.29	3968.18	-1.3
TDEL0H04480	*None*	7605.79	2054.54	-1.89

*TDEL0B06230***	*Anc_1.384_YLR251W_SYM1*	115.5	55.21	-1.06
TDEL0A00950	*None*	4708.18	2187.3	-1.11
TDEL0D05820,***	*Anc_3.514_YGL205W_POX1*	697.91	305.94	-1.19
TDEL0C02900	*None*	2157.25	708.44	-1.61
TDEL0F00170	*None*	535.08	221.04	-1.28
*TDEL0B06310**	*Anc_1.375_YFR015C_GSY1_YLR258W_GSY2*	1318.21	570.62	-1.21
*TDEL0D04470***	*Anc_3.176_YAR035W_YAT1*	631.43	159.06	-1.99
TDEL0B00110	*None*	39.85	19.29	-1.05
TDEL0C00160	*None*	40.29	19.48	-1.05
TDEL0D03060	*Anc_4.146_YGR008C_STF2_YLR327C_TMA10*	2032.38	733.81	-1.47
*TDEL0E00130***	*Anc_3.217_YBR018C_GAL7*	5447.66	2480.8	-1.13
TDEL0A06070	*Anc_8.661_YPL147W_PXA1*	431.99	206.53	-1.06
TDEL0E00180	*None*	11043.2	4472.84	-1.3
*TDEL0B05680**	*Anc_1.435_YEL011W_GLC3*	841.87	411.07	-1.03
TDEL0B06280	*Anc_1.378_YLR257W_YLR257W*	426.12	195.76	-1.12

3.5 Discussion

In this study we exploited four opportunities provided by *Torulaspora delbrueckii* to explore theme and variation in the evolution of gene silencing. Specifically, *T. delbrueckii*, as a pre-whole-genome duplication ascomycete, has one of the oldest versions of the *SIR1* gene, perhaps the most enigmatic of all budding yeast silencing genes. We explored the functional trajectory of a gene from in its earliest recognized appearance in *Torulaspora delbrueckii* to its reduced role in *Saccharomyces cerevisiae*. Interestingly, we found that although the overall function of *SIR1* in the formation of heterochromatin has remained constant, its precise role in that process has evolved considerably. The effect of deleting *SIR1* on silencing in *S. cerevisiae* is relatively minor on a cell population basis. In contrast, in *T. delbrueckii*, deletion of *KOS3* completely abolished silencing. Second, in addition to having the oldest *SIR*-silencing components, *T. delbrueckii* also has genes orthologous to budding yeast *AGO1* and *DCR1*, whose function(s) in *T. delbrueckii* were not known. Third, the silencer composition of the only other pre-duplication species examined, *K lactis*, differs from *S. cerevisiae*. Hence, *T. delbrueckii* offered the chance to explore which composition was most ancestral. Finally, *T. delbrueckii* offered the opportunity to explore to what extent unusual features of the molecular topography of silenced chromatin were intrinsic to the mechanism of silencing.

3.5.1 ScSir1 Associated With Silencers Except For The *HMR-I* Silencer

Our ChIP-Seq results show that Sir1 clearly binds to three of the four silencers in *S. cerevisiae*. Sir1 was strikingly enriched at *HML-E, HML-I, and HMR-E*, but not at *HMR-I.* Sir1 bound to those silencers that are sufficient on their own to maintain silencing (MAHONEY and BROACH 1989). Sir1 directly interacts with Orc1, a component of the Origin of Recognition Complex, and this interaction likely brings Sir1 to the silencer (TRIOLO and STERNGLANZ 1996; HSU *et al.* 2005). However, the ORC complex presumably associates with all four silencers, as an ARS consensus sequence is present at each one, and all four are capable of functioning as an

origin of replication when on plasmids. Both *HMR-E* and *HMR-I* are origins of replication in their chromosomal context (FOX *et al.* 1993; RIVIER *et al.* 1999). Therefore, it is perplexing why ScSir1 enrichment was absent from *HMR-I*.

3.5.2 *KOS3* Was Essential for Silencing, Whereas *SIR1* Is Not

Two observations emphasize the importance of Kos3 in silencing: (1) *T. delbrueckii kos3*Δ strains exhibited a complete loss of silencing at *HML*, *HMR*, and telomeres; and (2) in the absence of Kos3, enrichment of Sir2 and Sir4 at these positions was greatly reduced. In *S. cerevisiae,* Sir1 and Sir4 interact (BOSE *et al.* 2004). Rap1 is also present at the silencer, and the interaction between Rap1 and Sir4 is well documented (LUO *et al.* 2002). Therefore, in addition to the interaction between Sir1 and Sir4, the interaction between Rap1 and Sir4 may provide an additional route to bring silencing proteins to the silencer in *Saccharomyces*. Our putative Rap1 binding site mutations in the silencers of *T. delbrueckii* suggest that Rap1 bound those silencers and contributed to silencing the adjacent loci. However, a Sir4-Rap1 interaction may not exist in *T. delbrueckii*, resulting in Kos3 being necessary in both the establishment and maintenance of silencing.

3.5.3 Kos3 Functioned At Telomeres, Whereas ScSir1 Did Not

Early studies of telomeric silencing in *S. cerevisiae* found no role for *ScSIR1* in "telomere position effect," as measured by reporter genes adjacent to synthetic telomeres. Our ChIP-seq data of Sir1 and RNA-Seq data of the *sir1*Δ mutant corroborated these early observations and extended them to all telomeres. We saw no Sir1 protein enrichment at telomeres (except for at *HML*α) and no subtelomeric genes were de-repressed in the *sir1*Δ mutant. In contrast, TdKos3 bound to telomeric and subtelomeric sequences in *T. delbrueckii*, where it's enrichment pattern closely matched that of Sir2 and Sir4. These data suggest that the ancestral *SIR1* was once a part of a core silencing complex, one that may be composed of Orc1/Kos3/Sir4/Sir2, and that this is functionally equivalent to the ScSir2/Sir3/Sir4 complex.

3.5.4 *T. delbrueckii SIR2* Had Roles In Addition To Silencing

SIR2 in *S. cerevisiae* has other roles in the cell in addition to its role in heterochromatin at telomeres and the silent mating type loci, such as suppression of recombination at rDNA repeats and lifespan regulation (SMITH and BOEKE 1997; LIN *et al.* 2000). Our RNA-Seq data suggested that even in *T. delbrueckii*, *SIR2* regulates many genes and likely performs many functions outside of silencing, as there were 146 expression changes that were specific to the *sir2*Δ mutant (124 genes increased and 22 decreased in expression). *T. delbrueckii SIR2* is the pre-whole genome duplication ancestor of the *S. cerevisiae SIR2* and *HST1* duplicates; thus, *T. delbrueckii SIR2* may also repress genes that in *S. cerevisiae* are repressed by *HST1*. *S. cerevisiae* Hst1, in complex with Sum1 and Rfm1, functions in promoter-specific repression of middle-sporulation genes (XIE *et al.* 1999). *K. lactis* SIR2, another pre-whole-genome duplication ortholog of *S. cerevisiae* SIR2 and *HST1*, possesses functions of both *S. cerevisiae SIR2* and *HST1* (HICKMAN and RUSCHE 2009; FROYD and RUSCHE 2011). Interestingly, two middle-sporulation genes

repressed by Hst1 in *S. cerevisiae* were de-repressed in the *T. delbrueckii sir2*Δ mutant: *SPS4* and *DIT1*. Many other meiotic genes were also de-repressed (21 marked genes in Table 3.7), and some had Sir2 peaks in their promoters: *DIT2*, *SPO19*, *SPS101*, *SPS2*, *SPS4*, and *IME2*. The presence of promoter-specific Sir2 peaks suggests that like *S. cerevisiae* Hst1, *T. delbrueckii SIR2* is capable of acting as both a promoter-specific repressor as well as a long-range, promoter-independent repressor of gene expression.

3.5.5 Silencer Conservation And Diversity Among Budding Yeasts

Pairs of silencers flank both *HML* and *HMR* in *S. cerevisiae*, which are all bound by Sir2, Sir3 and Sir4 and, as shown here, by Sir1, with the exception of *HMR-I*. Based upon our ChIP-Seq data, it appears that a single prominent site bound by Kos3, Sir2 and Sir4 adjacent to *HML* and a close pair of sites adjacent to one side of *HMR* mediated silencing of these loci in *T. delbrueckii* . Although the analysis of these binding sites has only just begun, these sites were, in fact, silencers. The Rap1 binding site motif was clearly critical for silencing at both loci. The *HMR* silencer supported autonomous replication of a plasmid, implying the existence of an origin of replication and thus an ORC binding site. Abf1 binding site motifs were also evident. Further analysis will be required to map more precisely the functional elements of the silencer, but already there are notable differences between the structure of silenced chromatin in *T. delbrueckii* from that of *S. cerevisiae*.

In *K lactis*, Reb1 substitutes for the Rap1 protein in silencer function (SJÖSTRAND *et al.* 2002), even though Rap1 is critical for telomeric gene silencing (GUREVICH *et al.* 2003). In *T. delbrueckii*, Rap1 sites were clearly important for silencer function, and based upon the Rap1 binding sites in telomeric repeats of *T. delbrueckii*, we speculate that Rap1 is important for telomeric gene silencing as well. Thus the substitution of Reb1 for Rap1 was not an event associated with the whole genome duplication. Because *K. lactis* lacks any Sir1 ortholog and uses Reb1 at silencers, it is possible that Sir1 and its orthologs may drive the diversification of silencer binding proteins. If this view has merit, then the absence of a Sir1 ortholog should predict variation in the proteins that nucleate heterochromatin. In this regard, we note that *Candida glabrata* lacks any Sir1 ortholog, and depends upon the Rif1 protein to nucleate Sir-protein based gene silencing at telomeres (ROSAS-HERNANDEZ *et al.* 2008). However, Rap1 is important for silencing in *Candida glabrata* as well, suggesting that it may be at the silencer, and thus that the presence or absence of Sir1 cannot be the sole driver of silencer variation (Alejandro de las Peñas, personal communication).

3.5.6 The Presence Of Sir1 And Kos3 At Centromeres

Heterochromatin is characteristically assembled at centromeres of eukaryotes including *Schiszosaccharomyces pombe*, yet in *Saccharomyces* and other organisms with point centromeres, heterochromatin is not found at centromeres based upon the observation that no genes near centromeres were found to be de-repressed in *sir* mutants in *T. delbreuckii*. Earlier work established that the Sir1 protein of *Saccharomyces cerevisiae* is present at some centromeres, where it plays both positive and negative effects on centromere function, and serves to recruit the chromatin assembly factor CAF to centromeres (SHARP *et al.* 2003). Using our

genome-wide data of Sir1 binding, we found specific enrichment of Sir1 at all but one centromere. Interestingly, though earlier work found no enrichment of ScSir2, Sir3, or Sir4 at centromeres, we found evidence for enrichment of Sir2 and Sir3 at a handful of centromeres, using the ChIP-Seq data on GFP chromatin association to filter out artifactual associations. All three Sir proteins in *T. delbrueckii* (Kos3, Sir2, and Sir4) were found at all eight centromeres in this organism. However, we have been unable to express the GFP protein in *T. delbrueckii* and hence were unable to use this established metric to evaluate whether these peaks represented biological or artifactual associations. One interpretation is that Kos3 in *T. delbreuckii*, like Sir1 in *Saccharomyces*, plays some conserved function in centromere function. Whether the other Sir proteins with a ChIP-Seq enrichment signal at a subset of centromeres represent some latent function of these proteins at centromeres, or a new class of ChIP-Seq artifacts, awaits further study.

3.5.7 The Role Of RNAi In *T. delbrueckii*

Our RNA-Seq data of *ago1*Δ and *dcr1*Δ mutants of *T. delbreuckii* revealed that *AGO1* and *DCR1* did not function in silencing at *HML, HMR*, or telomeres. Thus if these proteins contribute to RNAi function in *T. delbrueckii,* RNAi must have a role other than in heterochromatin function. Of the 77 genes found to significantly change in expression across all candidate RNAi mutants, ~32% are genes of unknown function that have no ortholog in *S. cerevisiae*. Moreover, budding yeast *DCR1* is not directly orthologous to *S. pombe DCR1,* but rather is a duplicate of *RNT1* which encodes a ribonuclease involved in the processing of rRNA transcripts (CATALA *et al.* 2008). Therefore, *DCR1* may have inherited a separate set of interaction partners and functional constraints from its *RNT1* ancestor and may be on a different evolutionary trajectory from *AGO1*. Additionally, the *AGO1* and *DCR1* genes of *N. castellii* that repress Ty elements are thought to mediate repression at the post-transcriptional level, not at the epigenetic level via interactions with chromatin modifying enzymes (such as histone deacetylases and demethylases). Furthermore, *Candida albicans DCR1,* an ortholog of both the *T. delbrueckii* and *N. castellii DCR1,* functions in rRNA and spliceosomal RNA processing, strengthening the case for an RNA-processing function for *T. delbrueckii DCR1* (BERNSTEIN *et al.* 2012). As of yet, there exists no evidence tying budding yeast RNAi genes with any chromatin factors involved in the establishment or maintenance of heterochromatin, although there are many direct interactions between chromatin modifiers and *DCR1* and *AGO1* in *S. pombe* (GREWAL 2010).

Argonaute itself has had a complex evolutionary journey. Eukaryotic Argonaute proteins bind short RNA guide molecules to target transcripts. Prokaryotic Argonaute proteins, however, can bind DNA and may participate in genome defense against mobile elements (SWARTS *et al.* 2014). Budding yeast Argonaute co-purifies with small-interfering RNAs generated by Dicer, which suggests that it functions like other eukaryotic Argonaute proteins (DRINNENBERG *et al.* 2009b). However, other binding properties for budding yeast Argonaute have yet to be explored. Little overlap was observed in gene sets between *ago1*Δ and *dcr1*Δ; however, the 48 genes whose expression is altered only in the *ago1*Δ*dcr1*Δ double mutant implies that these two proteins share some overlapping function. That overlapping function must not be one that the proteins carry out together; rather, either must be able to contribute to that function in the absence of the other.

ABRAHAM J., NASMYTH K. A., STRATHERN J. N., KLAR A. J., HICKS J. B., 1984 Regulation of Mating-type Information in Yeast. Negative Control Requiring Sequences Both 5' and 3' to the Regulated Region. J. Mol. Biol. **176**: 307–331.

AI W., BERTRAM P. G., TSANG C. K., CHAN T., ZHENG X. F. S., 2002 Regulation of Subtelomeric Silencing During Stress Response. Mol. Cell **10**: 1295–1305.

ALBERTIN W., CHASSERIAUD L., COMTE G., PANFILI A., DELCAMP A., SALIN F., MARULLO P., BELY M., 2014 Winemaking and Bioprocesses Strongly Shaped the Genetic Diversity of the Ubiquitous Yeast Torulaspora delbrueckii. PLoS One **9**: e94246.

ANDERS S., HUBER W., 2010 Differential Expression Analysis for Sequence Count Data. Genome Biol. **11**: R106.

ANDERS S., HUBER W., 2013 Differential Expression of RNA-Seq Data At the Gene Level – the DESeq Package.

APARICIO O. M., BILLINGTON B. L., GOTTSCHLING D. E., 1991 Modifiers of Position Effect Are Shared Between Telomeric and Silent Mating-Type Loci in S. cerevisiae. Cell **66**: 1279–1287.

APARICIO O. M., GEISBERG J. V, SEKINGER E., YANG A., MOQTADERI Z., STRUHL K., 2005 Chromatin Immunoprecipitation for Determining the Association of Proteins with Specific Genomic Sequences In Vivo. Curr. Protoc. Mol. Biol. **23**: 17.7.1–17.7.23.

ARMACHE K. J., GARLICK J. D., CANZIO D., NARLIKAR G. J., KINGSTON R. E., 2011 Structural Basis of Silencing: Sir3 BAH Domain in Complex with a Nucleosome at 3.0 A Resolution. Science (80-.). **334**: 977–982.

ÅSTRÖM S. U., OKAMURA S. M., RINE J., 1999 Yeast Cell-Type Regulation of DNA Repair. Nature **397**: 310.

BAILEY T. L., BODEN M., BUSKE F. a, FRITH M., GRANT C. E., CLEMENTI L., REN J., LI W. W., NOBLE W. S., 2009 MEME SUITE: Tools for Motif Discovery and Searching. Nucleic Acids Res. **37**: W202–8.

BANNISTER A. J., KOUZARIDES T., 2011 Regulation of Chromatin by Histone Modifications. Cell Res. **21**: 381–395.

BARSOUM E., SJOSTRAND J. O. O., ASTROM S. U., 2010 Ume6 Is Required for the MATa/MATα Cellular Identity and Transcriptional Silencing in Kluyveromyces lactis. Genetics **184**: 999–1011.

BERNSTEIN B. E., TONG J. K., SCHREIBER S. L., 2000 Genomewide Studies of Histone Deacetylase Function in Yeast. Proc. Natl. Acad. Sci. U. S. A. **97**: 13708–13.

BERNSTEIN D. A., VYAS V. K., WEINBERG D. E., DRINNENBERG I. A., BARTEL D. P., FINK G. R., 2012 Candida albicans Dicer (CaDcr1) is Required for Efficient Ribosomal and Spliceosomal RNA Maturation. Proc. Natl. Acad. Sci. U. S. A. **109**: 523–528.

BOEKE J. D., TRUEHEART J., NATSOULIS G., FINK G. R., 1987 5-Fluoroorotic Acid as a Selective Agent in Yeast Molecular Genetics. METHODS Enzymol. **154**: 164–175.

BOER C. G. DE, HUGHES T. R., 2012 YeTFaSCo: a Database of Evaluated Yeast Transcription Factor Sequence Specificities. Nucleic Acids Res. **40**: D169–79.

BOSE M. E., MCCONNELL K. H., GARDNER-AUKEMA K. A., LLER U. M., WEINREICH M., KECK J. L., FOX C. A., 2004 The Origin Recognition Complex and Sir4 Protein Recruit Sir1p to Yeast Silent Chromatin Through Independent Interactions Requiring a Common Sir1p Domain. Mol. Cell. Biol. **24**: 774–786.

BRAND A. H., BREEDEN L., ABRAHAM J., STERNGLANZ R., NASMYTH K., 1985 Characterization of a "silencer" in Yeast: A DNA Sequence with Properties Opposite to Those of a Transcriptional Enhancer. Cell **41**: 41–48.

BYRNE K. P., WOLFE K. H., 2005 The Yeast Gene Order Browser: Combining curated homology and syntenic context reveals gene fate in polyploid species. **15**: 1456–1461.

CATALA M., TREMBLAY M., SAMSON E., CONCONI A., ABOU ELELA S., 2008 Deletion of Rnt1p Alters the Proportion of Open Versus Closed rRNA Gene Repeats in Yeast. Mol. Cell. Biol. **28**: 619–629.

COLLART M. A., OLIVIERO S., 2001 Preparation of Yeast RNA. In: *Current Protocols in Molecular Biology*, John Wiley & Sons, Inc., pp. 13.12.1–13.12.5.

CRAMPTON A., CHANG F., PAPPAS D. L. J., FRISCH R. L., WEINREICH M., 2008 An ARS Element Inhibits DNA Replication Through a SIR2-Dependent Mechanism. Mol. Cell **30**: 156–166.

DODSON A. E., RINE J., 2015 Heritable Capture of Heterochromatin Dynamics in Saccharomyces cerevisiae. Elife **4**: 1–22.

DOMERGUE R., CASTAN I., PEÑAS A. D. Las, ZUPANCIC M., LOCKATELL V., HEBEL J. R., JOHNSON D., CORMACK B. P., 2005 Nicotinic Acid Limitation Regulates Silencing of Candida Adhesins During UTI. Science (80-.). **308**: 866–870.

DRINNENBERG I. A., WEINBERG D. E., XIE K. T., MOWER J. P., WOLFE K. H., FINK G. R., BARTEL D. P., 2009a RNAi in Budding Yeast. Science (80-.). **326**: 544–550.

DRINNENBERG I. A., WEINBERG D. E., XIE K. T., MOWER J. P., WOLFE K. H., FINK G. R., BARTEL D. P., 2009b RNAi in Budding Yeast. Science (80-.). **326**: 544–550.

DRINNENBERG I. a, FINK G. R., BARTEL D. P., 2011 Compatibility with Killer Explains the Rise

of RNAi-deficient Fungi. Science (80-.). **333**: 1592.

DUJON B., 2010 Yeast evolutionary genomics. Nat. Publ. Gr. **11**: 512–524.

EHRENTRAUT S., WEBER J. M., DYBOWSKI J. N., HOFFMANN D., EHRENHOFER-MURRAY A. E., 2010 Rpd3-Dependent Boundary Formation at Telomeres By Removal of Sir2 Substrate. Proc. Natl. Acad. Sci. U. S. A. **107**: 5522–5527.

ELLAHI A., THURTLE D., RINE J., 2015 The Chromatin and Transcriptional Landscape of Native Saccharomyces cerevisiae Telomeres and Subtelomeric Domains. Genetics **200**: 1–17.

FELDMANN E. a., BONA P. DE, GALLETTO R., 2015 The Wrapping Loop and Rap1 C-terminal (RCT) Domain of Yeast Rap1 Modulate Access to Different DNA Binding Modes. J. Biol. Chem. **290**: 11455–11466.

FOUREL G., REVARDEL E., KOERING C. E., GILSON É., 1999 Cohabitation of Insulators and Silencing Elements in Yeast Subtelomeric Regions. EMBO J. **18**: 2522–2537.

FOX C. a., LOO S., RIVIER D. H., FOSS M. a., RINE J., 1993 A Transcriptional Silencer as a Specialized Origin of Replication That Establishes Functional Domains of Chromatin. Cold Spring Harb. Symp. Quant. Biol. **58**: 443–455.

FROYD C. A., RUSCHE L. N., 2011 The Duplicated Deacetylases Sir2 and Hst1 Subfunctionalized by Acquiring Complementary Inactivating Mutations. Mol. Cell. Biol. **31**: 3351–3365.

GALGOCZY D. J., CASSIDY-STONE A., LLINAS M., O'ROURKE S. M., HERSKOWITZ I., DERISI J. L., JOHNSON A. D., 2004 Genomic Dissection of The Cell-Type-Specification Circuit in Saccharomyces cerevisiae. Proc. Natl. Acad. Sci. U. S. A. **101**: 18069–18074.

GALLAGHER J. E. G., BABIARZ J. E., TEYTELMAN L., WOLFE K. H., RINE J., 2009 Elaboration, Diversification and Regulation of the Sir1 Family of Silencing Proteins in Saccharomyces. Genetics **181**: 1477–1491.

GEITZ D. R., 2014 Yeast Transformation by the LiAc/SS Carrier DNA/PEG Method. In: Smith JS, Burke DJ (Eds.), *Yeast Genetics: Methods and Protocols, Methods in Molecular Biology, vol. 1205*, Springer Science+Business Media, New York, pp. 1–12.

GOLDBERG A. D., ALLIS C. D., BERNSTEIN E., 2007 Epigenetics: A Landscape Takes Shape. Cell **128**: 635–638.

GORDON J. L., ARMISEN D., PROUX-WERA E., OHEIGEARTAIGH S. S., BYRNE K. P., WOLFE K. H., 2011 Evolutionary Erosion of Yeast Sex Chromosomes by Mating-type Switching Accidents. Proc. Natl. Acad. Sci. **108**: 1–6.

GOTTLIEB S., ESPOSITO R. E., 1989 A New Role for a Yeast Transcriptional Silencer Gene, SIR2, in Regulation of Recombination in Ribosomal DNA. Cell **56**: 771–776.

GOTTSCHLING D. E., APARICIO O. M., BILLINGTON B. L., ZAKIAN V. A., 1990a Position Effect at S. cerevisiae Telomeres: Reversible Repression of Pol II Transcription. Cell **63**: 751–762.

GOTTSCHLING D. E., APARICIO O. M., BILLINGTON B. L., ZAKIAN V. A., 1990b Position Effect at S. cerevisiae Telomeres: Reversible Repression of Pol II Transcription. Cell **63**: 751–762.

GREISS S., GARTNER A., 2009 Sirtuin/Sir2 Phylogeny, Evolutionary Considerations and Structural Conservation. Mol. Cells **28**: 407–415.

GREWAL S., 2010 RNAi-dependent Formation of Heterochromatin and Its Diverse Functions. Curr. Opin. Genet. Dev. **20**: 134–141.

GRUNSTEIN M., GASSER S. M., 2013 Epigenetics in Saccharomyces cerevisiae. Cold Spring Harb. Perspect. Biol. **5**: a017491–a017491.

GUILLEMETTE B., DROGARIS P., LIN H.-H. S., ARMSTRONG H., HIRAGAMI-HAMADA K., IMHOF A., BONNEIL É., THIBAULT P., VERREAULT A., FESTENSTEIN R. J., 2011 H3 Lysine 4 Is Acetylated at Active Gene Promoters and Is Regulated by H3 Lysine 4 Methylation (HD Madhani, Ed.). PLoS Genet. **7**: e1001354.

GUIZETTI J., SCHERF A., 2013 Silence, Activate, Poise and Switch! Mechanisms of Antigenic Variation in Plasmodium falciparum. Cell. Microbiol. **15**: 718–26.

GUREVICH R., SMOLIKOV S., MADDAR H., KRAUSKOPF A., 2003 Mutant Telomeres Inhibit Transcriptional Silencing at Native Telomeres of the Yeast Kluyveromyces lactis. Mol. Genet. Genomics **268**: 729–738.

HABER J. E., 2012 Mating-Type Genes and MAT Switching in Saccharomyces cerevisiae. Genetics **191**: 33–64.

HALME A., BUMGARNER S., STYLES C., FINK G. R., 2004 Genetic and Epigenetic Regulation of the FLO Gene Family Generates Cell-Surface Variation in Yeast. Cell **116**: 405–415.

HARRISON P., KUMAR A., LAN N., ECHOLS N., SNYDER M., GERSTEIN M., 2002 A Small Reservoir of Disabled ORFs in the Yeast Genome and its Implications for the Dynamics of Proteome Evolution. J. Mol. Biol. **316**: 409–19.

HAZELRIGG T., LEVIS R., RUBIN G. M., 1984 Transformation of white Locus DNA in Drosophila: Dosage Compensation, zeste Interaction, and Position Effects. Cell **36**: 469–81.

HECHT A., STRAHL-BOLSINGER S., GRUNSTEIN M., 1996 Spreading of Transcriptional Repressor SIR3 from Telomeric Heterochromatin. Nature **383**: 92–96.

HEINTEL T., ZAGORC T., SCHMITT M. J., 2001 Expression, Processing and High Level Secretion of a Virus Toxin in Fission Yeast. Appl. Microbiol. Biotechnol. **56**: 165–172.

HERNANDEZ-LOPEZ M. J., PRIETO J. A., RANDEZ-GIL F., 2003 Osmotolerance and Leavening

Ability in Sweet and Frozen Sweet Dough. Comparative Analysis Between Torulaspora delbrueckii and Saccharomyces cerevisiae Baker's Yeast Strains. Antonie Van Leeuwenhoek **84**: 125–134.

HICKMAN M. A., RUSCHE L. N., 2009 The Sir2-Sum1 Complex Represses Transcription Using Both Promoter-Specific and Long-Range Mechanisms to Regulate Cell Identity and Sexual Cycle in the Yeast Kluyveromyces lactis (HD Madhani, Ed.). PLoS Genet. **5**: e1000710.

HICKMAN M. A., RUSCHE L. N., 2010 Transcriptional Silencing Functions of the Yeast Protein Orc1/Sir3 Subfunctionalized After Gene Duplication. Proc. Natl. Acad. Sci. U. S. A. **107**: 19384–19389.

HICKMAN M. A., FROYD C. A., RUSCHE L. N., 2011 Reinventing Heterochromatin in Budding Yeasts: Sir2 and the Origin Recognition Complex Take Center Stage. Eukaryot. Cell **10**: 1183–1192.

HITTINGER C. T., 2013 Saccharomyces Diversity and Evolution: A Budding Model Genus. Trends Genet. **29**: 309–317.

HOMANN O. R., JOHNSON A. D., 2010 MochiView: Versatile Software for Genome Browsing and DNA Motif Analysis. BMC Biol. **8**: 1–8.

HONGAY C. F., GRISAFI P. L., GALITSKI T., FINK G. R., 2006 Antisense Transcription Controls Cell Fate in Saccharomyces cerevisiae. Cell **127**: 735–45.

HOPPE G. J., TANNY J. C., RUDNER A. D., GERBER S. A., DANAIE S., GYGI S. P., MOAZED D., 2002 Steps in Assembly of Silent Chromatin in Yeast: Sir3-Independent Binding of a Sir2/Sir4 Complex to Silencers and Role for Sir2-Dependent Deacetylation. Mol. Cell. Biol. **22**: 4167–80.

HOU Z., DANZER J. R., MENDOZA L., BOSE M. E., MULLER U., WILLIAMS B., FOX C. A., 2009 Phylogenetic Conservation and Homology Modeling Help Reveal a Novel Domain within the Budding Yeast Heterochromatin Protein Sir1. Mol. Cell. Biol. **29**: 687–702.

HSU H.-C., STILLMAN B., XU R.-M., 2005 Structural Basis for Origin Recognition Complex 1 Protein-Silence Information Regulator 1 Protein Interaction in Epigenetic Silencing. Proc. Natl. Acad. Sci. **102**: 8519–24.

IGLESIAS N., REDON S., PFEIFFER V., DEES M., LINGNER J., LUKE B., 2011 Subtelomeric Repetitive Elements Determine TERRA Regulation by Rap1/Rif and Rap1/Sir Complexes in Yeast. EMBO Rep. **12**: 587–93.

IMAI S.-I., ARMSTRONG C. M., KAEBERLEIN M., GUARENTE L., 2000 Transcriptional Silencing and Longevity Protein Sir2 is an NAD-dependent Histone Deacetylase. Nature **403**: 795–800.

KÖNIG P., GIRALDO R., CHAPMAN L., RHODES D., 1996 The Crystal Structure of the DNA-binding Domain of Yeast RAP1 in Complex with Telomeric DNA. Cell **85**: 125–136.

KURDISTANI S. K., ROBYR D., TAVAZOIE S., GRUNSTEIN M., 2002 Genome-wide Binding Map of the Histone Deacetylase Rpd3 in Yeast. Nat. Genet. **31**: 248–254.

LI H., DURBIN R., 2009 Fast and Accurate Short Read Alignment with Burrows-Wheeler Transform. Bioinformatics **25**: 1754–60.

LI H., HANDSAKER B., WYSOKER A., FENNELL T., RUAN J., HOMER N., MARTH G., ABECASIS G., DURBIN R., 2009 The Sequence Alignment/Map Format and SAMtools. Bioinformatics **25**: 2078–2079.

LI M., VALSAKUMAR V., POOREY K., BEKIRANOV S., SMITH J. S., 2013 Genome-wide Analysis of Functional Sirtuin Chromatin Targets in Yeast. Genome Biol. **14**: R48.

LIN S.-J., DEFOSSEZ P. a, GUARENTE L., 2000 Requirement of NAD and SIR2 for Life-Span Extension by Calorie Restriction in Saccharomyces cerevisiae. Science (80-.). **289**: 2126–2128.

LONEY E. R., INGLIS P. W., SHARP S., PRYDE F. E., KENT N. A., MELLOR J., LOUIS E. J., 2009 Repressive and Non-Repressive Chromatin at Native Telomeres in Saccharomyces cerevisiae. Epigenetics Chromatin **2**: 18.

LONGTINE M. S., MCKENZIE III A., DEMARINI D. J., SHAH N. G., WACH A., BRACHAT A., PHILIPPSEN P., PRINGLE J. R., 1998 Additional Modules for Versatile and Economical PCR-Based Gene Deletion and Modification in Saccharomyces cerevisiae. Yeast **14**: 953–961.

LOO S., RINE J., 1994 Silencers and Domains of Generalized Repression. Science **264**: 1768–1771.

LOUIS E. J., 1995 The Chromosome Ends of Saccharomyces cerevisiae. Yeast **11**: 1553–1573.

LUO K., VEGA-PALAS M. a, GRUNSTEIN M., 2002 Rap1-Sir4 Binding Independent of Other Sir, yKu, or Histone Interactions Initiates the Assembly of Telomeric Heterochromatin in Yeast. Genes Dev. **16**: 1528–39.

MA B., PAN S.-J., DOMERGUE R., RIGBY T., WHITEWAY M., JOHNSON D., CORMACK B. P., 2009 High-Affinity Transporters for NAD+ Precursors in Candida glabrata Are Regulated by Hst1 and Induced in Response to Niacin Limitation. Mol. Cell. Biol. **29**: 4067–79.

MAHONEY D. J., BROACH J. R., 1989 The HML Mating-Type Cassette of Saccharomyces cerevisiae Is Regulated by Two Separate but Functionally Equivalent Silencers. Mol. Cell. Biol. **9**: 4621–4630.

MARTIN A. M., POUCHNIK D. J., WALKER J. L., WYRICK J. J., 2004 Redundant Roles for Histone

H3 N-Terminal Lysine Residues in Subtelomeric Gene Repression in Saccharomyces cerevisiae. Genetics **167**: 1123–32.

MARVIN M. E., BECKER M. M., NOEL P., HARDY S., BERTUCH A. A., LOUIS E. J., 2009 The Association of yKu with Subtelomeric Core X Sequences Prevents Recombination Involving Telomeric Sequences. Genetics **183**: 453–467.

MILLAR C. B., GRUNSTEIN M., 2006 Genome-wide Patterns of Histone Modifications in Yeast. Nat. Rev. Mol. Cell Biol. **7**: 657–666.

MOAZED D., KISTLER A. M. Y., AXELROD A. M. Y., RINE J., JOHNSON A. D., 1997 Silent information regulator protein complexes in Saccharomyces cerevisiae: A SIR2/SIR4 complex and evidence for a regulatory domain in SIR4 that inhibits its interaction with SIR3. PNAS **94**: 2186–2191.

MORETTI P., FREEMAN K., COODLY L., SHORE D., 1994 Evidence That a Complex of SIR Proteins Interacts with the Silencer and Telomere-binding Protein RAP1. Genes Dev. **8**: 2257–2269.

PACHECO A., SANTOS J., CHAVES S., ALMEIDA J., LEO C., JOO M., 2012 The Emerging Role of the Yeast Torulaspora delbrueckii in Bread and Wine Production: Using Genetic Manipulation to Study Molecular Basis of Physiological Responses BT - (null). In: InTech.

PAPPAS D. L. J., FRISCH R., WEINREICH M., 2004 The NAD(+)-Dependent Sir2p Histone Deacetylase Is a Negative Regulator of Chromosomal DNA Replication. Genes Dev. **18**: 769–781.

PARK D., LEE Y., BHUPINDERSINGH G., IYER V. R., 2013 Widespread Misinterpretable ChIP-seq Bias in Yeast. PLoS One **8**: e83506.

PEÑAS A. D. Las, PAN S., CASTAÑO I., ALDER J., CREGG R., CORMACK B. P., 2003 Virulence-Related Surface Glycoproteins in the Yeast Pathogen Candida glabrata Are Encoded in Subtelomeric Clusters and Subject to RAP1- and SIR-Dependent Transcriptional Silencing. Genes Dev. **17**: 2245–2258.

PILLUS L., RINE J., 1989 Epigenetic Inheritance of Transcriptional States in S. cerevisiae. Cell **59**: 637–747.

PRYDE F. E., LOUIS E. J., 1999 Limitations of Silencing at Native Yeast Telomeres. EMBO J. **18**: 2538–2550.

RADMAN-LIVAJA M., RUBEN G., WEINER A., FRIEDMAN N., KAMAKAKA R., RANDO O. J., 2011 Dynamics of Sir3 Spreading in Budding Yeast: Secondary Recruitment Sites and Euchromatic Localization. EMBO J. **30**: 1012–26.

RENAULD H., APARICIO O. M., ZIERATH P. D., BILLINGTON B. L., CHHABLANI S. K.,

GOTTSCHLING D. E., 1993 Silent Domains Are Assembled Continuously from the Telomere and Are Defined by Promoter Distance and Strength, and by SIR3 Dosage. Genes Dev. **7**: 1133–1145.

REYES-TURCU F. E., GREWAL S. I. S., 2011 Different Means, Same End—Heterochromatin Formation by RNAi and RNAi-independent RNA processing Factors in Fission Yeast. Curr. Opin. Genet. Dev. **22**: 1–8.

RIVIER D. H., EKENA J. L., RINE J., 1999 HMR-I Is An Origin of Replication and A Silencer in Saccharomyces cerevisiae. Genetics **151**: 521–9.

ROSAS-HERNANDEZ L. L., JUAREZ-REYES A., ARROYO-HELGUERA O. E., LAS PENAS A. DE, PAN S.-J., CORMACK B. P., CASTANO I., 2008 yKu70/yKu80 and Rif1 Regulate Silencing Differentially at Telomeres in Candida glabrata. Eukaryot. Cell **7**: 2168–2178.

ROSSMANN M. P., LUO W., TSAPONINA O., CHABES A., STILLMAN B., 2011 A Common Telomeric Gene Silencing Assay Is Affected by Nucleotide Metabolism. Mol. Cell **42**: 127–136.

RUSCHE L. N., KIRCHMAIER A. L., RINE J., 2002 Ordered Nucleation and Spreading of Silenced Chromatin in Saccharomyces cerevisiae. Mol. Biol. Cell **13**: 2207–2222.

RUSCHE L. N., KIRCHMAIER A. L., RINE J., 2003 The Establishment, Inheritance, and Function of Silenced Chromatin in Saccharomyces cerevisiae. Annu. Rev. Biochem. **72**: 481–516.

SCHMITT M. J., BREINIG F., 2006 Yeast Viral Killer Toxins: Lethality and Self-protection. Nat. Rev. Microbiol. **4**: 212–221.

SCHULTZ J., 1947 The Nature of Heterochromatin. Cold Spring Harb. Symp. Quant. Biol. **12**: 179–191.

SHANKARANARAYANA G. D., MOTAMEDI M. R., MOAZED D., GREWAL S. I. S., 2003 Sir2 Regulates Histone H3 Lysine 9 Methylation and Heterochromatin Assembly in Fission Yeast. Curr. Biol. **13**: 1240–1246.

SHARP J. A., KRAWITZ D. C., GARDNER K. A., FOX C. A., KAUFMAN P. D., 2003 The Budding Yeast Silencing Protein Sir1 Is a Functional Component of Centromeric Chromatin. Genes Dev. **17**: 2356–2361.

SINGER M. S., GOTTSCHLING D. E., 1994 TLC1: Template RNA Component of Saccharomyces cerevisiae Telomerase. Science **266**: 404–409.

SJÖSTRAND J. O. O., KEGEL A., ASTRÖM S. U., 2002 Functional Diversity of Silencers in Budding Yeasts. Eukaryot. Cell **1**: 548–557.

SMITH J. S., BOEKE J. D., 1997 An Unusual Form of Transcriptional Silencing in Yeast

Ribosomal DNA. Genes Dev. **11**: 241–254.

STEAKLEY D. L., RINE J., 2015 On the Mechanism of Gene Silencing in Saccharomyces cerevisiae. G3 (Bethesda). **5**: 1751–1763.

STRAHL-BOLSINGER S., HECHT A., LUO K., GRUNSTEIN M., 1997 SIR2 and SIR4 Interactions Differ in Core and Extended Telomeric Heterochromatin in Yeast. Genes Dev. **11**: 83–93.

SVEJSTRUP J. Q., 2002 Mechanisms of Transcription-Coupled DNA Repair. Nat. Rev. Mol. Cell Biol. **3**: 21–29.

SWARTS D. C., MAKAROVA K., WANG Y., NAKANISHI K., KETTING R. F., KOONIN E. V, PATEL D. J., OOST J. VAN DER, 2014 The Evolutionary Journey of Argonaute Proteins. Nat. Struct. Mol. Biol. **21**: 743–753.

TAKAHASHI Y.-H., SCHULZE J. M., JACKSON J., HENTRICH T., SEIDEL C., JASPERSEN S. L., KOBOR M. S., SHILATIFARD A., 2011 Dot1 and Histone H3K79 Methylation in Natural Telomeric and HM Silencing. Mol. Cell **42**: 118–126.

TERLETH C., SLUIS C. A. VAN, PUTTE P. VAN DE, 1989 Differential Repair of UV Damage in Saccharomyces cerevisiae. Nucleic Acids Res. **17**: 4433–4439.

TEYTELMAN L., EISEN M. B., RINE J., 2008 Silent But Not Static: Accelerated Base-Pair Substitution in Silenced Chromatin of Budding Yeasts (GS Barsh, Ed.). PLoS Genet. **4**: e1000247.

TEYTELMAN L., THURTLE D. M., RINE J., OUDENAARDEN A. VAN, 2013 Highly Expressed Loci Are Vulnerable to Misleading ChIP Localization of Multiple Unrelated Proteins. Proc. Natl. Acad. Sci. **110**: 18602–18607.

THURTLE D. M., RINE J., 2014a The molecular topography of silenced chromatin in Saccharomyces cerevisiae. Genes Dev. **28**: 245–58.

THURTLE D. M., RINE J., 2014b The Molecular Topography of Silenced Chromatin in Saccharomyces cerevisiae. Genes Dev. **28**: 245–258.

TONKIN C. J., CARRET C. K., DURAISINGH M. T., VOSS T. S., RALPH S. A., HOMMEL M., DUFFY M. F., SILVA L. M. Da, SCHERF A., IVENS A., SPEED T. P., BEESON J. G., COWMAN A. F., 2009 Sir2 Paralogues Cooperate to Regulate Virulence Genes and Antigenic Variation in Plasmodium falciparum. PLoS Biol. **7**: e1000084.

TOONE W. M., JOHNSON A. L., BANKS G. R., TOYN J. H., STUART D., WITTENBERG C., JOHNSTON L. H., 1995 Rmel, a Negative Regulator of Meiosis, Is Also a Positive Activator of G1 Cyclin Gene Expression. EMBO J.

TRAPNELL C., PACHTER L., SALZBERG S. L., 2009 TopHat: Discovering Splice Junctions with

RNA-Seq. Bioinformatics **25**: 1105–11.

TRAPNELL C., ROBERTS A., GOFF L., PERTEA G., KIM D., KELLEY D. R., PIMENTEL H., SALZBERG S. L., RINN J. L., PACHTER L., 2012 Differential Gene and Transcript Expression Analysis of RNA-Seq Experiments with TopHat and Cufflinks. Nat. Protoc. **7**: 562–578.

TRIOLO T., STERNGLANZ R., 1996 Role of Interactions Between the Origin Recognition Complex and SIR1 in Transcriptional Silencing. Nature **381**: 251–253.

TSUKAMOTO Y., KATO J., IKEDA H., 1997 Silencing Factors Participate in DNA Repair and Recombination in Saccharomyces cerevisiae. Nature **388**: 900–903.

VALENCIA-BURTON M., OKI M., JOHNSON J., SEIER T. a, KAMAKAKA R., HABER J. E., 2006 Different Mating-Type-Regulated Genes Affect the DNA Repair Defects of Saccharomyces RAD51, RAD52 and RAD55 Mutants. Genetics **174**: 41–55.

VALENZUELA L., DHILLON N., DUBEY R. N., GARTENBERG M. R., KAMAKAKA R. T., 2008 Long-range Communication Between the Silencers of HMR. Mol. Cell. Biol. **28**: 1924–1935.

WELLINGER R. J., ZAKIAN V. A., 2012 Everything You Ever Wanted to Know About Saccharomyces cerevisiae Telomeres: Beginning to End. Genetics **191**: 1073–1105.

WELTHAGEN J. J., VILJOEN B. C., 1998 Yeast Profile in Gouda Cheese During Processing and Ripening. Int. J. Food Microbiol. **41**: 185–194.

WYRICK J. J., HOLSTEGE F. C. P., JENNINGS E. G., CAUSTON H. C., SHORE D., GRUNSTEIN M., LANDER E. S., YOUNG R. A., 1999 Chromosomal Landscape of Nucleosome-Dependent Gene Expression and Silencing in Yeast. Nature **402**: 418–21.

XIE J., PIERCE M., GAILUS-DURNER V., WAGNER M., WINTER E., VERSHON A. K., 1999 Sum1 and Hst1 Repress Middle Sporulation-specific Gene Expression During Mitosis in Saccharomyces cerevisiae. EMBO J. **18**: 6448–6454.

YOSHIDA K., BACAL J., DESMARAIS D., PADIOLEAU I., TSAPONINA O., CHABES A., PANTESCO V., DUBOIS E., PARRINELLO H., SKRZYPCZAK M., GINALSKI K., LENGRONNE A., PASERO P., 2014 The Histone Deacetylases Sir2 and Rpd3 Act on Ribosomal DNA to Control the Replication Program in Budding Yeast. Mol. Cell **54**: 691–697.

ZHANG Y., LIU T., MEYER C. a, EECKHOUTE J., JOHNSON D. S., BERNSTEIN B. E., NUSBAUM C., MYERS R. M., BROWN M., LI W., LIU X. S., 2008 Model-Based Analysis of ChIP-Seq (MACS). Genome Biol. **9**: R137.

ZHU X., GUSTAFSSON C. M., 2009 Distinct Differences in Chromatin Structure at Subtelomeric X and Y' Elements in Budding Yeast. PLoS One **4**: e6363.

ZILL O. A., SCANNELL D., TEYTELMAN L., RINE J., 2010 Co-Evolution of Transcriptional Silencing Proteins and the DNA Elements Specifying Their Assembly (EJ Louis, Ed.). PLoS Biol. **8**: e1000550.